An Investigation of Dry Band Arcing on Optical Fibre

T.W. Pretorius

B.Eng.

Dissertation submitted in partial fulfilment of the academic requirements of the

Masters in Engineering Degree (Electronic)

at the

North-West University

SUPERVISOR: Prof. A.S.J. Helberg

APRIL 2004

POTCHEFSTROOM

ABSTRACT

Communication companies are spending millions of Rands on installing optic fibre cables and links, with the purpose of increasing network bandwidth, reliability and stability. Several utilities, that combine power supply and telecommunication over the same servitudes, are confronted with quite a serious problem. The cables are being subjected to extreme electromagnetic (EM) force fields, which cause certain phenomena, damaging the fibres. The fibres that cause problems are usually installed in polluted areas or in salt rich air areas (e.g. along the coast).

The purpose of this study is to determine why and where Dry-Band arcing (DBA) occurs, or where it will be most likely to occur. The simulations done showed that DBA is not supposed to happen under normal circumstances, if the cables are correctly installed. There is therefore a certain set of additional phenomena and conditions required before DBA occurs.

UITTREKSEL

Kommunikasie maatskappye spandeer jaarliks miljoene rande op die installasie van optiese vesel kabels en verbindings. Dit word gedoen met die oog op die verbetering van netwerk stabiliteit, betroubaarheid en hoër bandwydte. Verskeie entiteite, wat kragtoevoer en telekommunikasie kombineer, word gekonfronteer met 'n ernstige probleem. Die kabels word onderwerp aan sterk elektromagnetiese velde, wat sekere verskynsels veroorsaak, wat die kabels beskadig. Die kabels wat probleme veroorsaak is gewoonlik die wat naby aan die kus en in hewig besoedelde omgewings voorkom.

Die doel van hierdie studie is om te bepaal hoekom en waar, droë-band vonking (Dry-Band Arcing) voorkom, of waar dit heel waarskynlik sal voorkom. Die simulasies wat gedoen is toon dat droë-band vonking nie veronderstel is om voor te kom onder normale omstandighede nie, dit is as die kabels korrek geïnstaleer is. Dus is daar 'n stel bykomende faktore nodig, voordat droë-band vonking sal plaasvind.

ACKNOWLEDGEMENTS

First and foremost I want to thank the Lord Jesus Christ for giving me the opportunity to broaden my knowledge and for the ability that he gave me to do so. Without Him I am nothing.

Secondly I want to thank my wife, Heleen, for all the support she gave me. Many times I became discouraged, but she just kept on encouraging me and helping me to stay focused and positive.

To my parents, you're the best. Many times you had to really shake me just so that I could realize that I can do it and I just have to carry on and finish what I started. Thank you for your inspiration, I really appreciate it.

I would also like to thank my supervisor, Prof. Albert Helberg for all the hours he put into my studies and for all the direction and ideas he supplied. As we all know, you won't get anywhere without the help of your supervisor.

I would also like to thank the staff at TRANSTEL for all their help and valuable contributions, especially to my supervisor at TRANSTEL, Michael Nuttall for his support and ideas and for putting me in touch with the right people.

All the staff at the University, especially Tannie Louise Cilliers for all the problem solving she had to do, thank you for your support, you are a great team.

SHALOM

Table of Contents

List of Abbreviations

ADSS	-	All Dielectric Self-Supporting
DBA	-	Dry-Band Arcing
EM(F)	-	Electromagnetic (Force Field)
FEA	-	Finite Element Analysis
LED	-	Light Emitting Diode
OFC	-	Optical Fibre Cable
OPGW	-	Optical Ground Wire
OVD	-	Outside Vapour Deposition
PE	-	Polyethylene
VCSEL	-	Vertical Cavity Surface Emitting Laser
2D	-	Two – Dimensional
3D	-	Three – Dimensional
DC	-	Direct Current
AC	-	Alternating Current

List of Symbols

$\boldsymbol{E}$	-	Electric Field (Vector)
$\boldsymbol{F}$	-	Force
q	-	Unit Charge
q_o	-	Positive test Charge
q_{enc}	-	Enclosed Charge
$\boldsymbol{\Phi}$	-	Electric Flux
$d\boldsymbol{A}$	-	Surface increment
A	-	Area
π	-	3.141593
k	-	Dielectric constant (8.85×10^{-12})
r	-	Radius
h	-	Height
ε_o	-	Permittivity Constant
λ	-	Current density
V	-	Electric Potential
v	-	Instantaneous voltage
ΔV	-	Potential Difference
U	-	Potential Energy
$d\boldsymbol{s}$	-	Line Segment
dq	-	Differential element of charge
dx	-	Differential element for line of charge
dW	-	Differential element of work required
∂x	-	Partial derivative of x
C	-	Capacitance
d	-	Distance between plates of a capacitor
C_{eq}	-	Total equivalent capacitance
L	-	Length
Xc	-	Capacitive reactance
f	-	frequency
I_{chg}	-	Charging Current
G	-	Conductance

List of Figures

CHAPTER 1 – PROBLEM STATEMENT

1. INTRODUCTION AND BACKGROUND

Communication companies are spending millions on installing optic fibre cables and links, with the purpose of increasing network bandwidth, reliability and stability. Several utilities, that combine power supply and telecommunication over the same servitudes, are confronted with quite a serious problem. The cables are being subjected to large electromagnetic (EM) force fields, which cause certain phenomena, damaging the fibres. The fibres that cause problems are usually installed in polluted areas or in salt rich air areas (e.g. along the coast).

It is believed that these polluted areas cause a conductive layer to form on top of and around the fibre cable. This conductive band, under the influence of EM force fields, causes a current to flow on and around the cable, causing problems such as dry-band arcing (DBA) and CORONA, which causes the fibre to be damaged to such an extent that it eventually burns off and causes a total collapse of that part of the network. The possible conditions leading to the formation of DBA will be investigated and possible solutions will be given.

P.D Pedrow, R.G. Olsen and K.S. Edwards of the School of Electrical Engineering and Computer Science at the Washington State University [5] have done some research concerning the phenomena of DBA and Corona. Optic fibre cable of the type Aerial Dielectric Self Supporting (ADSS) is known to have a limited installation lifetime in some environments when installed near high voltage transmission lines.

Dry band arcing as well as corona have been identified as a contributing factor in the short service life, for some of these cables. It has been hypothesized that contamination on the jacket of the optic fibre cable will be an indicator of cable installations that will have a short service life.

It is therefore very important to investigate the exact causes and environmental effects, contributing to these phenomena. An understanding of the causes will then

lead to cable design changes or different installation techniques in high mast environments. The following sections describe the two phenomena in more detail.

1.1. Corona

Corona is an electric discharge, caused by a very high electric field, which occurs at the tips of the wires supporting the optic fibre cable; the possible position of the corona is illustrated in figure 1. It can also be described as a low energy discharge occurring at the tips of the armour rods and is initiated by high electric fields and attachment hardware that have a small radius of curvature.

This electric discharge, figure 2, causes damage to the fibre cable in that the heat from the discharge causes the cable jacket to melt, and damage to the fibre core is experienced. This discharge also causes discoloration of the cable jacket [1]. This results in communication loss and high expenses due to extra labour costs and replacement of cable segments.

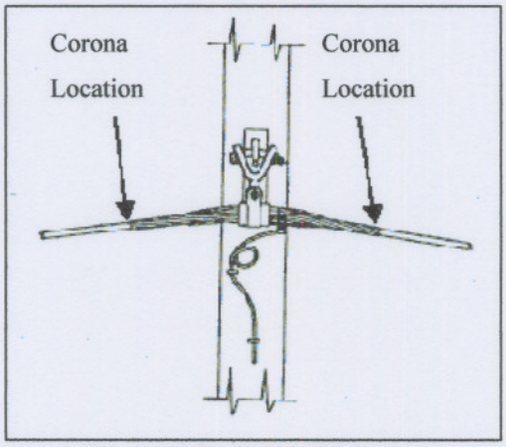

Figure 1: Location of Corona

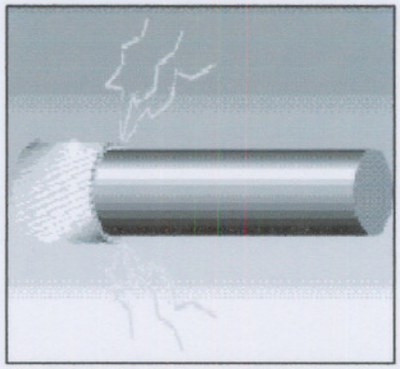

Figure 2: Corona Discharge

1.2. DBA (Dry-Band Arcing)

DBA usually occurs near the supporting wires. It is almost the same as corona, except that in this case the arc does not come from the wires, but it appears on the cable itself. This arc is also of much greater intensity than that of corona, and some cables have even ignited, causing a total collapse of the line [2]. Chapter 3 illustrates some of the damage that has been reported.

Research [3] has found that charge residing much further out in the span cannot contribute to the earth-leakage current, because the time taken to drain it is longer than the interval between polarity inversions. So generally there are no currents flowing over most of the central portion of the span, but they grow in magnitude nearer the span ends and reach a maximum at the support, where a wet cable will tend to dry preferentially, forming dry bands. A short length of dry cable represents very high resistive impedance to the leakage currents, which are prevented from flowing.

When a dry band first forms, the potential on the support side will fall to zero, whereas that on the span side will rise rapidly. If the resultant axial electric field in the dry band exceeds the breakdown strength of air, then flashover will occur, figure 3, and low-current arcing will take place. It is this process that causes the damage [3].

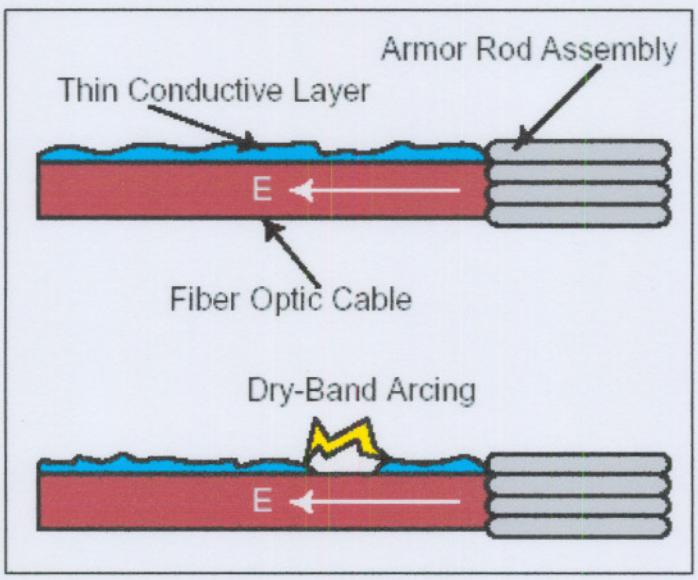

Figure 3: Dry-band arcing

2. PHENOMENA

DBA and Corona are the biggest contributors to cable destruction. Since the arc voltage is quite severe, DBA and Corona cause severe damage and poses a high risk to the stability and reliability of the network. The purpose of this research will be to study the effect of DBA and the factors leading to the occurrence of DBA on ADSS optic fibre cables installed on railway lines. A simulation model will be used to help to determine the extent of electric fields leading to DBA.

3. RESEARCH QUESTIONS

The following points need to be answered and guidelines need to be given, to identify the possibility of these phenomena before installation of optic fibre cables. There are several factors to be considered.

- Where should the OFC be installed, meaning at what distance from the feeder and at what distance from the mast itself?
- What type of insulation is to be used and should the cable be insulated or not?
- What is the magnitude of the potential needed in order for DBA to occur?
- How much does the pollution on the cable contribute to the occurrence of DBA?
- What materials/conditions are needed to enable DBA to occur?
- Which factors need to be considered for a solution to DBA?

4. ORGANIZATION OF STUDY

The study to be performed will include the following phases/stages.

- In Chapter 2, the result of a literature survey is presented which covers the necessary theory needed to understand the occurrence of Dry Band Arcing.
- In Chapter 3, a qualitative research was done using the field observations and known data taken from the relevant entity. This information was considered prior to the design of the simulation model. Chapter 3 also shows physical evidence of the destructive power of DBA.
- In Chapter 4, a quantitative study was done using an article that was used to predict the desired placement of an ADSS cable in a double three-phase system. The same model was fed into the software package to be used on the

simulation model, in order to test and see whether the software model would give the same results as that obtained in the article. Differences where noted and explained.

- In Chapter 5, the model designed from the consideration of field observations obtained in chapter 3 was simulated using the software package as validated in Chapter 4. Various scenarios was looked at and explained. Also in Chapter 5, the same model was used in a mathematical program to see what the current distribution on the cable would be under various conditions, such as cable sag, distance from the mast and so forth.
- In Chapter 6 the results are explained and conclusions are drawn. Further ideas for future work are also presented.
- The appendices gives the code used in the mathematical program.

CHAPTER 2 – LITERATURE SURVEY

1. INTRODUCTION

Fibre optics has found many uses in a variety of industries, but nowhere has it had such a profound effect as it has in telecommunications. Originally considered by many to be a prohibitively expensive technology in search of practical applications, it has now transformed the very infrastructure of private telephone operators (PTO's). It has achieved this because of two very simple advantages it has over copper: (1) the ability to transmit data at higher transmission rates and with lower losses and, (2) the ability to do this at lower error rates. Copper cables are being replaced with smaller fibre cables having increased capacity. The basic optic-fibre cable consists of a number of strands of optically pure **glass** as thin as a human hair that carries digital information over long distances [4].

If you look closely at a single optical fibre, figure 4, you will see that it consists of the following layers:

- **Core** - Thin glass centre of the fibre where the light travels,
- **Cladding** - Outer optical material surrounding the core that reflects the light back into the core,
- **Buffer coating** - Plastic coating that protects the fibre from damage and moisture.

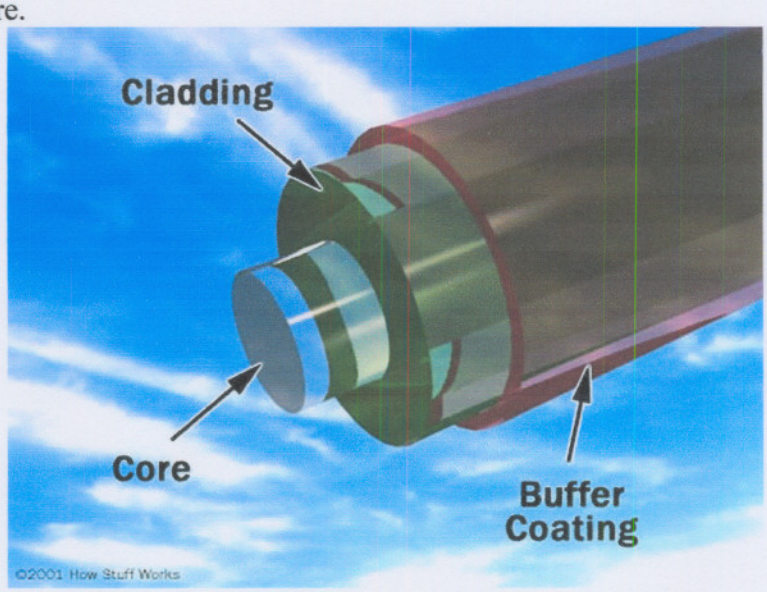

Figure 4: Parts of a single optical fibre

Typically 6-fibres are placed within a tube and then these tubes are placed inside a cable, therefore fibre counts are given in groups of six, e.g. 12, 24, etc. depending on how many fibres you need. Commonly over long distance the fibre count is low, about six-fibres and over short distances, such as in suburban areas, the fibre count is high, about 96-fibres or more. The cable's outer covering, called a jacket, protects this bundle. It is mainly and firstly this jacket that is being damaged by DBA, exposing the fibres themselves and then the total cable collapses as soon as all the fibres have been burned off. Some further reading can be found in [18] – [23].

2. INSTALLATION METHODS

Utilities are installing optic fibre cables on high voltage transmission lines in three different ways or three basic designs. These are *Optical ground Wire* (OPGW), *Wrap-type*, and *All dielectric self-supporting* (ADSS) configurations. The following sub-sections will discuss some of the advantages and disadvantages of each of the installation topologies.

2.1. OPGW (Optical ground wire)

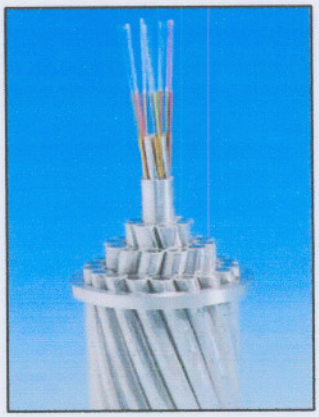

Figure 5: OPGW cable

OPGW is a composite wire, figure 5, which serves as a conventional overhead ground wire, with the added benefit of providing high-capacity and reliable fibre optic communications to service current and future needs.

OPGW has the following advantages.

- It is protected against lightning damage.
- It displays superior performance.

- The optical fibre itself is an insulator and protects against power transmission line and lightning induction, external noise and cross talk.
- Optical fibres are of low transmission loss, allowing long distance transmission.
- Wide-bandwidth transmission capacity of the optical fibres, allows high-speed transmission of large volumes of information through a single fibre. The small size and light-weight of the optical fibres, makes OPGW as compact in size and light in weight as conventional ground wire.

Figure 6 shows 3 different types of OPGW cables. Firstly the spacer type, then two types of stainless tube, one with a big core (top right) and one with smaller cores (bottom) carrying the fibre cables.

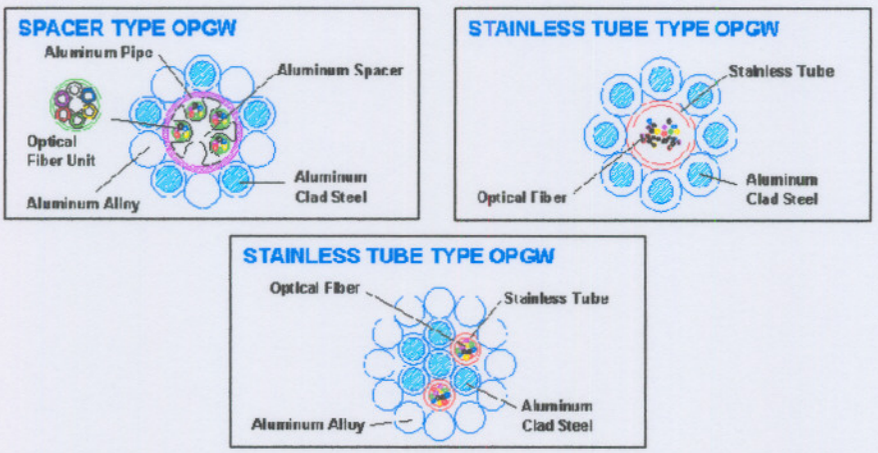

Figure 6: 3 Types of OPGW cable: Spacer type, and two types of Stainless tube

OPGW has the following disadvantages.

- Installation of OPGW requires long-term outage of the power lines, since it cannot be "hot" installed.
- It is also very expensive, about 8 times more so than ADSS.

2.2. Wrap-type

This type of cable can be wound around the shield wires and, in some instances, around energized conductors.

Advantages of wrap-type cables:

- They can be "hot" installed and
- Their low cost. Wrap-type cable is the cheapest cable available.

It does however, have a few disadvantages:

- Hot-line (while the carrier wire is still connected and power is flowing through it) installation of the cable is very difficult.
- Operation problems have however been observed such as vultures sitting on the cables causing it to break off, and birds sharpening their beaks against the cable, cutting the fibres.

2.3. ADSS (All Dielectric Self Supporting)

This cable can be mounted at various locations, typically 1 to 10 meters, depending on the voltage, below the phase (main) conductor/s and it is the cable most widely used.

ADSS has the following advantages.

- ADSS cables are much cheaper than OPGW cables but costs about twice that of wrap type cables, due to the Kevlar used in the sheath.
- It can have a higher fibre count than Wrap-type cables, giving it higher bandwidth and capacity.
- It can be installed on towers not designed for shielded wires, which means that you don't need to erect a support structure just for the optic cable. Available structures can therefore be utilised, making it more cost and labour effective.
- It is also suitable for "hot line" installation, meaning that the cable can be installed while the carrier wire is still connected.
- The sheath is made up of polyethylene (PE), high-density polyethylene and recently Anti-tracking sheaths (High resistance against DBA due to better heat and degradation resistance).

The ***disadvantages*** of ADSS are however of importance and will be researched in the rest of the study.

- Utilities have reported some cable failure due to high electric fields which causes:
    - Corona problems, and
    - Dry-band arcing, especially in polluted areas.

3. DEFINITIONS

In this section, some basic definitions are given. Where necessary, the definitions are elaborated on, otherwise it is taken that the reader has the necessary understanding and insight of the theory. The information was taken from [6].

3.1. Electric field

- An electric field **E** at a point *P* due to a charged object is defined as:

$$\mathbf{E} = \frac{\mathbf{F}}{q_0} \tag{2.1}$$

- with magnitude:

$$E = \frac{F}{q_0} \tag{2.2}$$

- and the direction of **E** is that of the force **F** that acts on the *positive* test charge.

3.2. Electric flux through a Gaussian surface

The electric flux Φ through a Gaussian surface is proportional to the net number of electric field lines passing through that surface.

$$\Phi = \oint \mathbf{E} \cdot d\mathbf{A} \tag{2.3}$$

Its SI unit is the Newton - square-meter per coulomb $(N \cdot m^2 / C)$.

3.3. Electric potential

It is necessary to know what the electric potential is between the fibre optic cable and the feeder cable. Although the effect of capacitance also plays a role, to be discussed in a later section, we take a look at the fundamental definition of electric potential which states that: The potential energy per unit charge at a point in an electric field is called the electric potential V at that point:

$$V = \frac{U}{q} \tag{2.4}$$

The electric potential difference ΔV between any two points i and f in an electric field is equal to the difference in potential energy per unit charge between the two points:

$$\Delta V = V_f - V_i = \frac{U_f}{q} - \frac{U_i}{q} = \frac{\Delta U}{q} = \frac{-W}{q} \tag{2.5}$$

The potential difference $V_f - V_i$ between any two points i and f in an electric field is equal to the negative of the line integral of $\mathbf{E} \cdot d\mathbf{s}$ from i to f:

$$V_f - V_i = -\int_i^f \mathbf{E} \cdot d\mathbf{s} \tag{2.6}$$

Thus, by integrating the path between points i and f one can calculate the electric potential between those two points.

3.3.1. Potential due to a continuous charge distribution

We now want to calculate the potential at a point P due to a continuous charge distribution. For a continuous charge distribution q, use a differential element of charge dq to determine the potential dV at point P due to dq, and then integrate over the entire charge distribution. With

$$dV = \frac{1}{4\pi\varepsilon_0}\frac{dq}{r} \tag{2.7a}$$

and r the distance between P and dq, the potential V at point P due to dq is given by:

$$V = \int dV = \frac{1}{4\pi\varepsilon_0}\int\frac{dq}{r} \tag{2.7b}$$

The integral is to be taken over the entire charge distribution. (Note that there are no vector components).

3.3.2. A Line of Charge

In figure 7, a thin non-conducting rod of length L has a positive charge of uniform linear density λ. We want to determine the potential V at point P due to the rod, a perpendicular distance d from the left end of the rod.

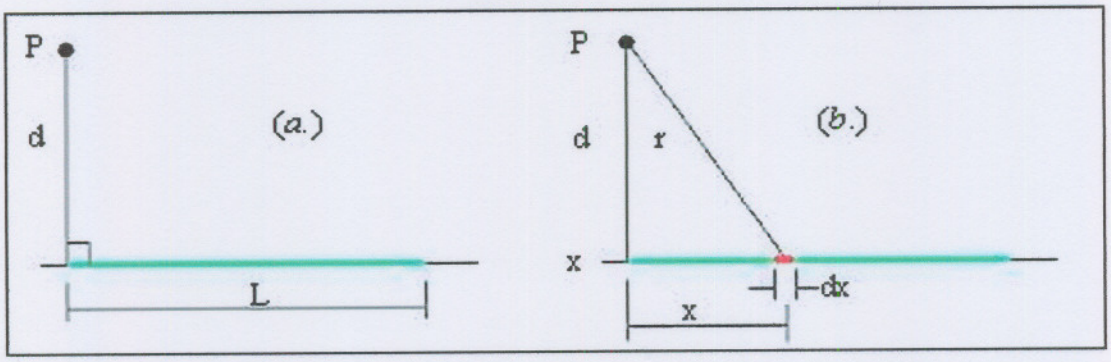

Figure 7: (a) A thin uniformly charged rod produces an electric potential *V* at point *P*. (b) An element of charge produces a differential potential *dV* at *P*.

Consider a differential element dx of the rod as shown in figure 7*b*. This (or any other) element of the rod has a differential charge of

$$dq = \lambda dx \tag{2.8}$$

This differential produces a potential dV at point P, which is a distance $r = (x^2 + d^2)^{1/2}$ from the element. Treating the element as a point charge, using $dV = \frac{1}{4\pi\varepsilon_0}\frac{dq}{r}$ to write the potential dV as

$$dV = \frac{1}{4\pi\varepsilon_0}\frac{dq}{r} = \frac{1}{4\pi\varepsilon_0}\frac{\lambda dx}{(x^2 + d^2)^{1/2}} \tag{2.9}$$

Since the charge on the rod is positive, and assuming $V = 0$ at infinity, dV in Equation (2.9) must be positive.

The total potential V produced by the rod at point P by integrating Equation (2.9) along the length of the rod, from $x = 0$ to $x = L$, gives:

$$\begin{aligned} V = \int dV &= \int_0^L \frac{1}{4\pi\varepsilon_0}\frac{\lambda}{(x^2 + d^2)^{1/2}} dx \\ &= \frac{\lambda}{4\pi\varepsilon_0}\int_0^L \frac{dx}{(x^2 + d^2)^{1/2}} \\ &= \frac{\lambda}{4\pi\varepsilon_0}\Big[\ln(x + (x^2 + d^2)^{1/2}\Big]_0^L \\ &= \frac{\lambda}{4\pi\varepsilon_0}\Big[\ln\Big[L + (L^2 + d^2)^{1/2}\Big] - \ln d\Big]. \end{aligned}$$

The result can be simplified by using the relation ln A – ln B = ln (A/B). This gives:

$$V = \frac{\lambda}{4\pi\varepsilon_0} \ln\left[\frac{L + (L^2 + d^2)^{1/2}}{d}\right]. \tag{2.10}$$

3.3.3. Calculating the field from the potential

Suppose a positive test charge q_o moves through a displacement ***ds*** from one equipotential surface to the adjacent surface, figure 8. The work done by the electric field on the test charge during the move is $-q_o\, dV$. From figure 8 it can also be seen that the work done by the electric field can be written as $(q_0\mathbf{E})\cdot d\mathbf{s}$ or $q_0 E(\cos\theta)\, ds$. Equating these two expressions for the work yields

$$-q_0 dV = q_0 E(\cos\theta) ds$$

or

$$E\cos\theta = -\frac{dV}{ds}. \tag{2.11}$$

Since $E\ cos\ \theta$ is the component of **E** in the direction of ***ds***, Equation (2.11) becomes

$$E_s = -\frac{\partial V}{\partial s}. \tag{2.12}$$

A subscript has been added to E and the partial derivative symbols have been added to emphasise that Equation (2.12) involves only the variation of V along a specified axis (here called the s-axis) and only the component of **E** along that axis. In words Equation (2.12) states: *The component of* **E** *in any direction is the negative of the rate of change of the electric potential with distance in that direction.*

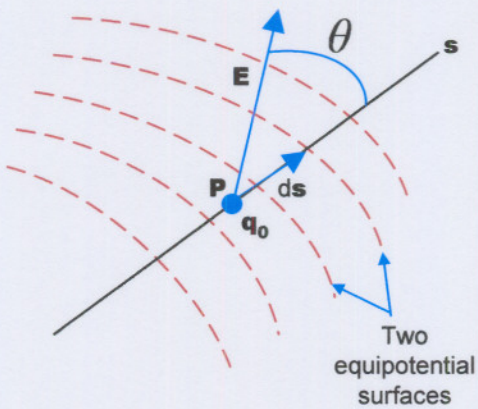

Figure 8: A test charge moving from one equipotential surface to another.

Likewise: If V is known for all points in the region around a charge distribution, that is, if the function $V(x,y,z)$ is known, the components of **E** at any point can be found by taking the partial derivatives:

$$E_x = -\frac{\partial V}{\partial x}; \quad E_y = -\frac{\partial V}{\partial y}; \quad E_z = -\frac{\partial V}{\partial z} \tag{2.13}$$

For a simple uniform field 2.13 reduces to:

$$E = -\frac{\Delta V}{\Delta s} \tag{2.14}$$

where s is perpendicular to an equipotential surface. The electric field is zero in any direction tangent to an equipotential surface.

3.4. Capacitance

According to research done by [2], [3] and [14] there exists a capacitive coupling between the 25kV Feeder and the "earthed" optical fibre cable. This capacitance leads to the build-up of a potential voltage between the lines and causes an leakage current to flow on the fibre cable. This leads to the occurrence of DBA.

A capacitor basically consists of two isolated conductors of arbitrary shape, called plates. A capacitor can be viewed as two parallel plates of area A that is separated by a distance d. When a capacitor is charged, its plates have equal but opposite charges of $+q$ and $-q$. However, the charge of a capacitor is being referred to as being q, the absolute value of these charges on the capacitor.

The charge q is proportional to the potential difference V, that is:

$$q = CV. \tag{2.15}$$

The proportionality constant C is called the capacitance of the capacitor. Its value depends only on the geometry of the plates and not on their charge or potential difference.

3.4.1. Calculating the capacitance

To calculate the capacitance of a capacitor one must:

a.) Calculate the electric field

b.) Calculate the potential difference

a.) Calculating the electric field

The electric field **E** between the plates of a capacitor is related to the charge q on a plate by Gauss' law:

$$\varepsilon_0 \oint \mathbf{E} \cdot d\mathbf{A} = q \tag{2.16}$$

Here q is the charge enclosed by a Gaussian surface, and $\oint \mathbf{E} \cdot d\mathbf{A}$ is the net electric flux through that surface. In all cases to be considered, the Gaussian surface will be such that whenever electric flux passes through it, **E** will have a magnitude E and the vectors **E** and $d\mathbf{A}$ will be parallel. Equation (2.16) then reduces to

$$q = \varepsilon_0 EA \tag{2.17}$$

in which A is the area of that part of the Gaussian surface through which flux passes.

b.) Calculating the Potential difference

The potential difference between the two plates of a capacitor is related to the electric field **E** by

$$V_f - V_i = \int_i^f \mathbf{E} \cdot d\mathbf{s} \tag{2.18}$$

in which the integral is to be evaluated along any path that starts on one plate and ends on the other. It is advisable to choose a path that follows an electric field line from the positive plate to the negative plate. For such a path, the vectors **E** and $d\mathbf{s}$ will always point in the same direction, so the dot product $\mathbf{E} \cdot d\mathbf{s}$ will be equal to the positive quantity $E\,ds$. Equation (2.18) then tells us that the quantity $V_f - V_i$ will always be negative. Since the desired result is V, the absolute value of the potential difference between the plates, set $V_f - V_i = -V$. Then, Equation (2.18) becomes:

$$V = \int_-^+ E\,ds \tag{2.19}$$

in which the + and – is a reminder that the path of integration starts on the positive plate and ends on the negative plate.

Now it is time to calculate the capacitance of a parallel-plate capacitor. Assume, as figure 9 suggests, that the plates of the parallel-plate capacitor are so large and so close together that the fringing of the electric field at the edges

of the plate can be neglected, taking **E** to be constant throughout the volume between the plates.

Figure 9: Charged parallel-plate capacitor.

Drawing a Gaussian surface that encloses just the charge q on the positive plate, as in figure 9, Equation (2.17) can be used with

$$q = \varepsilon_0 EA \tag{2.20}$$

where A is the area of the plate. Equation (2.20) yields:

$$V = \int_+ E\,ds = E\int_0^d ds = Ed. \tag{2.21}$$

In Equation (2.21), E can be placed outside the integral because it is a constant; the second integral then is simply the plate separation d.

Substituting q from Equation (2.20) and V from Equation (2.21) into the relation $q = CV$, gives

$$C = \frac{\varepsilon_0 A}{d} \tag{2.22}$$

which is the equation describing a parallel-plate capacitor. Thus the capacitance depends only on geometrical factors, namely, the plate area A and the plate separation d.

3.4.2. Calculations:

Calculating the total capacitance can be done with use of the following formulas:

a.) Capacitors in parallel:

$$C_{eq} = \sum_{j=1}^{n} C_j. \tag{2.23}$$

b.) Capacitors in series:

$$\frac{1}{C_{eq}} = \sum_{j=1}^{n} \frac{1}{C_j}. \tag{2.24}$$

3.5. Storing energy in an electric field

The work required to charge a capacitor, is stored in the form of electric potential energy U in the electric field between the plates.

Suppose that, at a given instant, a charge q' has been transferred from one plate to the other plate. The potential difference V' between the plates at that instant will be q'/C, if an extra increment of charge dq' in then transferred, the increment of work required will be, from Equation (2.8),

$$dW = V'dq' = \frac{q'}{C}dq'.$$

The work required to bring the total capacitor charge up to a final value q is

$$W = \int dW = \frac{1}{C}\int_0^q q'dq' = \frac{q^2}{2C}.$$

This work is stored as potential energy U in the capacitor, so that

$$U = \frac{q^2}{2C}. \tag{2.25}$$

From $q = CV$, this can also be written as

$$U = \frac{1}{2}CV^2. \tag{2.26}$$

Equations (2.25) and (2.26) hold no matter what the geometry of the capacitor is.

3.5.1. Energy Density

In a parallel-plate capacitor, neglecting fringing, the electric field has the same value for all points between the plates. Thus the energy density u, that is, the potential energy per unit volume between the plates, should also be uniform. We can find u by dividing the total potential energy by the volume Ad of the space between the plates. Using Equation (2.26),

$$u = \frac{U}{Ad} = \frac{CV^2}{2Ad} \tag{2.27}$$

With $C = \varepsilon_0 A/d$, this result becomes

$$u = \frac{1}{2}\varepsilon_0\left(\frac{V}{d}\right)^2 \tag{2.28}$$

But from Equation (2.14), V/d equals the dielectric field magnitude, so

$$u = \frac{1}{2}\varepsilon_0 E^2. \tag{2.29}$$

3.6. Capacitance of a transmission line

Capacitance of a transmission line is the result of the potential difference between the conductors; it causes them to be charged in the same manner as the plates of a capacitor when there is a potential difference between them.

The capacitance between the conductors is the charge per unit of potential difference. Capacitance between parallel conductors is a constant depending on the size and spacing of conductors.

For power lines less than 80 km long, the effect of capacitance is slight and is usually neglected. For longer lines of higher voltage, capacitance becomes increasingly important [7].

The flow of charge is current, and the current caused by the alternate charging and discharging of a line due to an alternating voltage is called the *charging current* of the line. Charging current flows in a transmission line even when it is open-circuited. It affects the voltage drop along the line as well as the efficiency and power factor of the line and the stability of the system of which the line is a part.

The total electric field emanating from a conductor is numerically equal to the number of coulombs of charge on the conductor. Electric flux density is the electric flux per square meter and is measured in coulombs per square meter.

If a long straight cylindrical conductor lies in a uniform medium such as air, has a uniform charge throughout its length, and is isolated from other charges so that the charge is uniformly distributed around its periphery, then ***the flux is radial.***

All points, equidistance from such a conductor, are points of equipotential and have the same electric flux density. The electric flux density at x meters away from the conductor can be computed by imagining a cylindrical surface concentric with the conductor and x meters in radius. The ***electric flux density*** is

$$D = \frac{q}{2\pi x} \quad \text{C/m}^2 \tag{2.30}$$

where q is the charge on the conductor in coulombs per meter of length and x is the distance in meters from the conductor to the point where the electric flux density is computed.

The electric field density, or the negative of the potential gradient, is equal to the electric flux density divided by the permittivity of the medium. Therefore, the ***electric field intensity*** is:

$$E = \frac{q}{2\pi xk} \quad V/m \tag{2.31}$$

Where k_0 = 8.85 x 10^{-12} F/m is the permittivity SI unit for free space. Relative permittivity k_r is the ratio of the actual permittivity k of a material to the permittivity of free space. Thus, $k_r = k/k_o$. For dry air k_r is 1.00054 and is assumed equal to 1.0 in calculations for overhead lines.

The instantaneous voltage drop between two points in volts is numerically equal to the work in joule per coulomb necessary to move a coulomb of charge between the two points.

$$v_{12} = \int_{D_1}^{D_2} E dx = \int_{D_1}^{D_2} \frac{q}{2\pi kx} dx = \frac{q}{2\pi k} \ln \frac{D_2}{D_1} \quad \text{V} \tag{2.32}$$

3.7. Capacitance of a two-wire line

Capacitance between the two conductors of a two-wire line, figure 10, was defined as the charge on the conductors per unit of potential difference between them. In the form of an equation, capacitance per unit length of the line is

$$C = \frac{q}{v} \quad \text{F/m} \tag{2.33}$$

where q is the charge of the line in coulombs per meter and v is the potential difference between the conductors in volts. Therefore the voltage between the two conductors with radius r_a and r_b can be written as follows

$$V_{ab} = \frac{q_a}{2\pi k} \ln \frac{D^2}{r_a r_b} \quad \text{V} \tag{2.34}$$

with D the distance between q_a and q_b.

The capacitance between the conductors is

$$C_{ab} = \frac{q_a}{V_{ab}} = \frac{2\pi k}{\ln(D^2 / r_a r_b)} \quad \text{F/m} \tag{2.35}$$

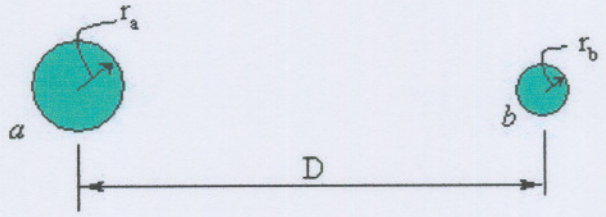

Figure 10: Capacitance between a two-wire line

If $r_a = r_b = r$, then

$$C_{ab} = \frac{\pi k}{\ln(D/r)} \quad \text{F/m} \tag{2.36}$$

Equation 2.34 gives the capacitance between the conductors of a two-wire line. Sometimes it is desirable to know the capacitance between one of the conductors and a neutral point between them. For instance, if a transformer having a grounded centre tap supplies the line, the potential difference between each conductor and the ground is half the potential difference between the two conductors. The *capacitance to ground,* or *capacitance to neutral*, is the charge on a conductor per unit of potential difference between the conductor and ground. Thus, the capacitance to neutral for the two-wire line is *twice* the *line-to-line capacitance* (capacitance between conductors).

If the line-to-line capacitance is considered to be composed of two equal capacitances in series, the voltage across the line divides equally between them and their junction is at the ground potential. Thus, the capacitance to neutral is that of one of the two equal series capacitances, or twice the line-to-line capacitance. Therefore,

$$C_n = C_{an} = C_{bn} = \frac{2\pi k}{\ln(D/r)} \quad \text{F/m to neutral.} \tag{2.37}$$

After the capacitance to neutral has been found, the capacitive reactance existing between one conductor and neutral for relative permittivity $k_r = 1$ is found by using the expression for C given in Eq. (2.35) to yield

$$X_C = \frac{1}{2\pi fC} = \frac{2.862}{f} \times 10^9 \ln\frac{D}{r} \quad \Omega\text{.m to neutral.} \tag{2.38}$$

Since C in Eq. (2.36) is in farads per meter, the proper units for X_C must be ohm-meters. Eq. (2.36) expresses the reactance from line to neutral for 1 m of line. Since capacitive reactance is in parallel along the line, X_C, in ohm-meters, it must be *divided* by the length of the line in meters to obtain the capacitive reactance in ohms to neutral for the entire length of the line.

The term *charging current* is applied to the current associated with the capacitance of a line. For a *single-phase* circuit, the charging current is the product of the line-to-line voltage and the line-to-line susceptance, or, as a phasor,

$$I_{\text{chg}} = j\omega C_{ab} V_{ab} \quad \text{A/m} \tag{2.39}$$

3.8. Conclusion

Several types of fibre optic cable installation methods exist, in this case-study the ADSS method is observed and the problems surrounding the installation of this cable in a railway environment is considered. Since the electric field generated by the power supply on these railway systems is the main contributor to DBA damage, two approaches will be followed to determine how, and to what extent the electromagnetic fields on the cable cause the occurrence of DBA: Firstly using a 2D modelling package the electric fields around the cables will be examined and from this, recommendations will be made as to where and how to install the fibre cables. Secondly a more mathematical approach will be used to create profiles, using a mathematical program, to indicate what the field strengths on the cable is along the span and close to the masts, again recommendations will be made as to where and how the fibre cables are to be installed.

Both methods should give similar results, and if not, possible explanations will be given.

CHAPTER 3 – FIELD OBSERVATIONS LEADING TO SIMULATION MODEL

1. INTRODUCTION

During my two years of study I had the privilege of joining the quality assurance department from TRANSTEL on an investigation trip to Richards Bay, South Africa. This chapter shows some of the destroyed cables and explains where and under what conditions DBA has been experienced.

Figure 11 shows examples of some cables that have been severely damaged by DBA. The problems occur on the OFC installed about 1.5m underneath a single-phase feeder cable carrying 25kV at 50Hz.

Figure 11: DBA damage on OFC cables

Severe cases have also occurred where the cable has actually been completely burned off (figure 12) and fell to the ground. The cable jackets of some of the cables have even ignited in some instances.

As one can see from figure 12, this specific cable has experienced severe DBA and needs to be replaced. Quite a number of such cases have occurred during the past few years particularly in an area called ELubana. The two root causes are:

- The presence of medium/high electric fields and
- The development, over time, of erratic (not yet predictable) pollution deposits that become sufficiently conductive under certain conditions and cycles to cause electrical currents in some sectors. The nature of these

currents is such that it physically destroys the cable sheaths and eventually the glass fibres themselves [8].

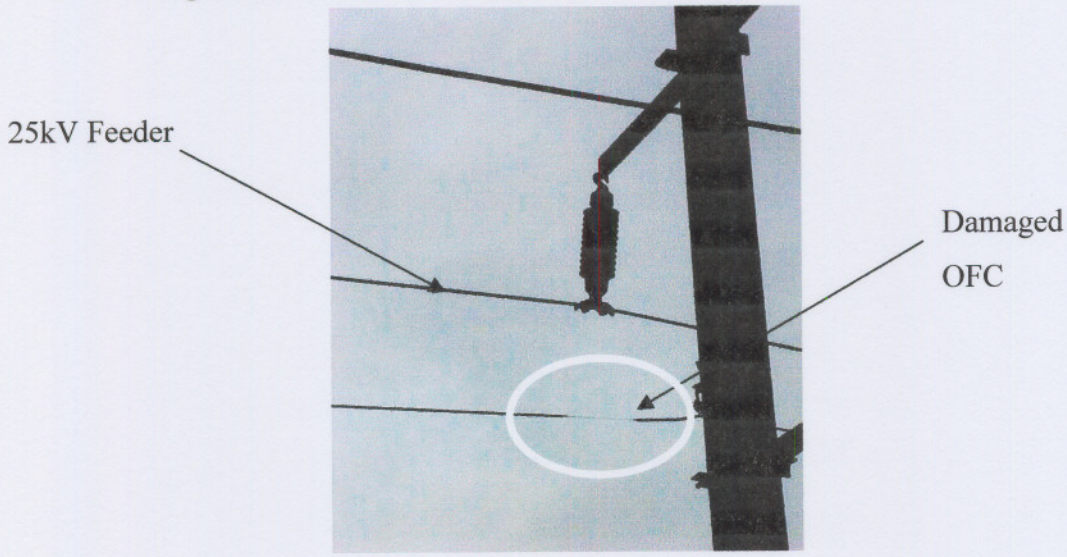

Figure 12: OFC cable damage on mast-pole, about to collapse

2. FIELD OBSERVATIONS

This section shows some of the photos taken of DBA activity along certain routes where DBA has mainly occurred. Currently a test section, about 500m in length, figure 13, is under observation and the cables used are of the type called ANTI-TRACKING. This type of cable is said to have a higher resistance to electrical tracking (arcing), currents on the cable sheath, than the normal polyethylene (PE) cables.

Figure 13: Test section at ELubana

This specific test section has been under observation for about 20 months and so far no signs of DBA have been observed. The previously installed PE cables had a service life of approximately 3 months. The fact that there are three cables installed in close proximity to each other does not seem to have any effect in the occurrence of DBA. The bobbin is used in order to insulate the cable from the mast since regulations state that all cables connected to the masts should be isolated and all masts should be earthed.

One problem that was observed during an inspection late August 2003, was a bobbin that had a hole burned right through it, figure 14. The OFC cable is connected to the mast with the use of these bobbins, which is plastic and supposed to be non-conductive. The support wires are wrapped around the bobbin and then around the cable with the use of a double wire.

Figure 14: Damaged bobbin at test section

It is speculated that the split-pin that holds the bobbin in place was bent at such an angle that the distance between the pin and support wire was short enough to cause extensive potential build-up between the split-pin and the wire wrapped around the OFC. This potential must have reached the breakdown value of air and also caused dielectric breakdown of the dielectric material of the bobbin, which resulted in an arc, which burned with such intensity over a period of time that a hole was burned right through the bobbin up to the suspension wires.

These types of bobbins have also been found to be hydrophilic, which means they have a tendency to retain water. In other words, when it is dry these bobbins are perfect insulators, however, when it starts raining or there is an excessive amount of moisture in the air, these bobbins lose some of their insulation properties and a small

current will be able to flow from the cable to the earthed mast. This current that is being drawn might in some cases be so high that when the wet layer on or around the OFC dries, this current that wants to flow causes a potential build-up and DBA occurs as explained in Chapter 1, Section 1.2.

Figures 15,16 and 17 show some more examples of cable jacket destruction and deterioration.

It is interesting to note that in all the cases DBA occurred close to the support wires. This is said to be due to the sharp pointed endings of the support wires that are being used to anchor the cables to the masts. This also causes a much steeper gradient for the potential and thus the higher intensity of Corona and DBA occurrences.

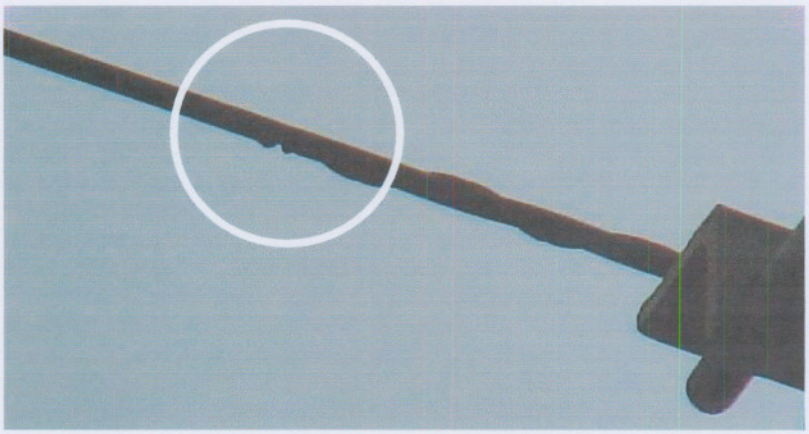

Figure 15: Photo of DBA damage

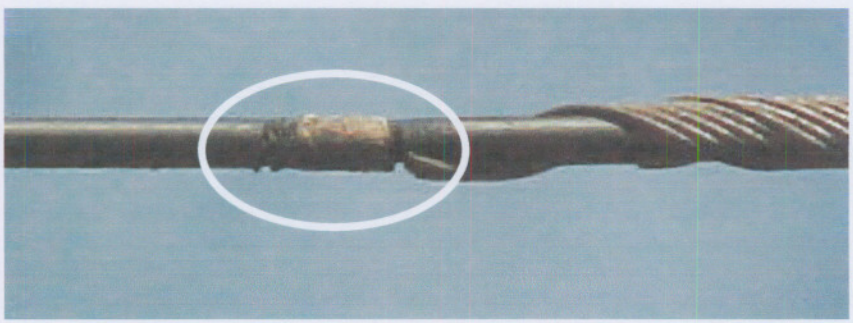

Figure 16: Photo of DBA damage

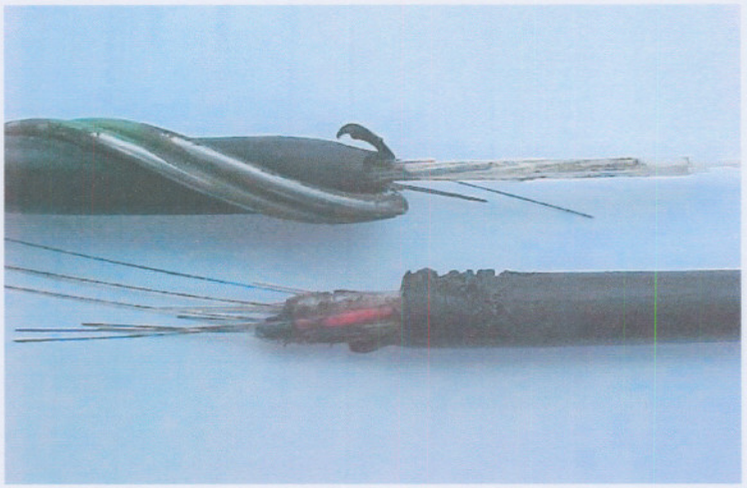

Figure 17: Photo of DBA damage, cable completely destroyed

3. CONCLUSION

This section has shown some of the physical damage done to OFC due to DBA. The exact causes and conditions needed for DBA to occur are not yet known. There are a lot of speculation but very little proof. The following chapters will be used to try and explain, theoretically, how, when and where DBA can be expected to occur and what could be done to prevent it. Note that the fibre cables are isolated from the masts with the use of the bobbins. This leads to very long, un-earthed spans, more on this later.

CHAPTER 4 – VALIDATION OF APPROACH

1. INTRODUCTION

This chapter will be used to determine whether or not the software package, MAXWELL 2D Field Simulator SV Version 9 [9], a software package for analysing electromagnetic fields in cross-sections of structures, to be used in the simulation process is suitable for the purpose of this study. Maxwell SV uses finite element analysis (FEA) to solve two-dimensional (2D) electromagnetic problems. A more detailed explanation of the package is given in chapter 5.

The article by C.N. Carter & M.A. Waldron [10] will be used as a basis to validate accuracy of the solution process of the MAXWELL software. The purpose for this is not only to see if the MAXWELL program can duplicate the results but its also to see whether or not I understand the workings of the package to such an extend that the model can be accurately simulated. Unfortunately the software package used by [10] is not mentioned. The article by [10] modelled a double 3-phase system and altered the relative phasing of the conductors. They used five different phase configurations as depicted in figure 18. Similar phased conductors of the two circuits are joined with a line as follows:

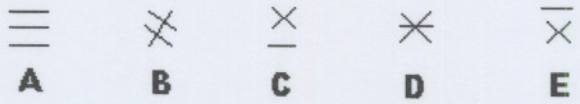

Figure 18: Relative phases used in simulation

Phase configuration A, for instance, would look as follows, figure 19.

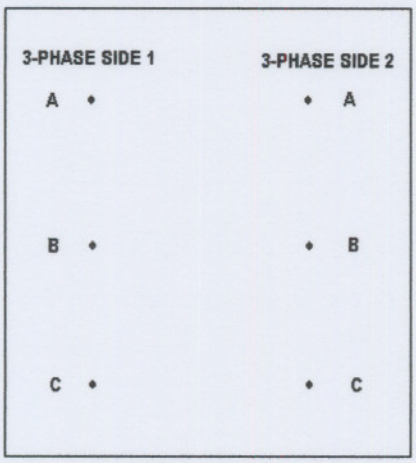

Figure 19: Double Three-Phase System with Phase Configuration A

In the next few sections each of these phases will be reviewed. The result taken from the article will be compared to that obtained by the use of the MAXWELL program. The areas of interest will be compared and conclusions will be drawn.

2. RESULTS

2.1. Phase configuration A

The first phase configuration is that depicted in figure 18.A. All the phases are exactly adjacent to their corresponding phase, e.g. 0^0 – 0^0, 120^0 – 120^0, 240^0 – 240^0. Figure 20 shows firstly the required result taken from [10], and secondly the acquired result obtained with the use of MAXWELL.

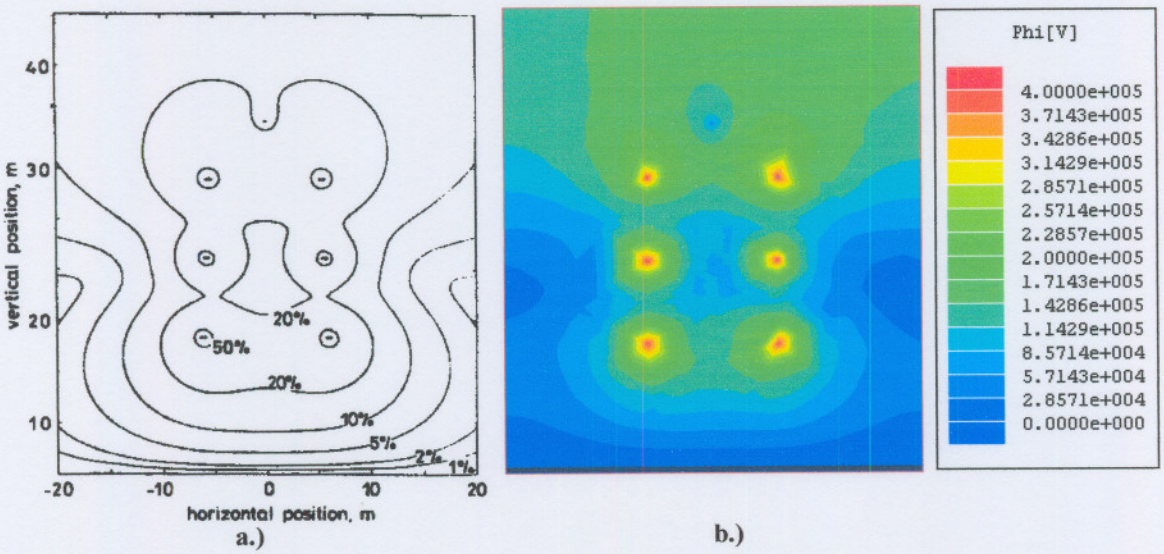

Figure 20: Results for phase configuration A

From figure 20 we see the following:

- The 50% area depicted in figure 20.a. has a value of 200kV, when one looks at figure 20.b. one can see that it correlates with the green area, which has a value of between 200kV and 228kV.
- The 20% region depicted in figure 20.a. corresponds to the light blue region in figure 20.b. which has a value of more or less 85.7kV – 114.2kV. Now 20% of 400kV gives 80kV, which is close to that acquired from MAXWELL.

- The 1% area in figure 20.a. has a value of about 4kV, just below that it is expected to drop to almost 0V, this is also displayed in figure 20.b.

From the above results it is apparent that the 20% region depicted in figure 20.a. coincides more or less with that depicted in figure 20.b obtained with MAXWELL. Although the values are not exactly the same it can be seen that the preferred location for the ADSS cable to be installed is at the same place. Figure 19.b does however show a deviation from the original graph at the top; this deviation might be due to the solution algorithm.

2.2. Phase configuration B

The second simulation was conducted using the phase configuration depicted in figure 18.B: $0^0 - 240^0$, $120^0 - 0^0$, $240^0 - 120^0$. Figure 21 shows the result.

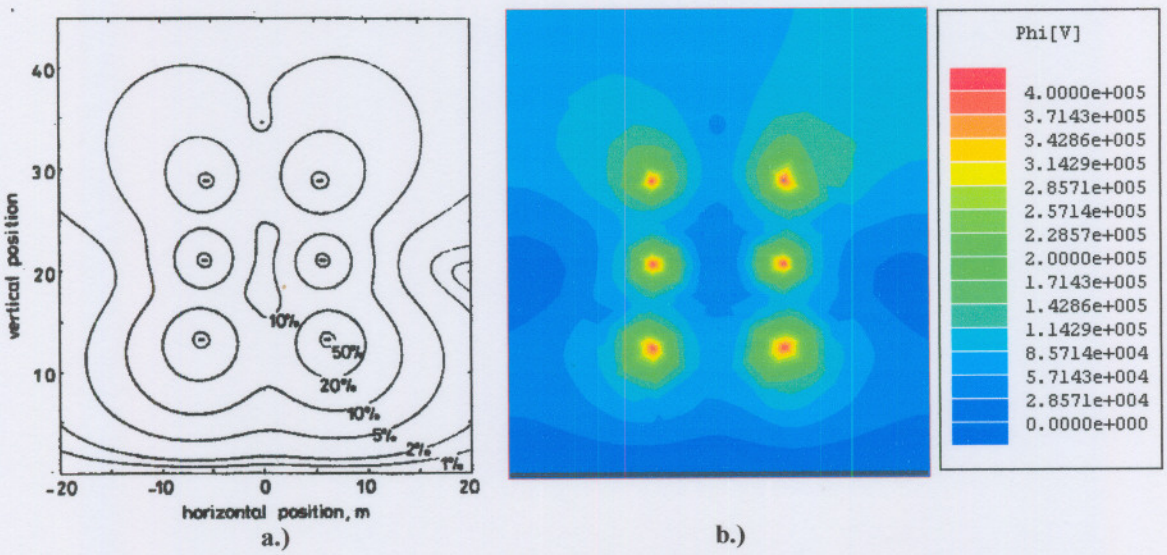

a.) b.)

Figure 21: Results for phase configuration B

From figure 21 we see the following:

- The 50% area depicted in figure 21.a. again has a value of 200kV, when one looks at figure 21.b. one can see that it correlates with the green area, which has a value of between 200kV and 228kV.
- The 20% region depicted in figure 21.a. corresponds to the light blue region in figure 21.b., which has a value of more or less 114.29kV – 142.86kV. Now 20% of 400kV gives 80kV. That is a minimum difference

of 34.29kV and a maximum difference of 62.86kV. This might be due to simulation parameter differences and the difference is not so that the values obtained from MAXWELL are totally unreliable. However, we are not so much interested in the area immediately surrounding the specific phases, we are more interested in the 10% area, since this is where the ADSS is to be installed.

- The 10% area in figure 21.a. has a value of about 40kV. This corresponds to the light blue area displayed in figure 21.b., which has an approximate value of between 28kV and 57kV. The ADSS will thus have been installed in the correct area of lowest voltage.

The MAXWELL package showed some differences in voltages close to the phase wires, but at the area of interest it correlated very well with the given values. Once again there is a deviation at the topside of the figure. This might also have something to do with boundary conditions.

2.3. Phase configuration C

The third simulation was conducted using the phase configuration depicted in figure 18.C: $0^0 - 0^0$, $120^0 - 240^0$, $240^0 - 120^0$. Figure 22 shows the result.

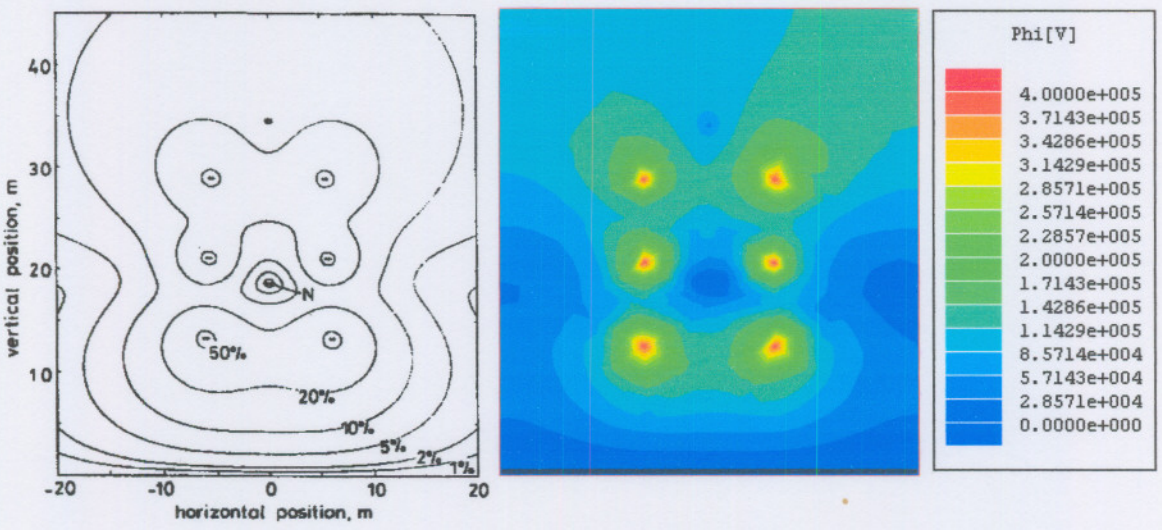

a.) b.)

Figure 22: Results for phase configuration C

From figure 22 we can see that the neutral point depicted in figure 22.a is also reflected in figure 22.b. This shows that for both programs the neutral point, the

best point for ADSS installation, is at more or less the same place. Note once again the deviation at the top.

2.4. Phase configuration D

The fourth simulation was conducted using the phase configuration depicted in figure 18.D: $0^0 - 240^0$, $120^0 - 120^0$, $240^0 - 0^0$. Figure 23 shows the result.

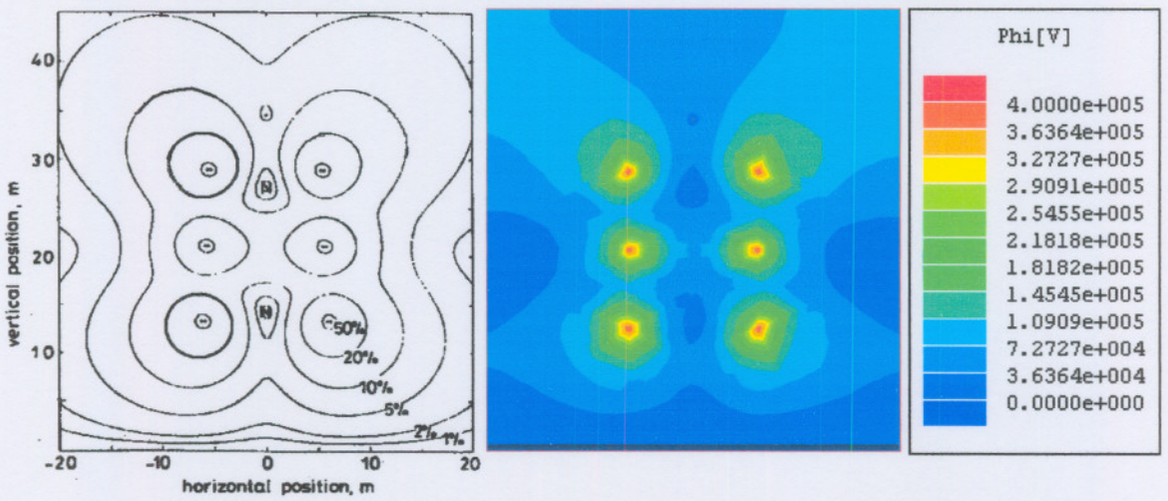

a.) b.)

Figure 23: Results for phase configuration D

From figure 23.a and b. it is clear that there are two neutral points. Each of these points exists at the same place. The deviation at the top can again only be described to the method of solution and selection of boundary conditions.

Therefore, if one where to use the results obtained by C.N. Carter & M.A. Waldron [10], or the results obtained with the use of MAXWELL, you would come to the same conclusion about where to place the OFC. This proves to show that the MAXWELL software program delivers the same type of results obtained by [10], and can therefore be expected to deliver acceptable results in the next chapter where the model and simulations are concerned.

2.5. Phase configuration E

The fifth and final simulation was conducted using the phase configuration depicted in figure 18.E: $0^0 - 120^0$, $120^0 - 0^0$, $240^0 - 240^0$. Figure 24 shows the result.

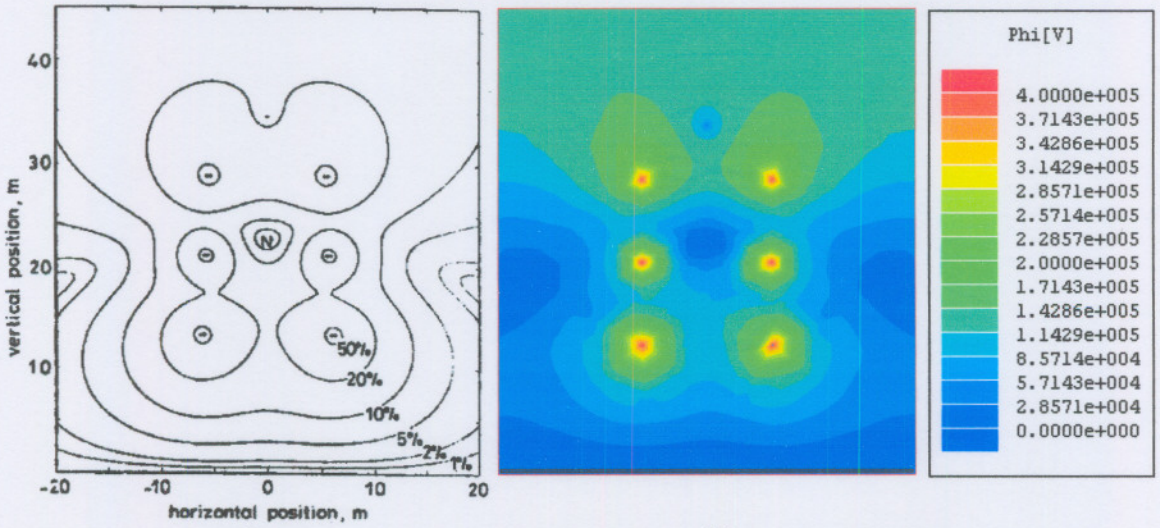

a.) b.)

Figure 24: Result for phase configuration E

From figure 24 it is apparent that the neutral point coincides. The N point in figure 24.a. is at more or less the same position as that of the darkish blue area in Figure 24.b., which has a value of 0kV – neutral. The other areas are the same as explained in the previous sections and once again MAXWELL can be expected to deliver the correct result in the following chapters.

3. CONCLUSION

From section 2 it is apparent that the MAXWELL program delivers acceptable results. The results obtained with the MAXWELL program did deviate from the expected result in some ways, mostly at the top, but this is believed to be as a result of the solution process and/or the boundary conditions. Note also that the results are of the same order of magnitude but that the deviation could be up to 30%.

The accuracy of the MAXWELL simulations are acceptable since MAXWELL will mainly be used to give us an idea of what the electric fields around the feeder and OFC might look like. The mathematical program MATLAB will be used to give us more specific values and a better idea of what the current and voltage distribution along the span of the cables look like.

we would like to install the fibre optic cable. In order to achieve this we omit the OFC from the simulation as was done in chapter 4 in order to see the supposed strength of the electric field at different distances from the ground.

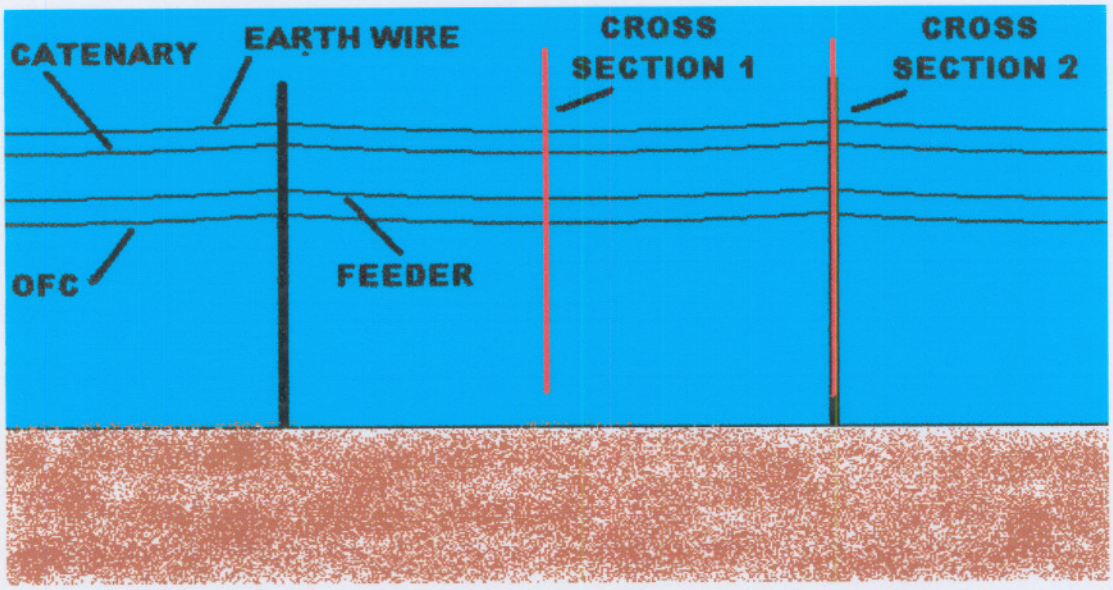

Figure 25: Side view of railway line indicating cross-sections

The first cross section consists of only the feeder, catenary and earth cables since it is at mid-span (See figure 26). The second cross section consists of the feeder, catenary and earth cable as well as the mast (See figure 29). The black line at the bottom of each figure represents the ground level.

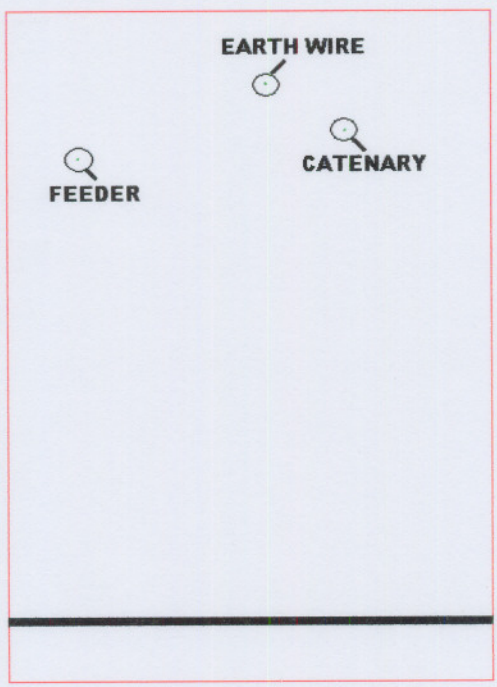

Figure 26: Cross section 1 - cables at mid-span

For the first cross section the target energy error for the solution process was set to 0.8%. That means that for each square to be solved, the error is to be less than 0.8%. When I conducted the first simulation I allowed the simulation program to create it's own mesh. After 10 iterations the energy error was no less than 14% and there it stayed, no matter how many iterations I used. With the help of "setup solution options" one can create your own mesh. I found that where the program created it's own mesh; it concentrated a lot of refinement on the ground level. This caused the amount of triangles in the background to be large and unrefined (figure 27).

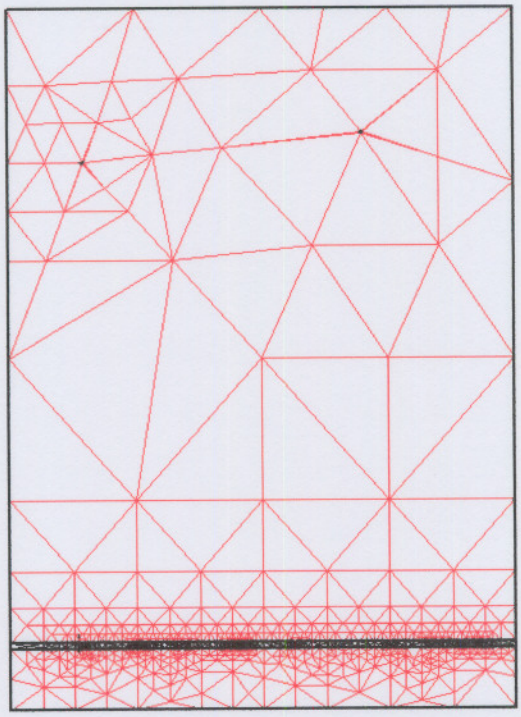

Figure 27: Mesh created by program for cross section 1

From this, one can clearly see that the program focused much more on the ground level as on any other part of the graph. The triangles are also much larger than that of figure 28, giving it a very low percent energy error value and making it less accurate.

Seeing that the solution is very inaccurate, I then decided to use the option "Manual Mesh", with which one can setup your own mesh. I decided to select the number of triangles to be as follows: around each cable - 1000, for the ground level - 500, and for the background - 7000. This reduced the percentage of the energy error to between 0.11% and 0.00747% after only a single iteration. The manual mesh can be seen in figure 28. From this, one can see that the fields around the cables will be much more accurate compared to that for the mesh created by the program.

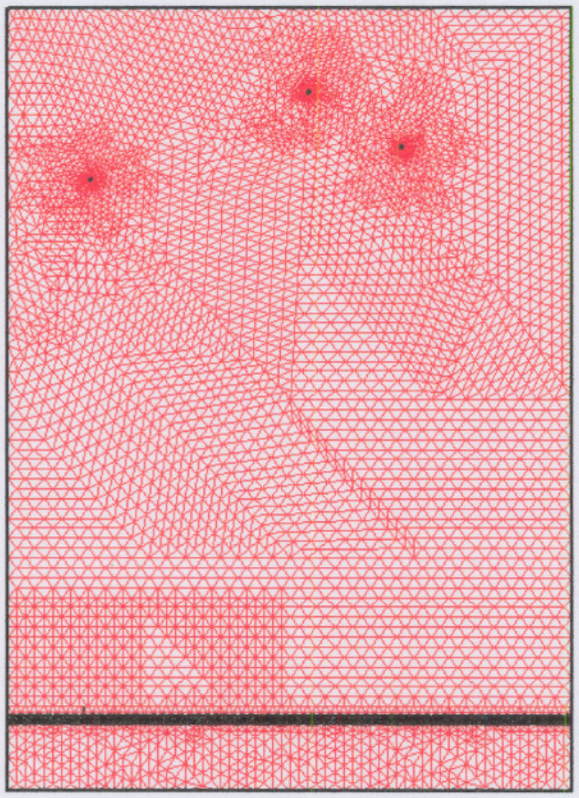

Figure 28: Manual mesh for cross section

The mesh file for cross section 2 (figure 29) can be seen in figure 30. Again the same procedure was followed as described for figure 26. For this setup each of the cables had a mesh of 1000, the background a mesh of 7000 and both the mast and ground level a mesh of 500 triangles.

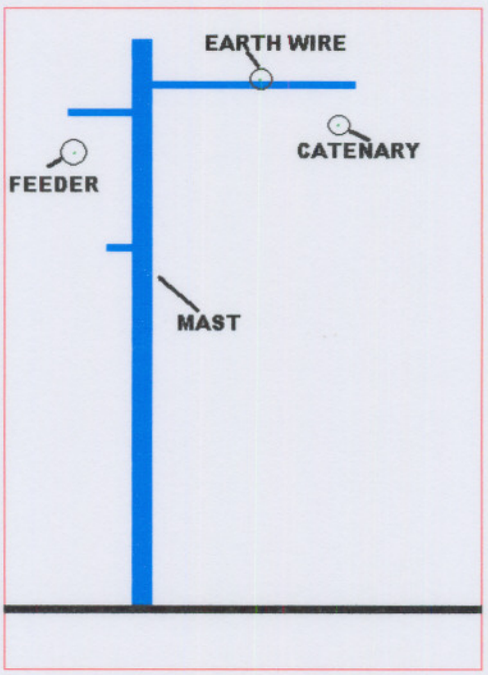

Figure 29: Cross section 2 - Cables and mast

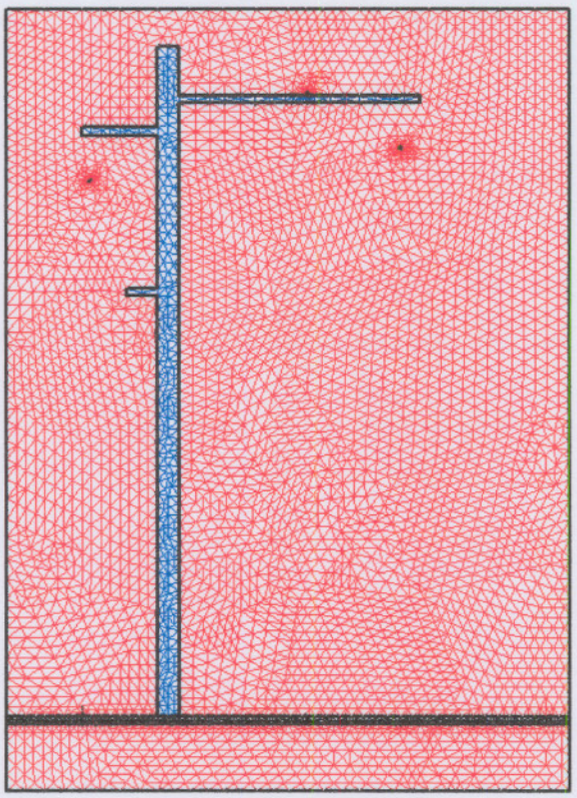

Figure 30: Manual mesh for cross section 2

Each of these cross sections will now be used in the simulation. The first series of simulations, as stated above, will be without the mast, and the second series of simulations will be with the mast. The third and final simulation will be used to see what effect the position of the OFC has on the occurrence of DBA.

2. GENERAL PROCEDURE FOR CREATING AND SOLVING A 2D MODEL

The general procedure to follow when using the software to create and solve a 2D problem is given below [9]:

1. Use the ***SOLVER*** command to specify which of the following electric or magnetic field quantities to compute:
   - Electrostatic
   - Magnetostatic
   - Eddy Current
   - DC Conduction
   - AC Conduction
   - Eddy Axial
2. Use the ***DRAWING*** command to select one of the following model planes:
   - **XY-Plane:** Cartesian models appear to sweep perpendicularly to the cross-section.
   - **RZ-Plane:** Axisymmetric models appear to revolve around an axis of symmetry in the cross-section.
3. Use the ***DEFINE MODEL*** command to create the geometric model. There are two options:
   - **Draw model:** Allows you to access the 2D modeller and build the object that make up the geometric model.
   - **Group model:** Allows you to group discrete objects that are actually one electrical object.
4. Use the ***SETUP MATERIAL*** command to assign materials to all objects in the geometric model.
5. Use the ***SETUP BOUNDARIES / SOURCES*** command to define the boundaries and sources for the problem. This determines the electromagnetic excitations and field behaviour for the model.
6. Use the ***SETUP EXECUTIVE PARAMETERS*** command to instruct the simulator to compute one or more of the following special quantities during the solution process:

- Matrix (Capacitance, Inductance, Admittance, Impedance, or Conductance matrix, depending on the selected solver).
- Force
- Torque
- Flux lines
- Post Processor macros
- Core loss
- Current Flow

7. Use the ***SETUP SOLUTION OPTIONS*** command to enter parameters that affect how the solution is computed.
8. Use the ***SOLVE*** command to solve for the appropriate field quantities.
9. Use the ***POST PROCESS*** command to analyse the solution.

3. FIRST SERIES OF SIMULATIONS

The model used in the first part of the modulation process is that depicted in figure 26. The first simulation was done using only the cables, the mast and the OFC was excluded. This was done in order to get an idea of what the electric field and potentials will be at about mid-span, halfway between the masts without the presence of the OFC. This corresponds to that done in chapter 4 where we evaluated the software package.

3.1. First simulation – Cables at mid-span

The first simulation had the following setup:

- The OFC was excluded and only the feeder, catenary and earth wire was taken into account.
- Figure 31 shows the expected complex magnitude of the instantaneous voltage.

The top circle in figure 31 shows more or less where the OFC is currently installed, about 5.44 meter above the ground. According to this, the instantaneous voltage at that specific place will be between 10.562kV and 13.158kV.

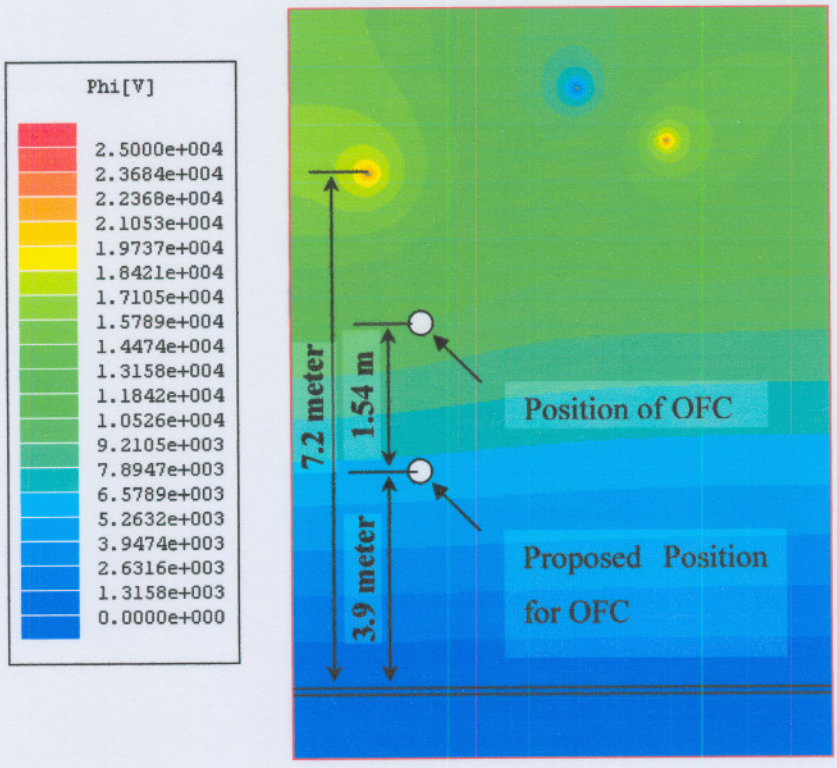

Figure 31: Complex Instantaneous voltage for the cables, with the OFC excluded

Now we wish to determine the current that will be expected to flow on the cable having a certain resistance and being at a certain voltage level.

In [12] it is stated that a magnitude of below 0.5mA is the threshold for dry-band arcing to occur, and damage will not be prevalent. For a wet polluted cable at a given level of induced voltage, the leakage current is highly dependent on the resistance per unit length of accumulated contamination and the cable's sheath.

This may explain why cable sheath degradation subject to marine type pollution is more prone to damage than cables subjected to pollution levels of a lesser degree. Therefore, if $i = Gv$, with i the current in *amperes*, v the voltage in *volts* and G the conductance in *siemens*, then the current that will be induced on the clean cable will be:

$$
\begin{aligned}
i &= Gv \\
&= 2e-8 * 13158 \\
&= 0.263e3 \\
&= 0.263mA
\end{aligned}
$$

This value of 0.263mA is well below the current needed to initiate DBA, which is also expected for a newly installed cable. When this cable becomes polluted (the time needed for this amount of pollution to occur is unknown) the conductivity of the cable rises to about 5.8823 x 10^{-8} siemens/meter [11]. The calculated current is about 0.774mA, which is more than enough to initiate DBA.

If the cable is lowered to where the potential field value is about 9.2kV, the leakage current will be more or less 0.54mA; this is also within the range for DBA to occur. Therefore, if DBA is to be eliminated, the current should be less than 0.4mA. The conductance stays the same therefore the cable should be installed in a position where the potential field is less than 6.8kV.

This proposed position for installation is indicated in figure 31, about 3.9m above the ground, which might present some problems of another nature such as theft. As will be seen later in the MATLAB simulations, lowering the OFC by over a meter should reduce the risk of DBA considerably.

4. THE SECOND SERIES OF SIMULATIONS

The next section describes the second set of simulations, the model used is that depicted in figure 29. For these simulations the mast was included to study the effect that it would have on the potential field acting in on the cables.

4.1. First Simulation – Cables and mast without OFC

The first simulation had the following setup:

- The OFC was excluded and the number of field lines was taken as 30 to give a better dispersion of the potential lines.
- Figure 32 shows the complex magnitude of the instantaneous voltage.

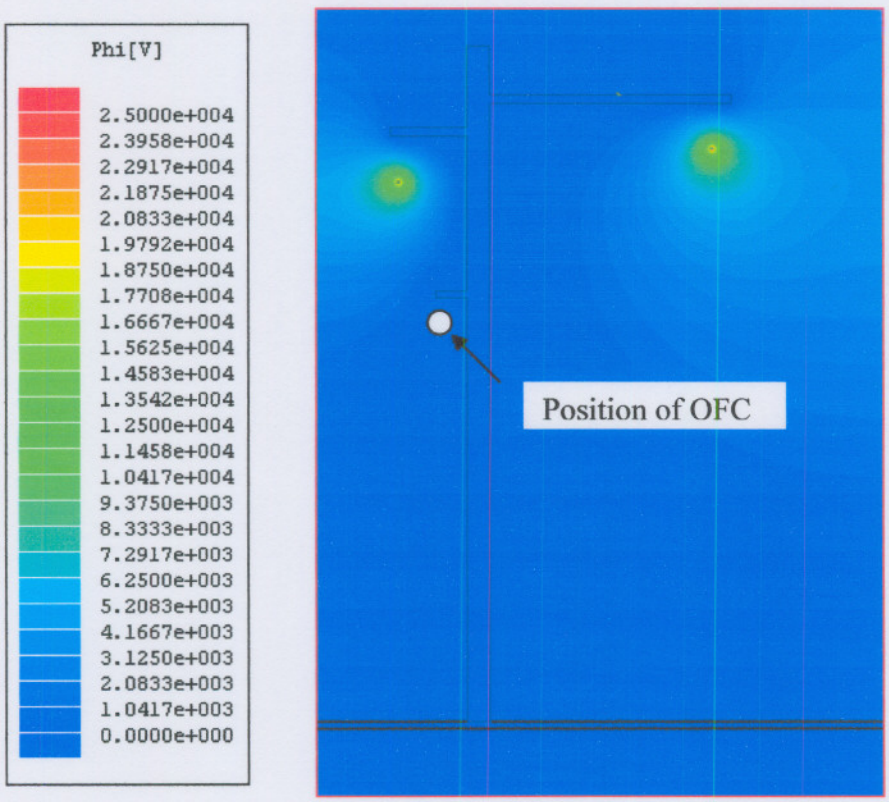

Figure 32: Complex instantaneous voltage for cables and mast without OFC

From figure 32 we can clearly see that the voltage level at the mast in the vicinity where the OFC is to be installed is 0kV. We will now take a look at the effect that this field has on the OFC installed on the mast structure.

4.2. Second simulation – Cables with the mast with clean OFC

- The OFC was installed at the designated position and chosen to be of polyethylene material which has a relative permittivity of 2.25 and a conductivity of 2×10^{-8} *siemens/meter* for a clean, newly installed cable.
- Figure 33 shows the complex magnitude of the instantaneous voltage
- Figure 34 shows a close-up view of the instantaneous voltage around and inside the OFC

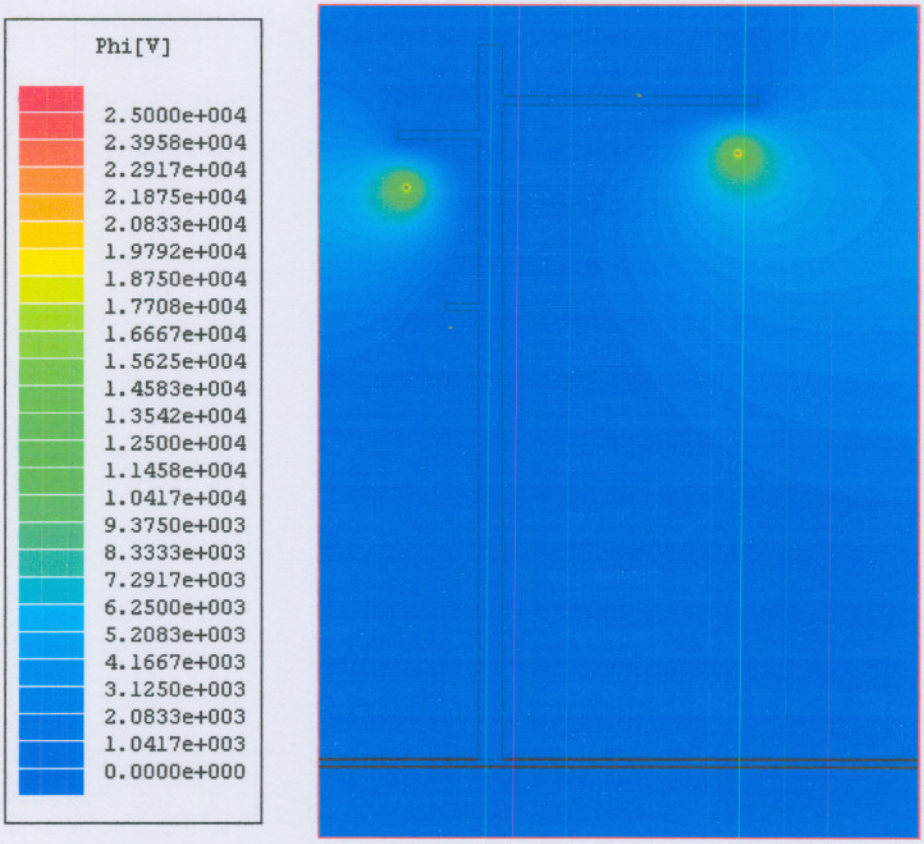

Figure 33: Complex Instantaneous voltage for OFC with conductivity = 2 x 10^{-8} siemens/meter

When one compares figure 33, OFC installed, to figure 32, no OFC, there is no difference in the electric field lines or in the values of the corresponding field lines. The fact that the OFC is installed on the masts does therefore not have any effect on what the field lines look like nor on their magnitude. However, the electric field does have an effect on the cable as can be seen in figure 34.

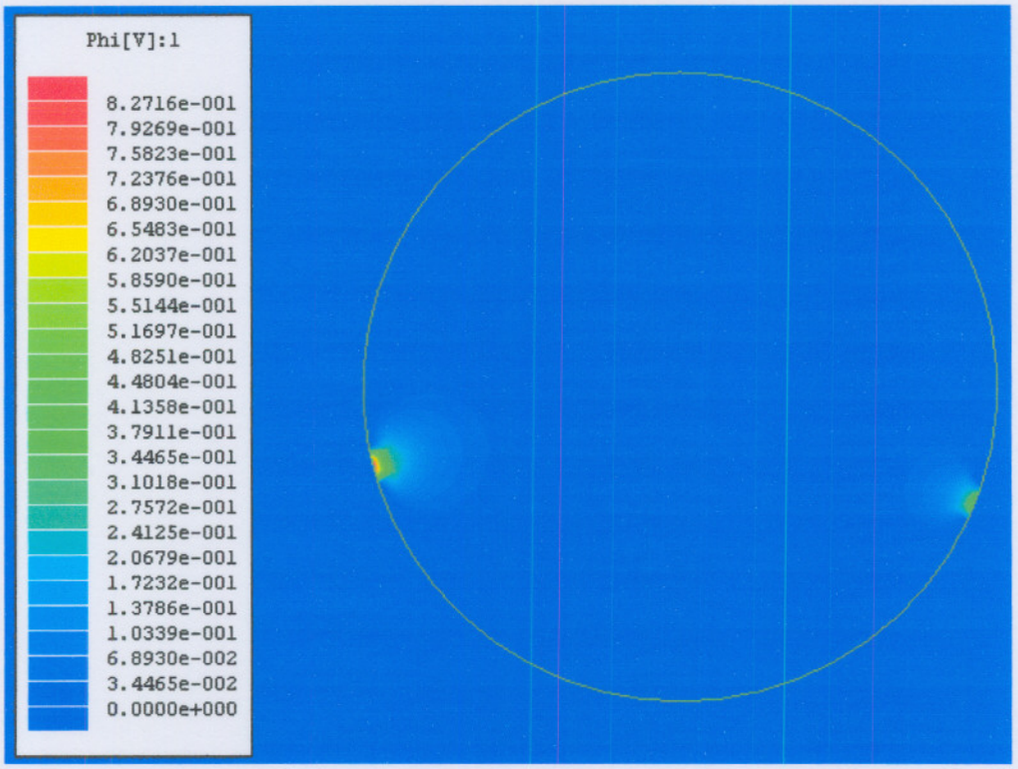

Figure 34: Close-up view of the instantaneous voltage in and around the OFC for a clean cable

From figure 34 it is interesting to note that there seems to be a small surface potential ("hot spot") present on the inside surface of the OFC. When one looks at the magnitude of this occurrence one can see that it is in the vicinity of 0.827V maximum, thus the potentials are of very low magnitude compared to that of the feeder and surrounding potential fields, but it could be an indication of where DBA might occur; if the pollutant is spread evenly around the cable. No explanation for the occurrence of the small "hot spot" could be postulated.

4.3. Third simulation – Cables with mast with polluted OFC

- Now the effect that a polluted fibre optic cable will have on the instantaneous voltage will be examined.
- The fibre optic cable was selected to have a relative permittivity of 2.25 and a conductivity of 5.8823×10^{-8} *siemens/meter* this is the value for a polluted cable obtained from [11].
- Figure 35 shows the complex magnitude of the instantaneous voltage
- Figure 36 shows a close-up view of the instantaneous voltage around and inside the OFC

One would expect the conductivity increase of the cable to have a major effect or at least some effect on the voltage fields. Looking at figure 35, and comparing it to figure 33, there doesn't seem to be any difference. This may be due to the fact that the OFC's effect on the voltage field is so small compared to that of the mast, that one can barely see the difference.

However when we start looking at what is happening inside the OFC, the picture changes. In figure 34 one could see two "hot spots"; these cannot be explained at this point in time. When we look at figure 36, we see *nothing*. There are no "hot spots" on the inside of the OFC. This might be due to the fact that the OFC is now conducting all the potential build-up away from these "hot spots".

The electric field in the vicinity of the OFC (from figure 35) is more or less between 1.04kV to about 2.08kV. This would give a leakage current value of about 0.12mA, which is below the 0.5mA threshold necessary to initiate DBA. Thus the simulation does not support DBA under these conditions, DBA does however occur. Near the coastal region where the mixture of salt rich air, high humidity and extreme pollution of coal dust plays a major role. The fact that the simulation does not proof the occurrence of DBA might be due to insufficient simulation parameters, or a combination of CORONA and DBA or 0.5mA is not applicable to these conditions as a threshold. Further investigation is required to determine these facts.

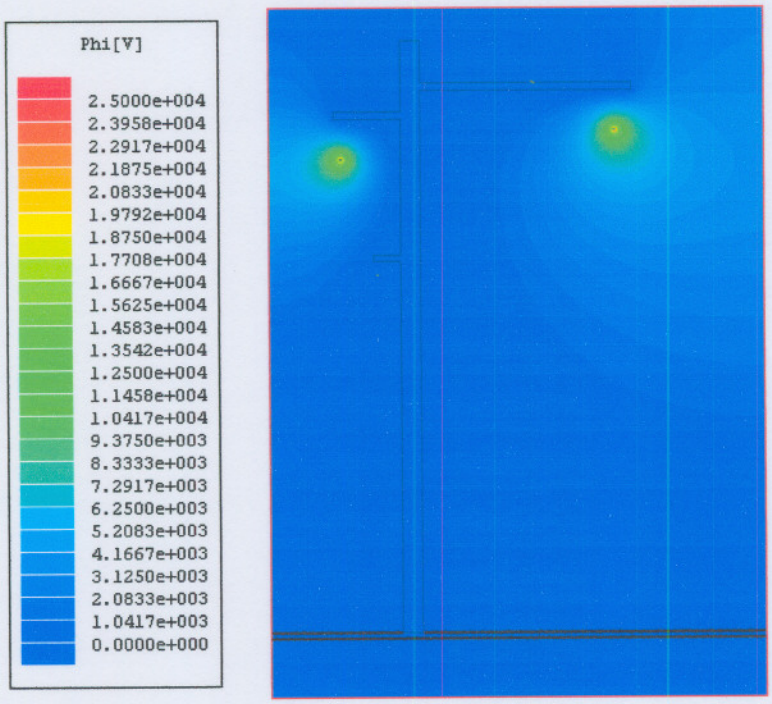

Figure 35: Complex Instantaneous voltage for OFC with conductivity = 5.8823 x 10^{-8} siemens/meter

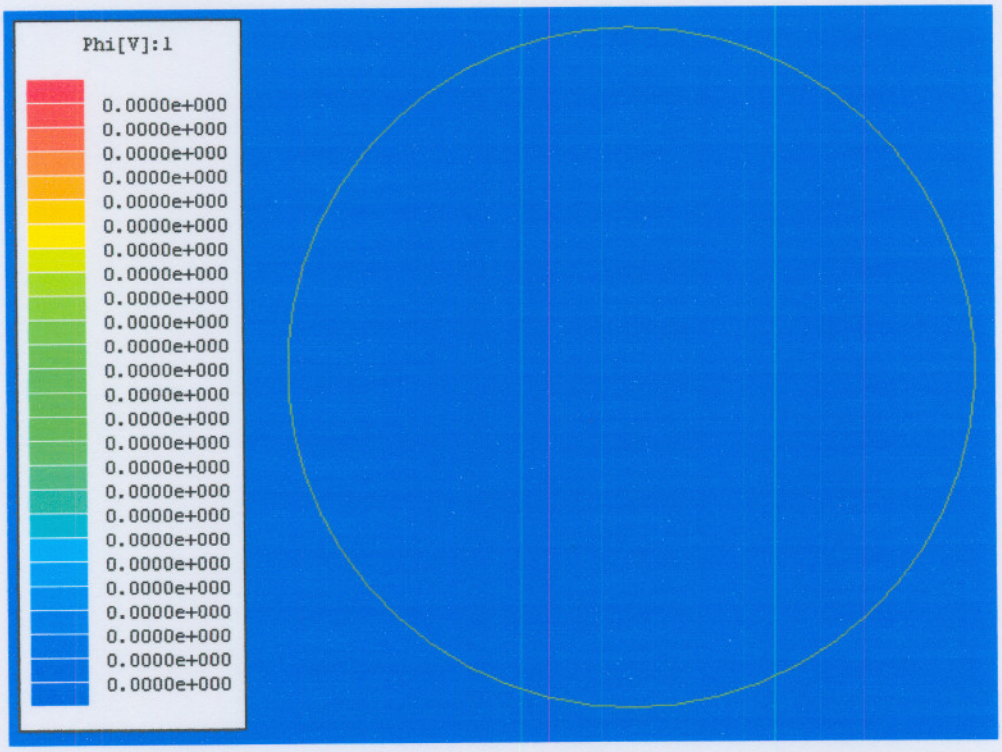

Figure 36: Close-up view of the instantaneous voltage in and around the OFC for a polluted cable

4.4. OFC lowered on mast

The next question to be asked is, "What effect would lowering the cable have on the occurrence of DBA?" One would expect that if the cable were lowered by more or less a meter and a half (1.5m), that DBA would stop occurring. This assumption is due the relation that the field becomes weaker as the square of the distance from the source increases.

Figure 37 shows the complex magnitude of the potential field around the cable with the mast and cables. One would expect the field to look quite different from that seen in figure 35. When one looks at figure 37, one can see that the OFC is now in a potential field of less than 1.043kV. That means that for a polluted cable the leakage current would be less than 0.6 x 10^{-6} A. That is far less than the required current of 0.5mA for DBA to occur.

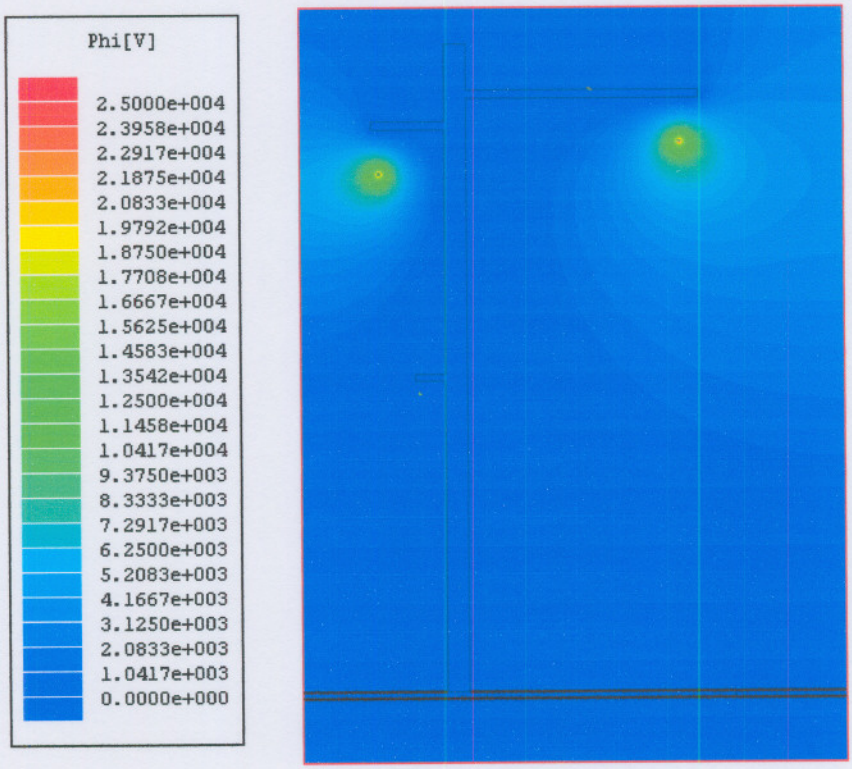

Figure 37: Complex Instantaneous voltage for lowered OFC with conductivity = 5.8823 x 10^{-8} siemens/meter

4.5. Discussion

Using the MAXWELL program, several things can be seen. The form and magnitude of the electric field around the feeder and catenary is mainly dependant on the form of the mast and not the location of the fibre support. This was done to show that by putting a fibre cable on the mast does not affect the electric field although the fibre cable is affected when placed within this field.

The real contribution of pollution to the occurrence of DBA on the fibre cable could not be satisfactorily described since the simulation package has only two dimensions. The following section makes use of a more mathematical approach in order to get a better understanding of the effect of things such as: span length, sag of the cables and distance of the fibre cable from the feeder on the occurrence of DBA. This approach is explained in more detail in section 5.

5. CAPACITANCE USED TO DETERMINE DBA

In the previous section, the MAXWELL program was used to determine the effect of the OFC, both clean and polluted, on the potential fields. In this section we will look at the effect that this potential field has on the fibre cable. The MAXWELL program is a 2D program and we used it to view the cross-section of the span at the mast and at mid-span. This gave us two reference points. With the use of the MATLAB program we will be able to model the span at X nodes along the span. For each node we will calculate the relative distances between the feeder, catenary and fibre cable. Using these distances we will be able to calculate the capacitance value between each of these and from this we will calculate the current and voltage on the cable.

The MATLAB program is based on a mathematical model designed by C.N. Carter and M.A. Waldron [3], and a complete derivation can be found in Appendix B. They [3] where among the first researchers to postulate a mathematical model to determine the leakage currents induced on the outer sheath of a fibre optic cable installed in a high voltage environment. M.F. Khan and D.A. Hoch [14] describe this model in detail.

Karady and Devarajan [13] have subsequently presented an algorithm that improves upon the method by [3]. In their calculation of leakage current, [3], made the assumptions that the line to voltage to fibre optic cable capacitance, the fibre optic cable to ground capacitance and the resistance of the wetted pollution layer were constant along the length of the span. This was an over-simplification as it is common practice for the sag on the fibre cable to be smaller than that of the phase conductor thereby altering both the phase to fibre optic capacitance and the fibre optic cable to ground capacitance along the span. Also, the assumption that the resistance of the pollution layer is constant throughout the entire length of the cable is not realistic. Whether windborne coastal pollution or industrial soot, or in this case, coal dust from the passing train, pollution does not settle uniformly on the ADSS cable. The algorithm presented by [13] can include both the effect of sag and the effect of non-uniform pollution.

Figure 38 is a diagrammatic representation of the equivalent circuit at a given point along the span. The numbers 1,2, and 3 represent the phase conductors and 0 represents the ADSS fibre optic cable.

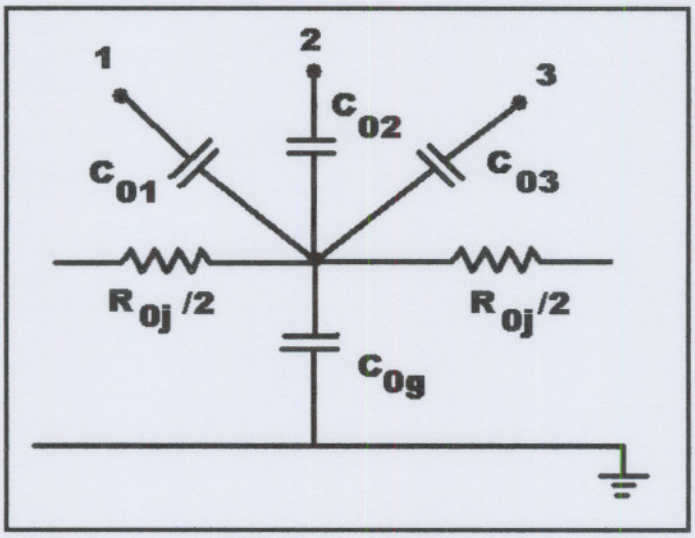

Figure 38: Equivalent circuit of polluted fibre optic cable

C_{01}, C_{02} and C_{03} are the respective phase to fibre optic cable capacitance and C_{0g} represents the fibre optic cable to ground capacitance. R_{0j} represents the wetted pollution layer on the outer sheath of the cable. A finite number of these sections in series approximate the distributed nature of the circuit such that numerical analysis would yield the leakage current induced on the cable sheath.

This algorithm will now be used to investigate the effects of pollution, span length, sag, distance from feeder and uneven pollution deposits on the induced leakage currents that flow on the outer sheath of the fibre optic cable.

5.1. Simulation parameters

The positioning of the fibre optic cable and feeder cable on the tower for these simulations is best illustrated in figure 39 below. (An enlarged view of this figure can also be seen in appendix A). The relative coordinates of the cables are used in the algorithm to determine the distances between the cables, taking into account the sag of the cables. Figure 40 shows the cross-section view of the cables with relative positions as will be used in the algorithm. The height of the fibre will vary according to the sag %.

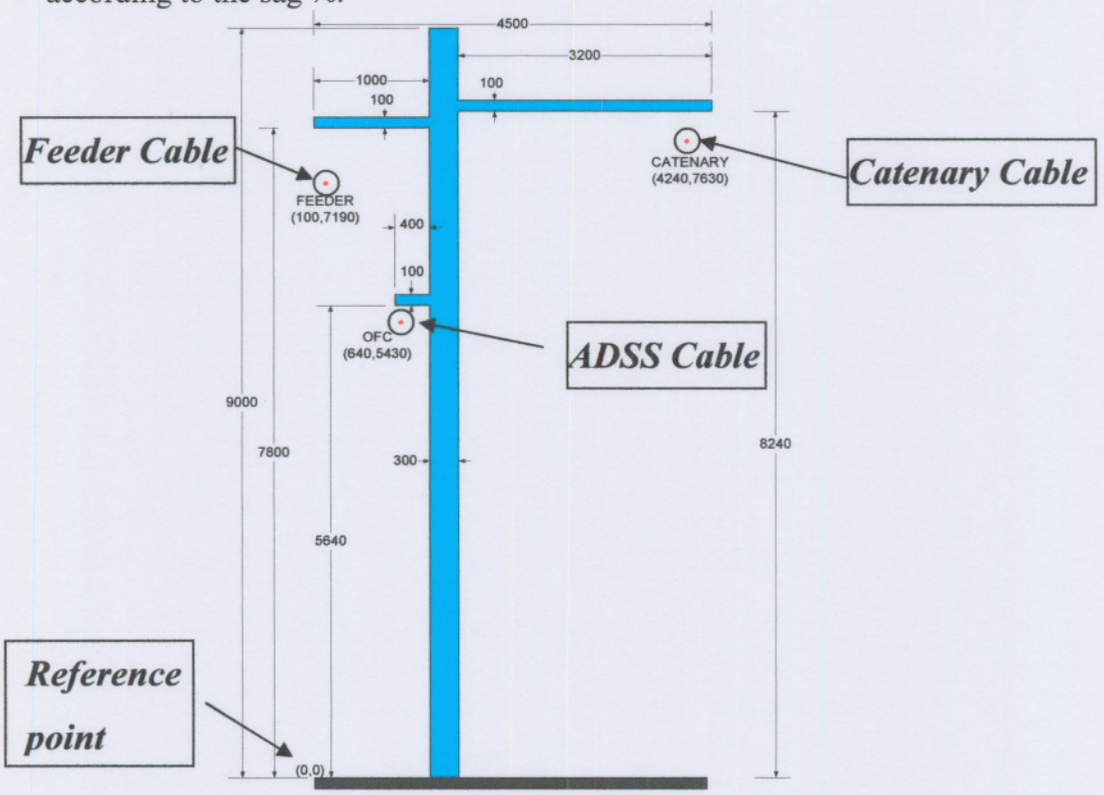

Figure 39: Two-dimensional diagram of tower, highlighting the position of the respective cables.

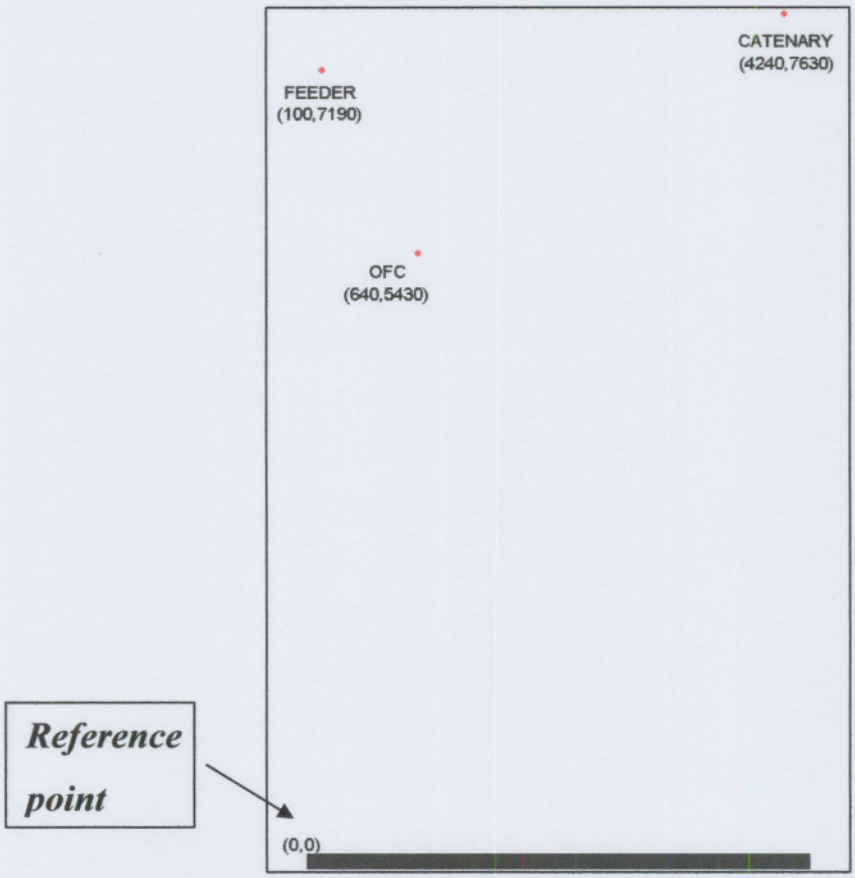

Figure 40: Diagram showing relative positions of cables along the span

The system voltage carried by the feeder cable is 25kV at a frequency of 50 Hz. The catenary is connected to the feeder, delivering the necessary voltage and current to the electric train. It is therefore a single-phase system, operating at 25kV rms.

The reference point, as indicated in figure 40, is located at the bottom left of the drawing and all coordinates are given with respect to this point.

Voltage	Fibre		Feeder		Catenary	
	X (m)	Y (m)	X (m)	Y (m)	X (m)	Y (m)
25000	0.640	5.430	0.100	7.190	4.240	7.630

Table 1: Spatial positions of the fibre optic cable and conductors on the tower window

A test span of between 50m and 100m was used in various scenarios. The span was generally divided into 1000 sections when performing the numerical algorithm. According to [14], increasing the number of nodes along the span was

found to increase the accuracy of the simulation but any further increases in the number of nodes was found to not change the result beyond any acceptable level.

5.2. Effects of pollution on leakage current at different span lengths

According to [3] and [14], the pollution layer can be represented as a resistance. This resistance is only applicable after the thin conductive pollution layer has been lightly wetted by light rain, fog or drizzle. The pollution layer, as described by [14], is difficult to categorize in absolute terms, as it is highly dependant on both the type of pollutant and the amount of moisture present. Three pollution levels that represent varying levels of conductivity have been considered in this study as defined by [14]. These are:

10^5 Ω/m	-	Heavy pollution	-	10^{-7} *siemens/meter*
10^6 Ω/m	-	Medium Pollution	-	10^{-8} *siemens/meter*
10^7 Ω/m	-	Light Pollution	-	10^{-9} *siemens/meter*

The voltage distribution for the 25kV system at a span length of 120m with cable sag of 2% for both the fibre and feeder can be observed in figure 43 below. The voltage distribution was found to be symmetrical with respect to the centre of the span.

From figure 41, it is apparent that the voltage goes to zero close to the mast. This is as expected since the mast is earthed and therefore at zero potential.

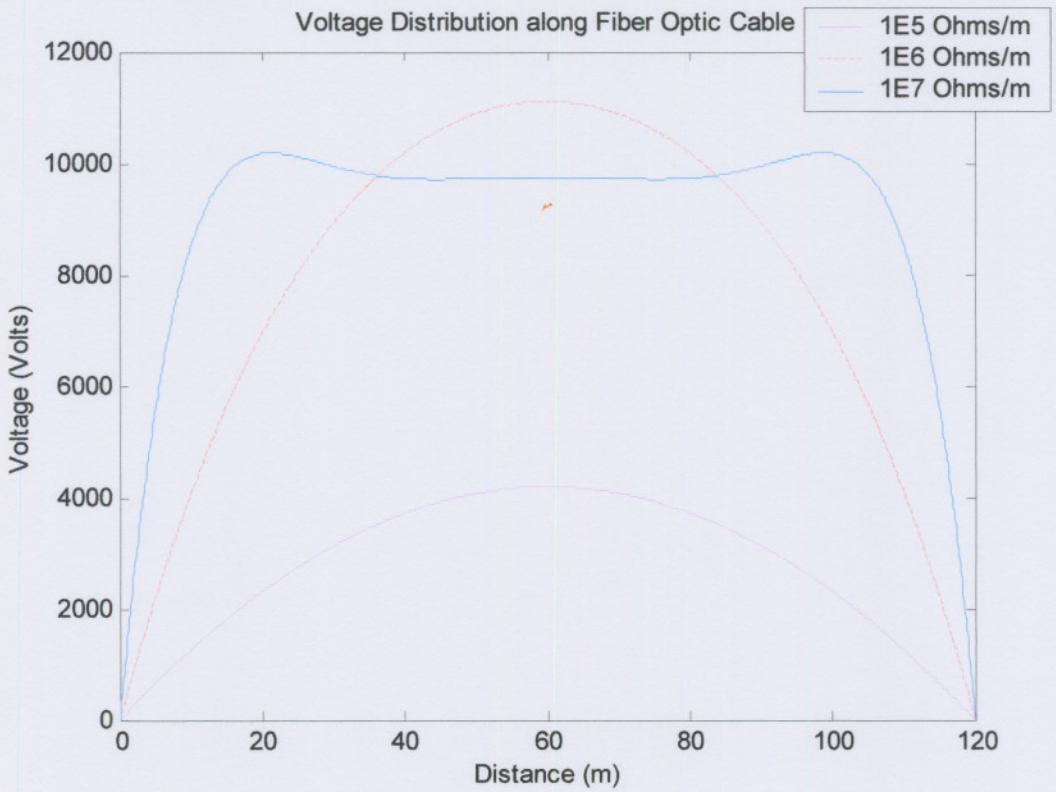

Figure 41: Voltage distribution along the fibre for a span of 120m, sag=2% for cabe and fibre, location as per drawing (0.640, 5.43).

Now, the span lengths will be varied between 50m and 100m, with 10m increments, the sag is kept at 2% for both the feeder and fibre cables. Five figures will be shown and a conclusion will be drawn at the end regarding the voltage distribution, then five more figures will be used to show the effect of span length on the leakage current, again a conclusion will be drawn after the last figure.

Results of voltage distribution for varying span length and sag of 2%

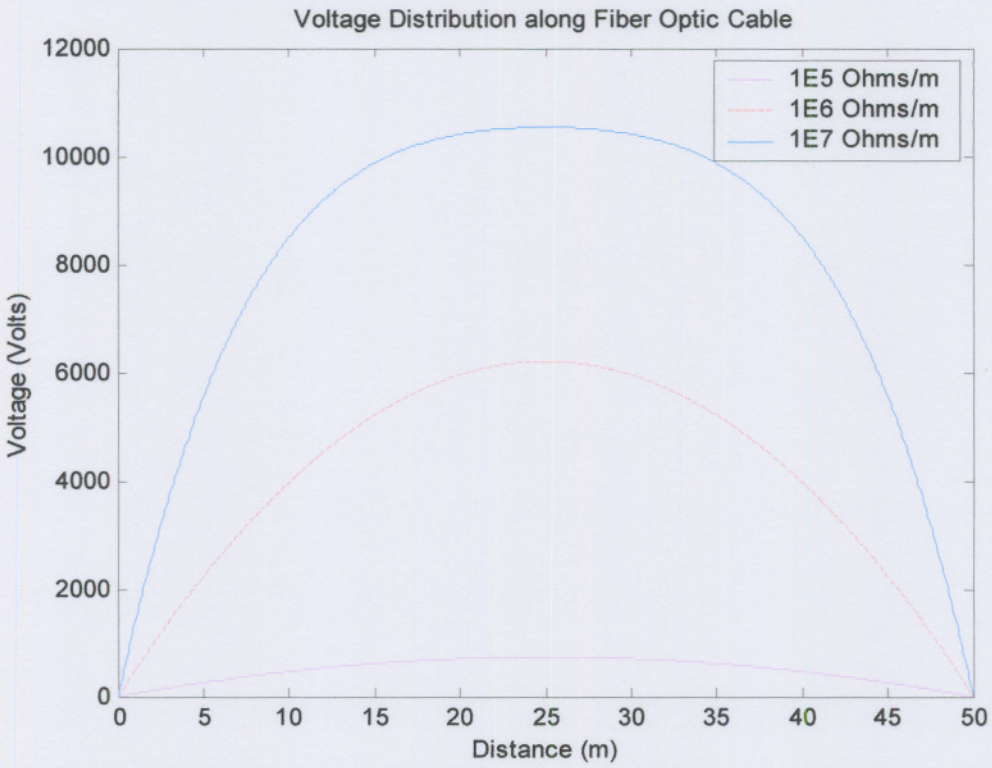

Figure 42: Voltage distribution for span length of 50m and sag = 2%

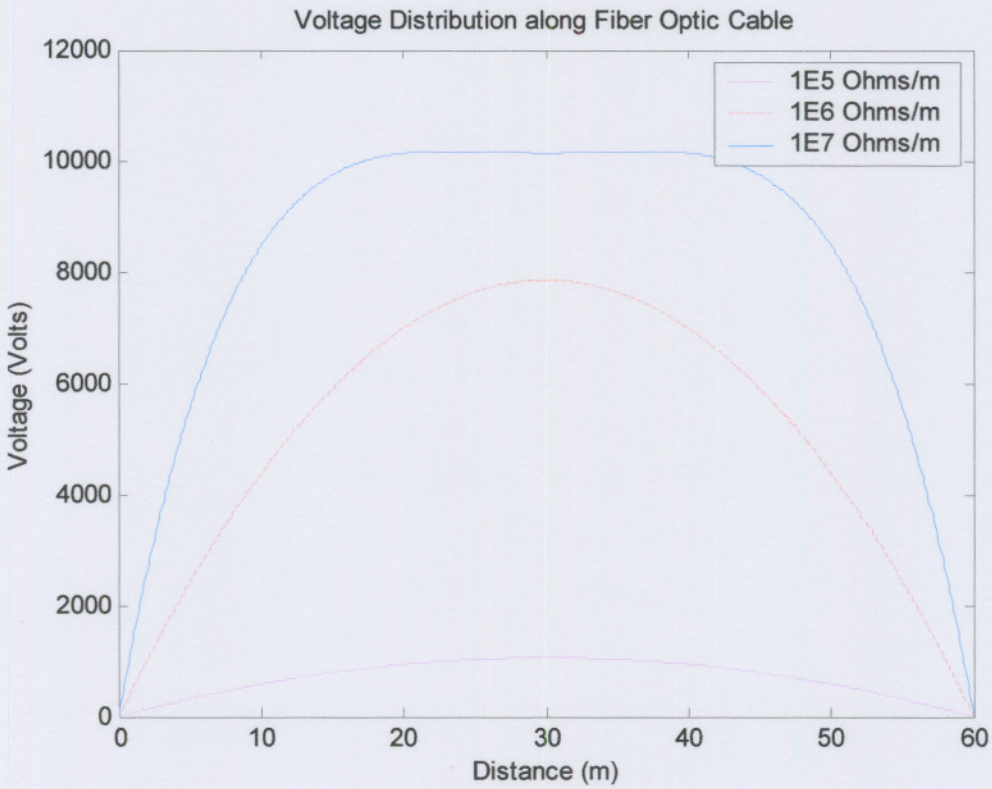

Figure 43: Voltage distribution for span length of 60m and sag = 2%

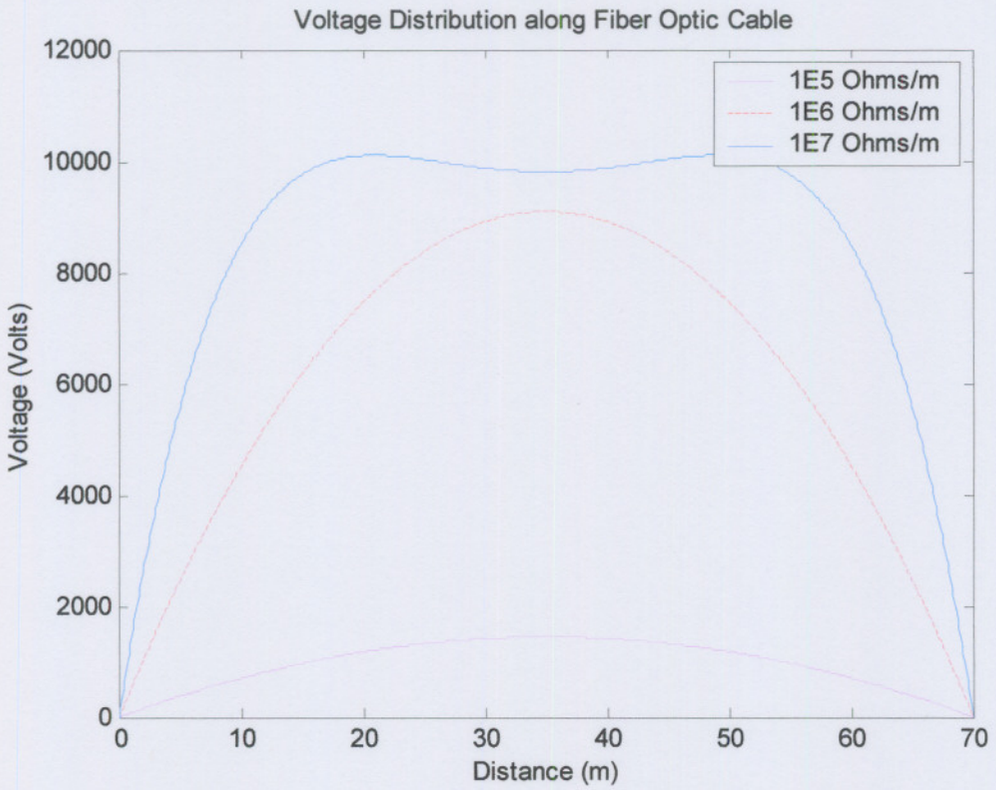

Figure 44: Voltage distribution for span length of 70m and sag = 2%

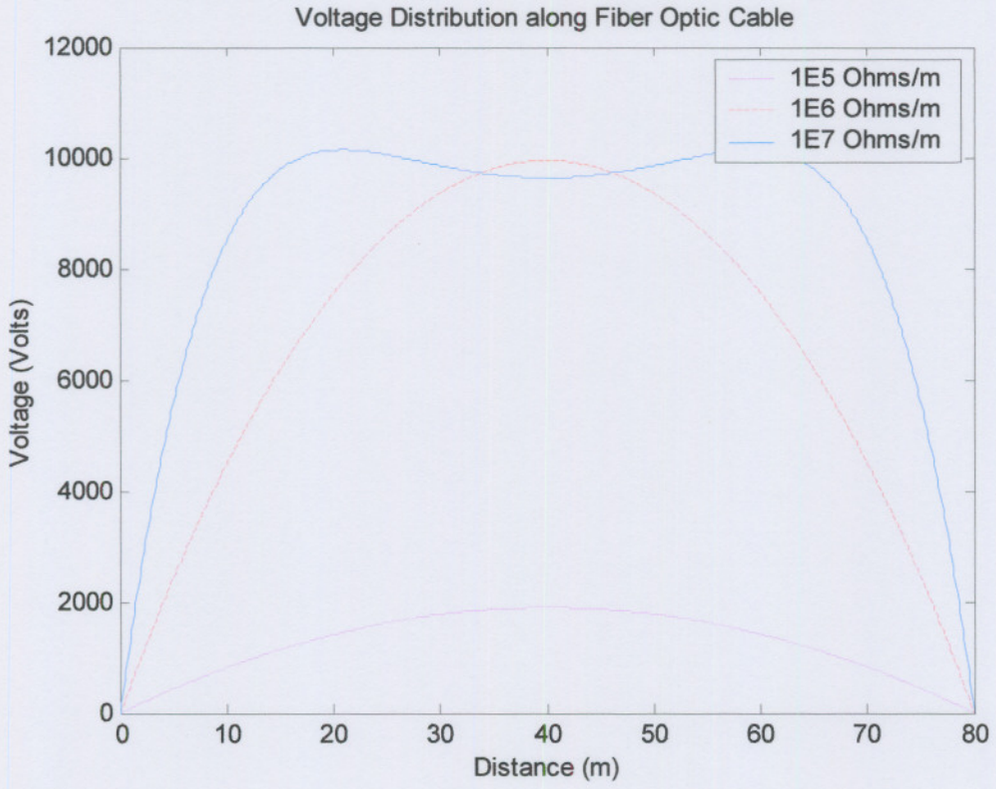

Figure 45: Voltage distribution for span length of 80m and sag = 2%

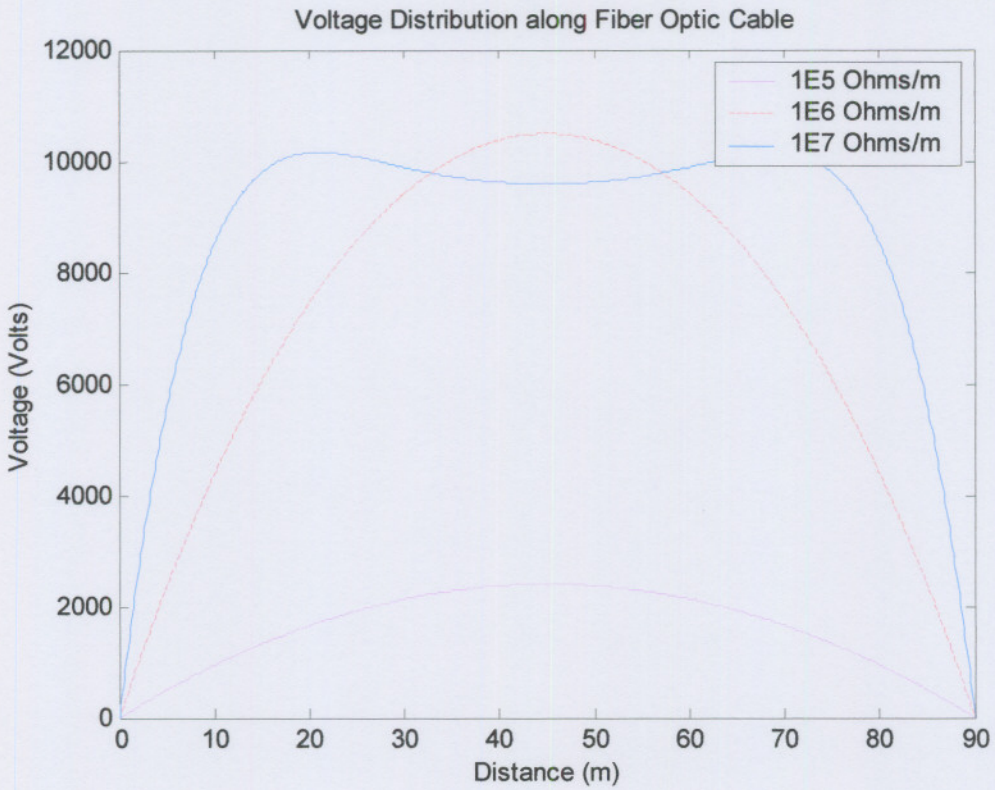

Figure 46: Voltage distribution for span length of 90m and sag = 2%

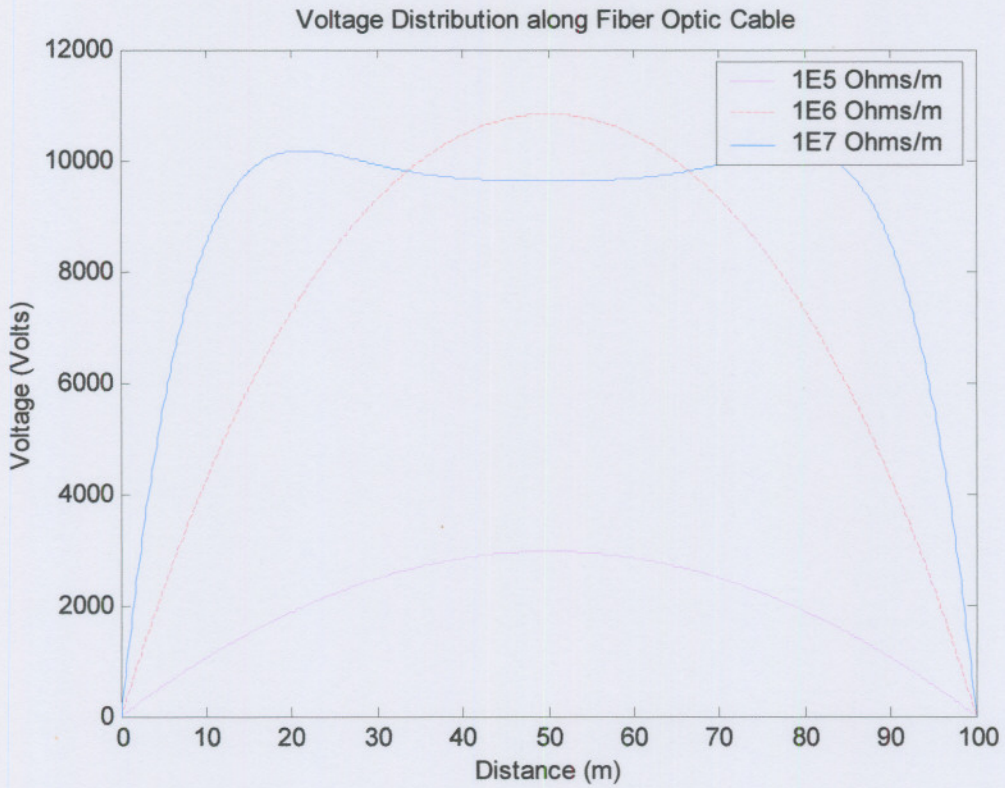

Figure 47: Voltage distribution for span length of 100m and sag = 2%

Discussion:

Starting with figure 42, and as will be seen in all figures relating to this section; one can clearly see that all the figures are symmetric to the centre of the span. This is due to the nature of potential build-up on the cable. As will be seen in the next section, the current follows the same profile. In figure 44, the voltage for a lightly polluted cable with resistance of 1E7 ohms/m is about 700 Volts, however, the voltage for a medium polluted cable increases by over 857.1% to 6000V. The voltage for a heavily polluted cable is even worse with a 1428.57% increase to 10200V. From figure 42 it is also apparent that the potential build-up is somewhat gradual on both sides sloping to a peak at the top.

In figure 43, this picture changes somewhat, almost forming a plateau. The peak value at the centre of the span starts levelling off at 10200V, and the profile tends to grow wider. The voltage for a lightly polluted cable with a span of 60m is about 1000V, the voltage for a medium polluted cable is 7800V, 780% increase, and the voltage for a heavily polluted cable is 10200V, a 1020% increase.

For figure 44 a strange thing happens. The voltage for a lightly polluted cable is now about 1500V, the voltage for a medium polluted cable is about 9200V, 613% increase, but although the peak voltage value for a heavily polluted cable is still 10200V, the value at the centre has decreased somewhat to 9800V.

For figure 45, the same applies. The voltage for a lightly polluted cable is now at 2000V, the voltage for a medium polluted cable is at 10000V and the voltage for a heavily polluted cable has stayed very much the same except for the fact that it tends to widen even more, getting closer and closer to the mast and the voltage at the centre is now 9600V.

In figure 46 the voltage for a lightly polluted cable is 2400V, the voltage for a medium polluted cable is now 10400V, about 200V more than what the voltage for a heavily polluted cable was for a 50m span, and the voltage for a heavily polluted cable is 9600V at the centre and 10200V at both sides. The centre portion seems to have reached a lower saturation limit and the two highs at both sides an

upper saturation limit. The voltage for a medium polluted cable seems to keep on increasing without any sign of levelling off.

In figure 47, the voltage for a lightly polluted cable is at 3000V, the voltage for a medium polluted cable is at 11000V, higher than what the voltage for a heavily polluted cable has been up to now and the voltage for a heavily polluted cable is still at 9600V in the middle and 10200V at either side.

Judging from the voltages that are being induced at different span lengths with varying pollution severities, it seems to be rational to suggest that a shorter span length should reduce the risk of DBA occurring.

When one compares the voltage values obtained in this section to that which was obtained from MAXWELL, we see that MAXWELL showed that at mid-span a voltage level of between 10562V and 13158V could be expected in the area where the OFC is to be installed. This correlates well with the values obtained for both medium and high pollution levels.

The MATLAB simulation does however give a much better indication of exactly what happens on the cable whereas MAXWELL gave us an overall indication of the voltage fields, without the OFC cable.

Results of Leakage current distribution for varying span length and sag of 2%

This section shows the effect of varying span length on the leakage current. An explanation will be given at the end.

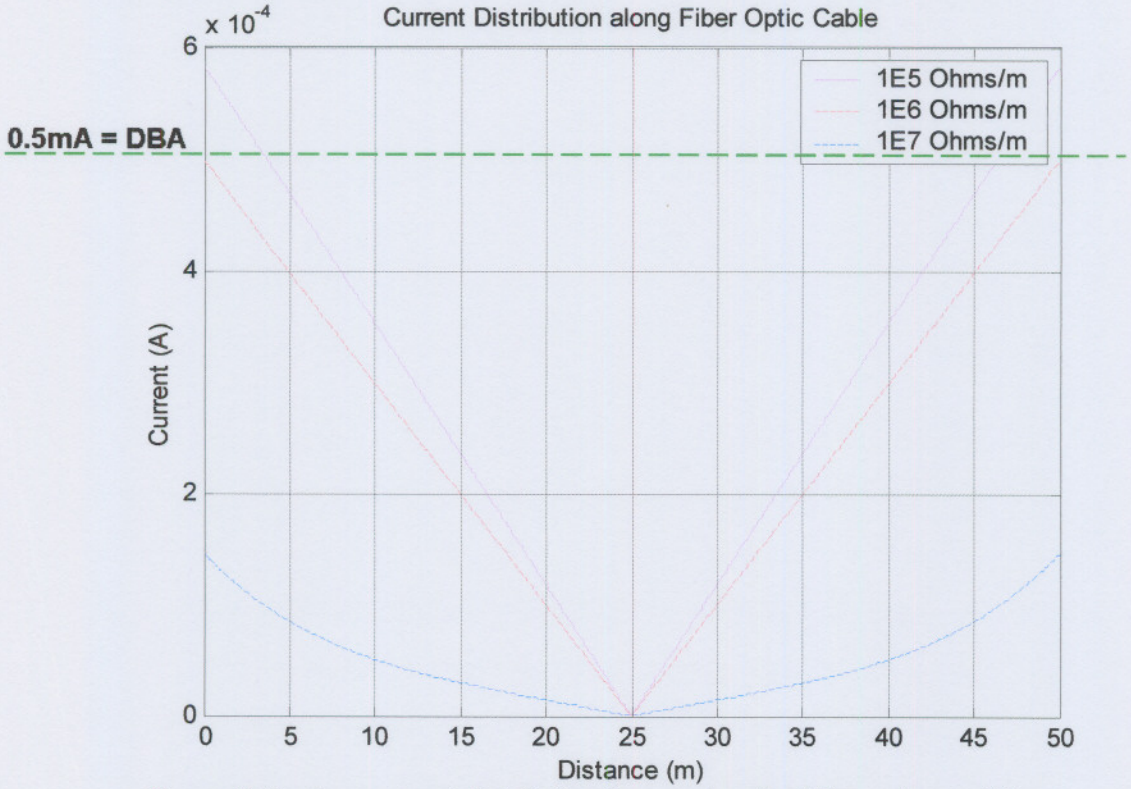

Figure 48: Leakage current distribution for span length of 50m and sag = 2%

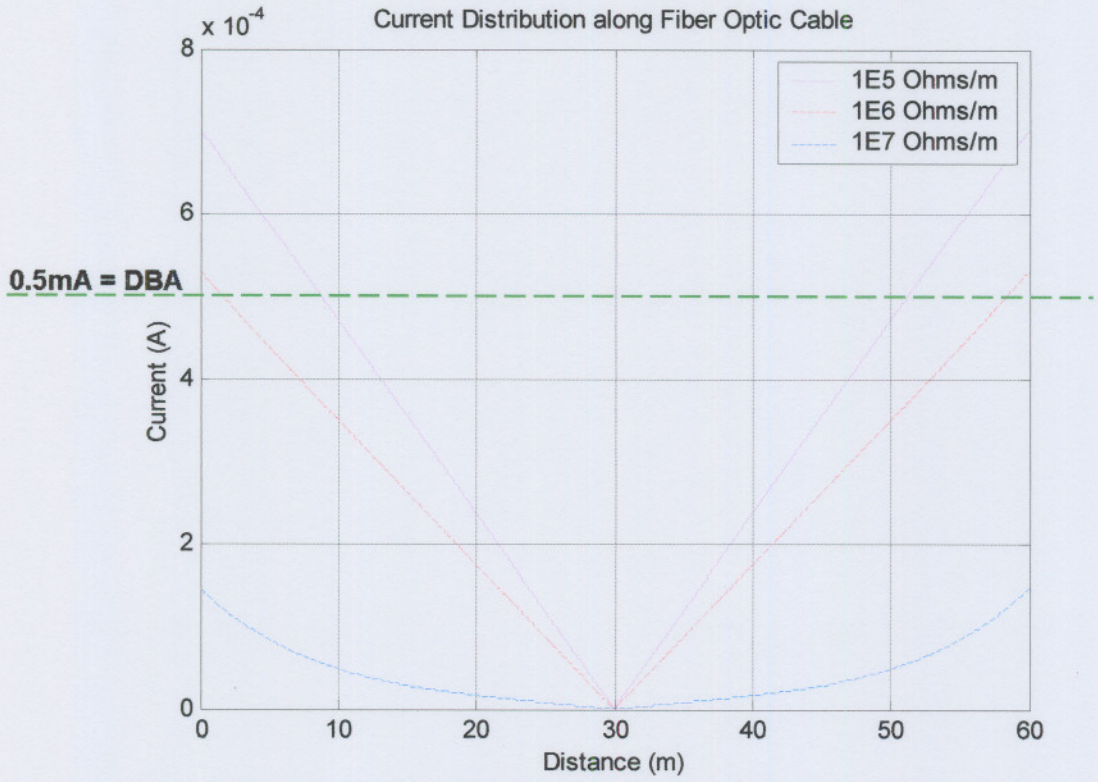

Figure 49: Leakage current distribution for span length of 60m and sag = 2%

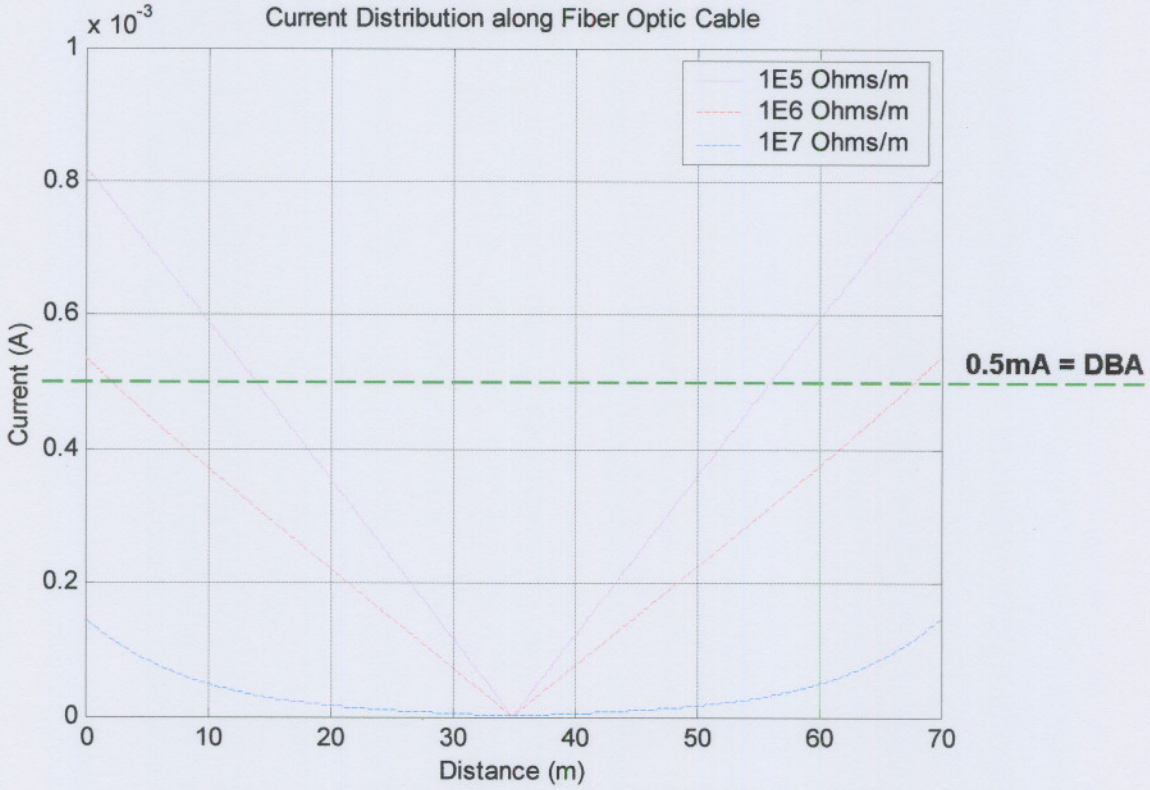

Figure 50: Leakage current distribution for span length of 70m and sag = 2%

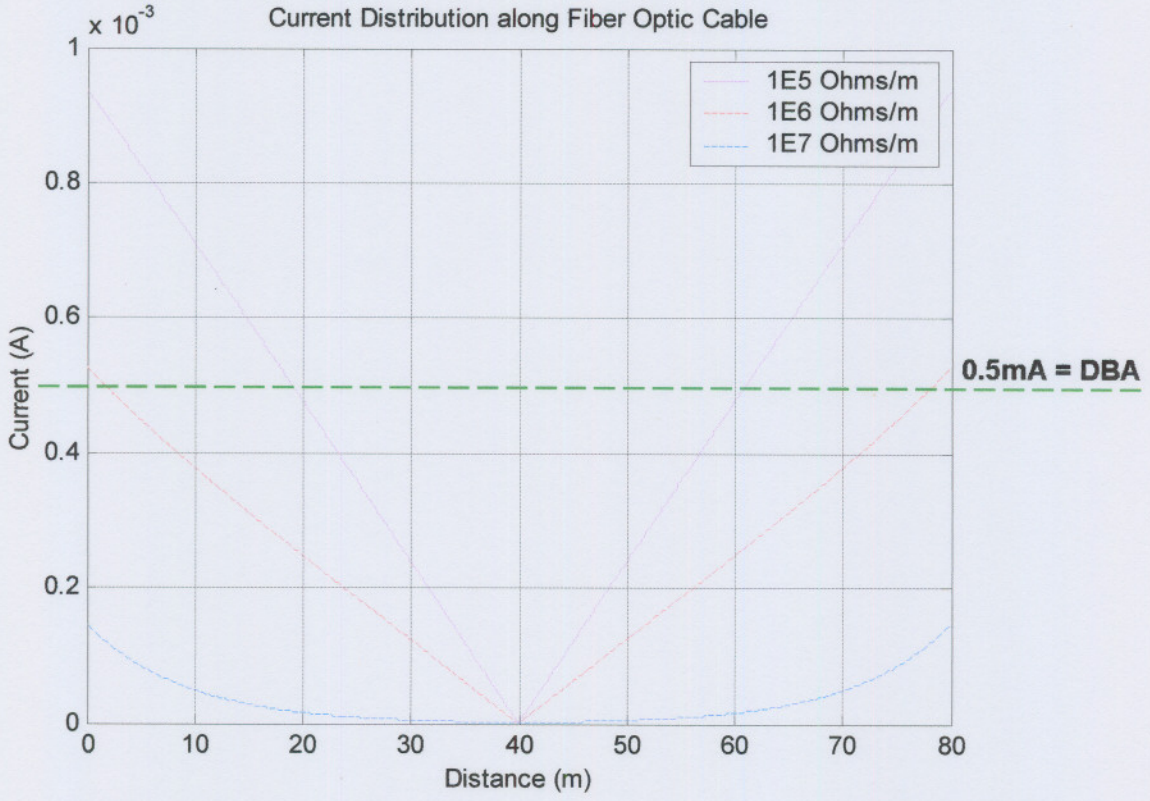

Figure 51: Leakage current distribution for span length of 80m and sag = 2%

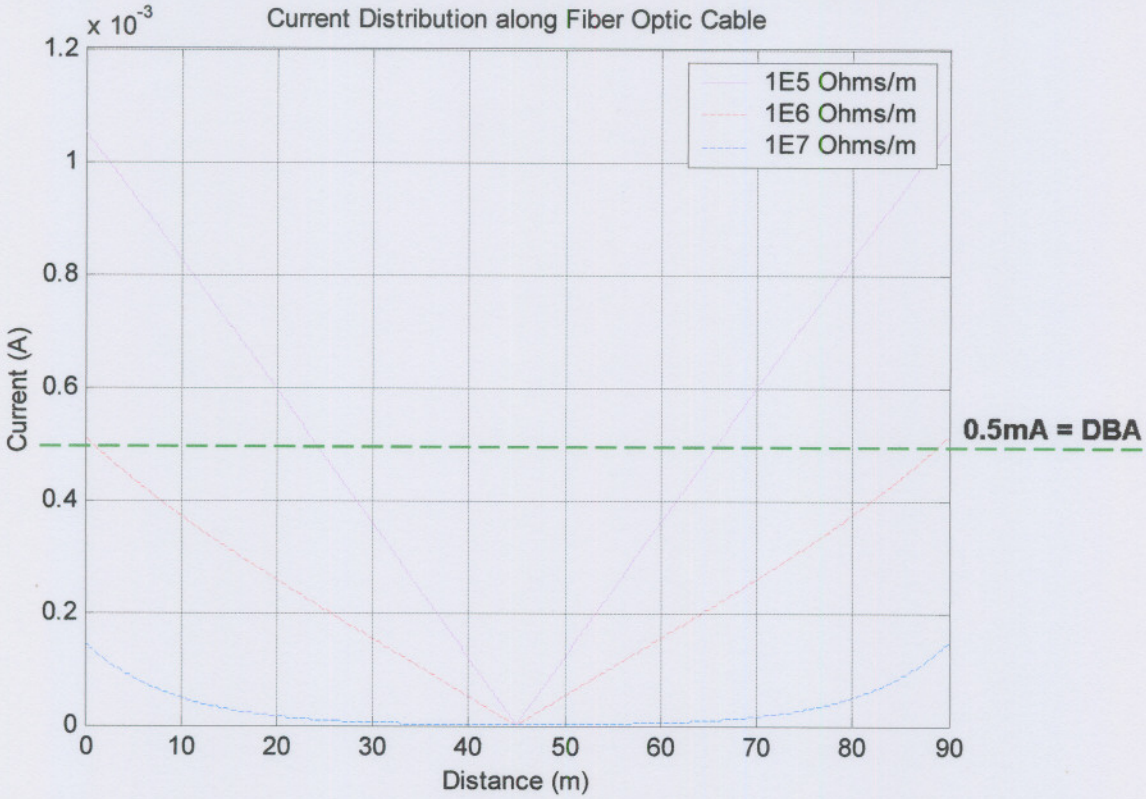

Figure 52: Leakage current distribution for span length of 90m and sag = 2%

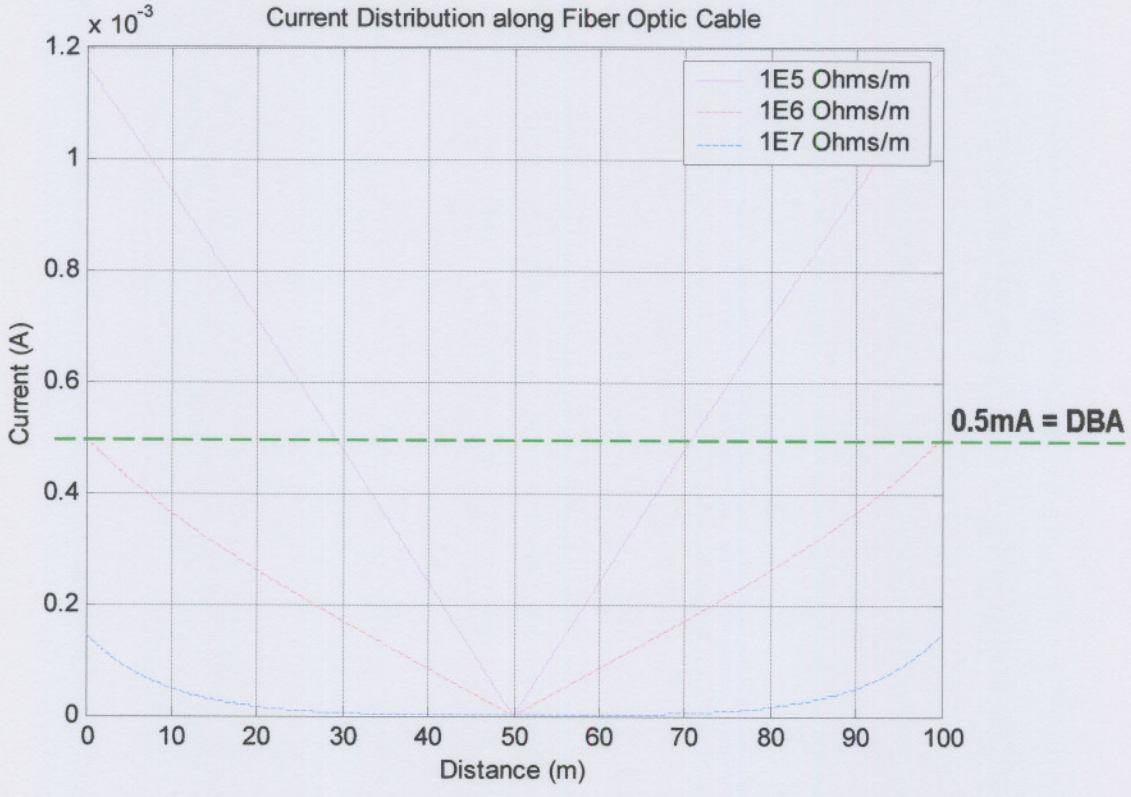

Figure 53: Leakage current distribution for span length of 100m and sag = 2%

Discussion:

One would expect that the resistance of a newly installed cable would be very high and that the pollution on this cable would be very low, if at all. Now this relates to a lightly polluted cable. Therefore, if the cable is new and clean, it should have a very high resistance to current that would want to flow on the cable due to the potential build-up on the cable. When one studies figures 48 to 53, this is exactly what happens, refer to the blue line at the bottom of each figure. Most dielectrics allow a very small leakage current to flow when placed in an electric field. In this case the current that is allowed to flow reaches a maximum at the mast of no more than 0.15mA for any given span length. This is supposed to be so since the cable is the same for all instances, that is, it has either no or very low pollution on it, having a very high resistance to any current that wishes to flow.

From MAXWELL we saw that in section 3.1, the leakage current on a newly installed cable is in the vicinity of 0.263mA and for a polluted cable it would be expected to be in the vicinity of 0.774mA. This is also the value that we obtain with the use of MATLAB.

As mentioned earlier in this study, the current reaches a maximum at the support towers and is zero at mid-span. This is due to the fact that the current that is induced at mid-span is too short lived to reach the support mast due to the fluctuation of the AC current.

Now, in figure 48, for a span length of 50m we see that for a cable lightly polluted or newly installed, the leakage current on the fibre cable reaches a maximum of 0.15mA at the support tower, this is far too low for DBA to occur. This is also what is observed in the field, for clean cables, no DBA occurs.

However, for a cable with medium pollution level, the leakage current reaches a maximum of 0.5mA at the support tower. This is the proposed threshold [3] value after which the occurrence of DBA is very likely. For a cable heavily polluted, the leakage current reaches a maximum of 0.58mA, which is also just above the threshold value. But due to the short span length it is highly unlikely that DBA

should occur since the current induced is barely above 0.5mA and the chances of an evenly spread high pollution layer on the fibre cable is unlikely.

Figure 49 shows the same value of leakage current for a cable lightly polluted, that is 0.15mA, and for cables with medium pollution the maximum leakage current is 0.53mA. This is 0.03mA more than what it was for a 50m span. Again it is highly unlikely for DBA to occur. For a cable with heavy pollution levels the situation is quite different. The leakage current increased to 0.7mA, which is 0.2mA above the threshold. The probability of DBA occurring becomes more realistic.

Figure 50 again shows the same value for leakage current of 0.15mA for a cable lightly polluted, for a cable with medium pollution the leakage current increased by 0.01mA to 0.54mA. This is just above the threshold value for DBA to occur. For a cable with a heavy pollution layer, the leakage current increased to about 0.82mA, 0.32mA above the threshold value. It is becoming clear that with increased span length, the leakage current for a cable with a heavy pollution layer becomes a critical factor in the occurrence of DBA.

In figure 51 the leakage current for a cable with a light pollution layer stayed at 0.15mA, for a cable with a medium pollution layer the leakage current stayed at 0.54mA,but for a cable that has a heavy pollution layer, the leakage current increased to 0.94mA. It is becoming apparent that with increased span length and increased pollution level, the probability of DBA occurring also increases.

In figure 52 the leakage current for a cable with light pollution levels stayed constant at 0.15mA but for a cable with medium pollution levels the leakage current is 0.52mA. For a cable with heavy pollution levels the leakage current once again increased and is now at a value of about 1.05mA.

Finally, for figure 53, the leakage current for a lightly polluted cable is at 0.15mA. The leakage current for a cable with medium pollution levels is at 0.5mA, but for the cable with a heavy pollution layer the leakage current increased to 1.16mA. That is more than double the threshold value of 0.5mA and DBA is most likely to appear.

From this I think it safe to presume that, independent of span length, a newly installed cable should not experience any DBA at all. However, when the cable becomes polluted to a point of medium pollution, span length plays an insignificant role since the value stayed at almost 0.5mA, with very small variations although the chances of DBA occurring does exist.

For a cable with a heavy pollution layer, the span length plays a significant role and has a significant effect on the amount of leakage current that is flowing on the cable. This might be why it takes up to a minimum of 18 months to two years before any DBA activity is noticed.

Judging from the voltage and leakage current distributions it is clear to see that polluted cables stand a far greater risk of experiencing DBA than clean or newly installed cables. It is also apparent that the greatest risk of DBA is situated close to the masts. This corresponds to what has been experienced in the field, namely that most of the reported cases of DBA occurred close to the mast, more or less at the tips of the support wires.

5.3. Effects of pollution on induced voltage and leakage current at different sag percentages

In this section we will take a look at the effect of the level of pollution on the leakage currents and voltages when the cable sag of the fibre cable is varied from 4% to 10%. The case for 2% sag has been shown in the previous section. The span length will be kept constant at 70m, and the voltage at 25kV, 50 Hz. A detailed description will once again be given at the end. Firstly the effect of sag on the induced voltage will be given and then the effect of sag on the leakage current.

Again the pollution levels are classified as follows:

10^5 Ω/m - Heavy pollution - 10^{-7} *siemens/meter*

10^6 Ω/m - Medium Pollution - 10^{-8} *siemens/meter*

10^7 Ω/m - Light Pollution - 10^{-9} *siemens/meter*

Results of voltage distribution for span length of 70m and varying sag%

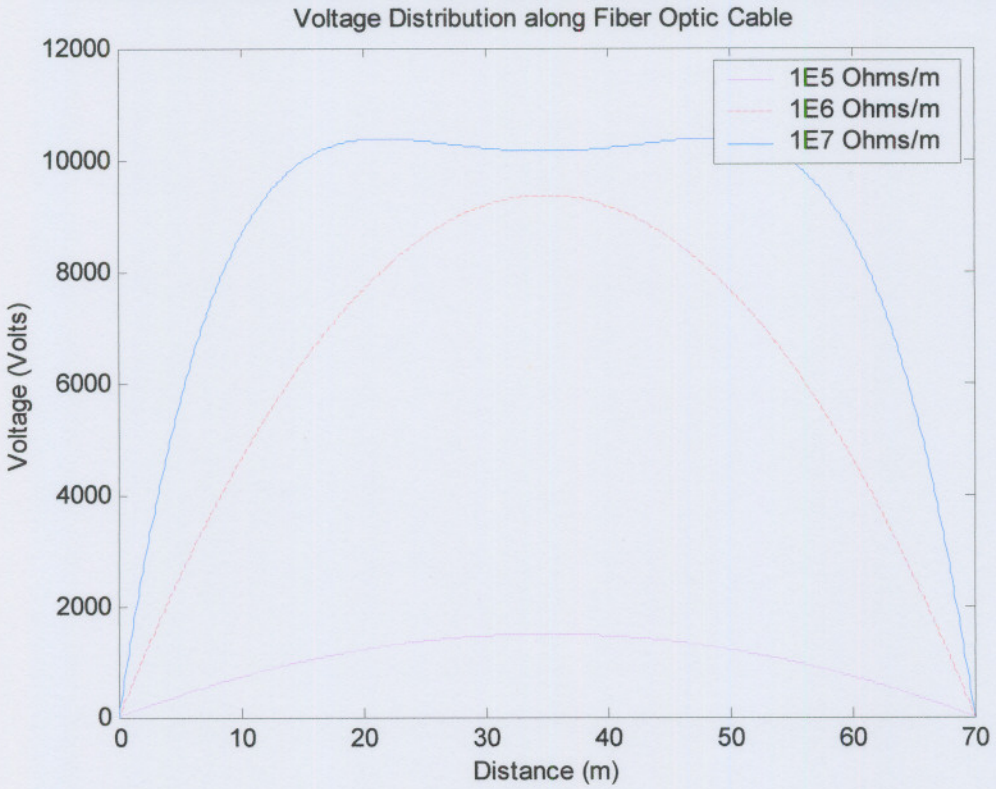

Figure 54: Voltage distribution for span length of 70m and sag = 4%

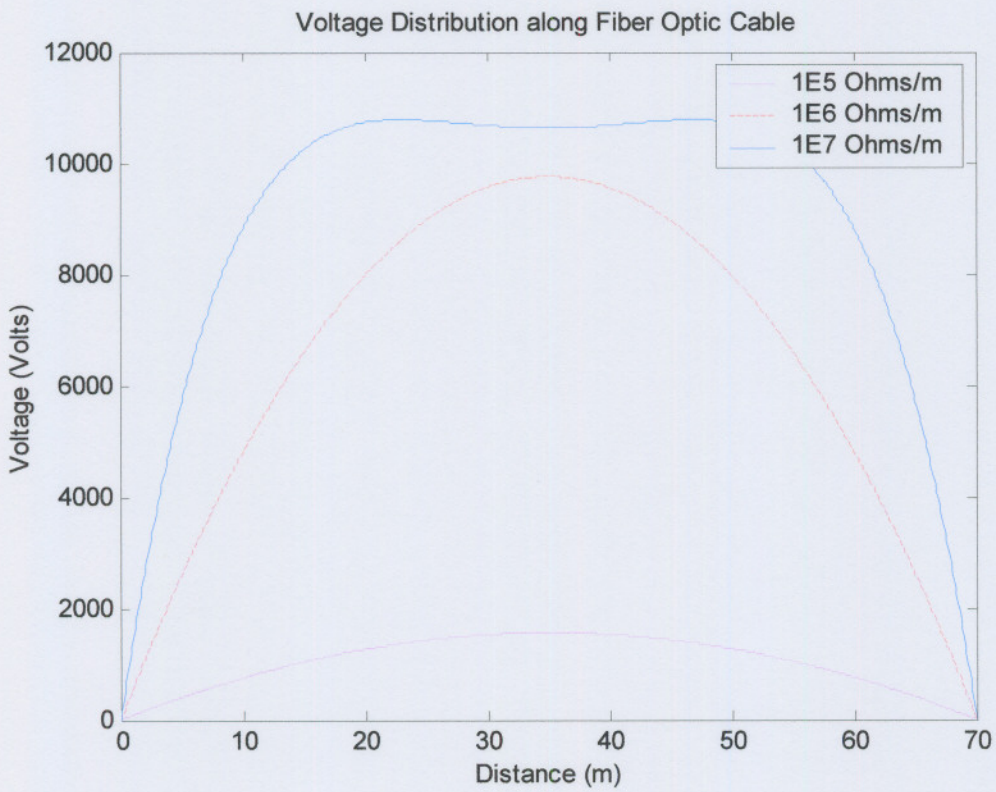

Figure 55: Voltage distribution for span length of 70m and sag = 6%

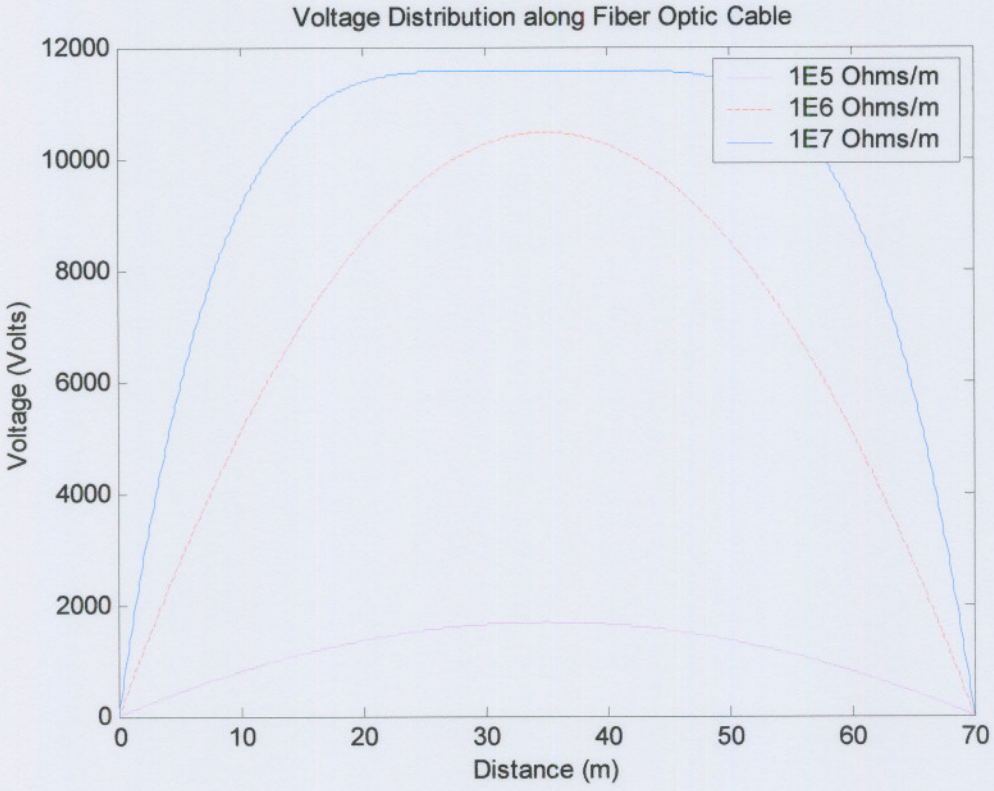

Figure 56: Voltage distribution for span length of 70m and sag = 8%

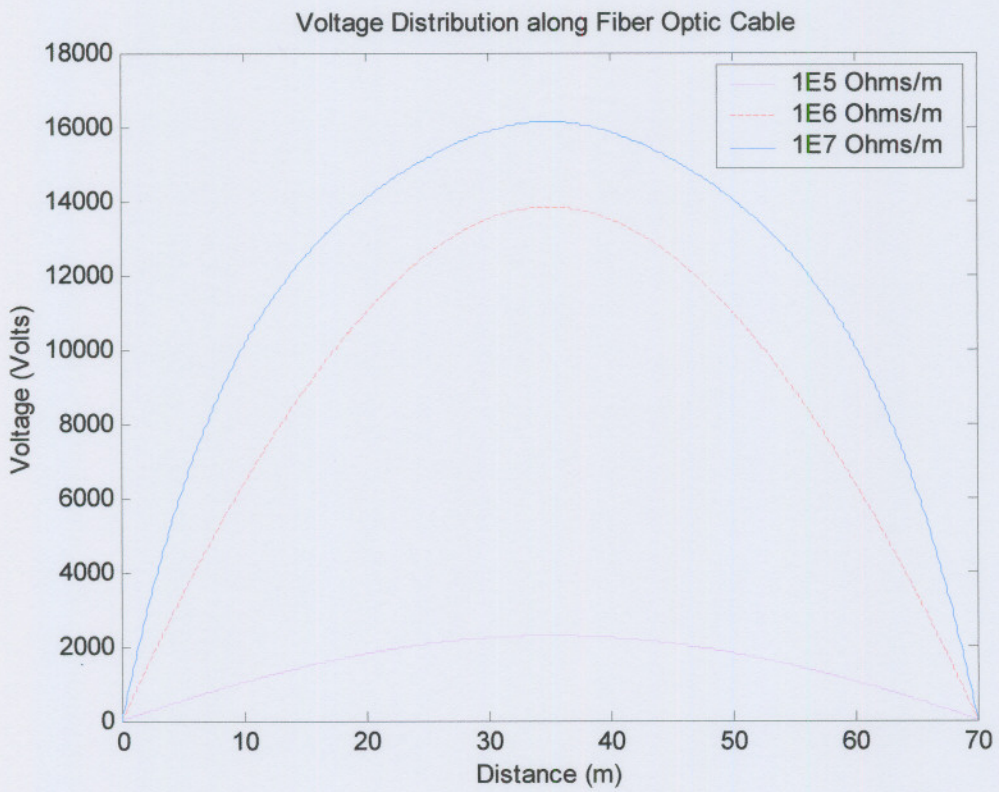

Figure 57: Voltage distribution for span length of 70m and sag = 10%

Discussion:

This section aims to see what the effect of the percentage of sag has on the amount of leakage current and the induced voltage distribution at a span length of 70m. In the first case, figure 44 (in the previous section), the sag is 2% and the span length is taken as 70m. Here we see that the maximum induced voltage for a lightly polluted cable is about 1500V, for cable with a medium pollution level the induced voltage is about 9200V and for a cable with a heavy pollution level the induced voltage at the centre is 9800V and on the side it is about 10200V.

In figure 54 the sag is increased to 4%. This increased the induced voltage for a cable with a light pollution level to about 1600V, the induced voltage for a cable with a medium pollution level is about 9600V and the induced voltage for a cable with a heavy pollution level is about 10200V at the centre and 10400V on either side. These values are a bit higher than for the case of 2% sag.

In figure 55 the sag is increased to 6%, this increased the induced voltage for a cable with a light pollution level to about 1700V, the induced voltage for a cable with a medium pollution level to about 9800V and the induced voltage for a cable with a heavy pollution level to about 9800V at the centre and 10800V and either side. It is becoming apparent that with increased sag% the voltages also increase, for a cable with a heavy pollution level it obviously increases more than for a cable with lower pollution levels.

In figure 56 the sag is increased to 8%, this increased the induced voltage for a cable with a light pollution level to about 1800V, the induced voltage for a cable with a medium pollution level to about 10600V and very interestingly the induced voltage for a cable with a heavy pollution level is becoming a straight line again at the top with a voltage level of about 11600V.

In figure 57 the whole picture changes when the sag% is increased to 10%. The induced voltage for a cable with a light pollution level is at about 2400V, a 600V increase from that of the 8% sag. The induced voltage for a cable with a medium pollution level is now at about 13800V, about 2200V more than that in figure 56 and the induced voltage for a cable with a heavy pollution level is in the form of

an arc with peak voltage at about 16400V. This is 4800V above that for the 8% sag.

This clearly indicates that the closer one gets to the ground, the bigger the value of the capacitance becomes between the fibre and ground and the bigger the voltage that is stored in this field. It is therefore advisable to hang the cables at as low sag% as possible.

Results of Leakage current distribution for span length of 70m and varying sag%

The next section shows what effect of the sag% has on the leakage current.

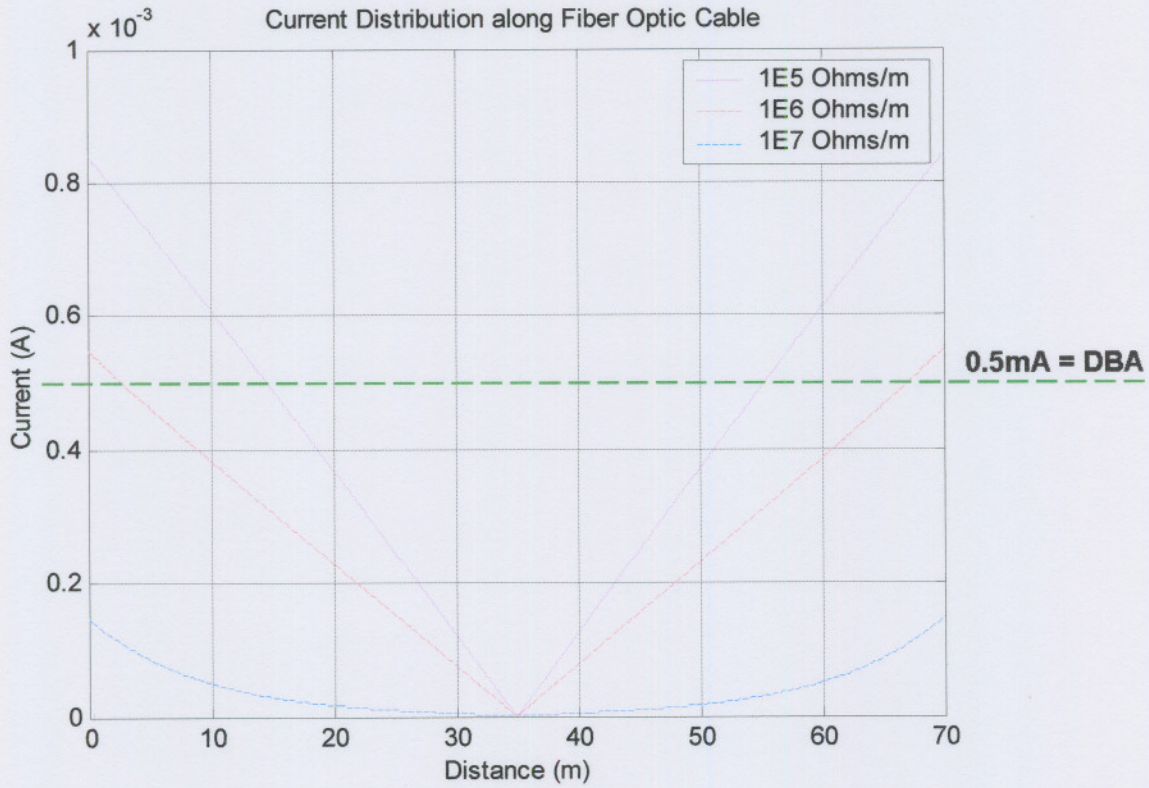

Figure 58: Leakage Current distribution for span length of 70m and sag = 4%

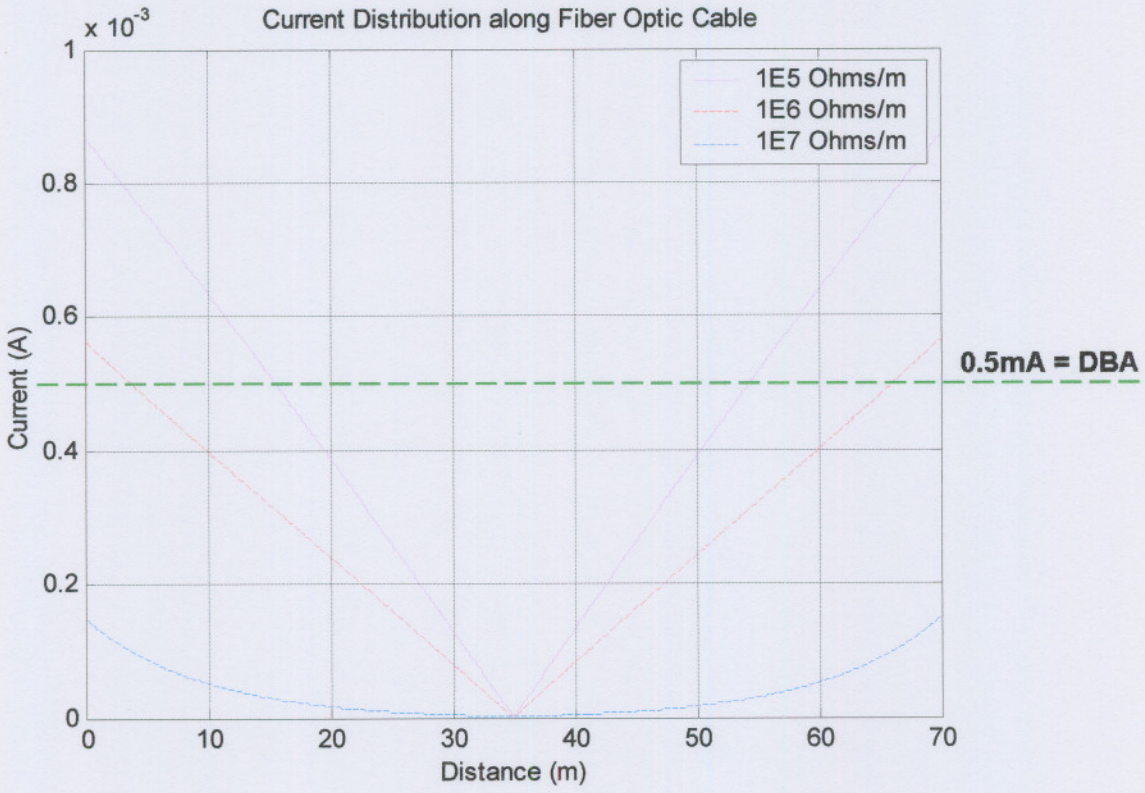

Figure 59: Leakage Current distribution for span length of 70m and sag = 6%

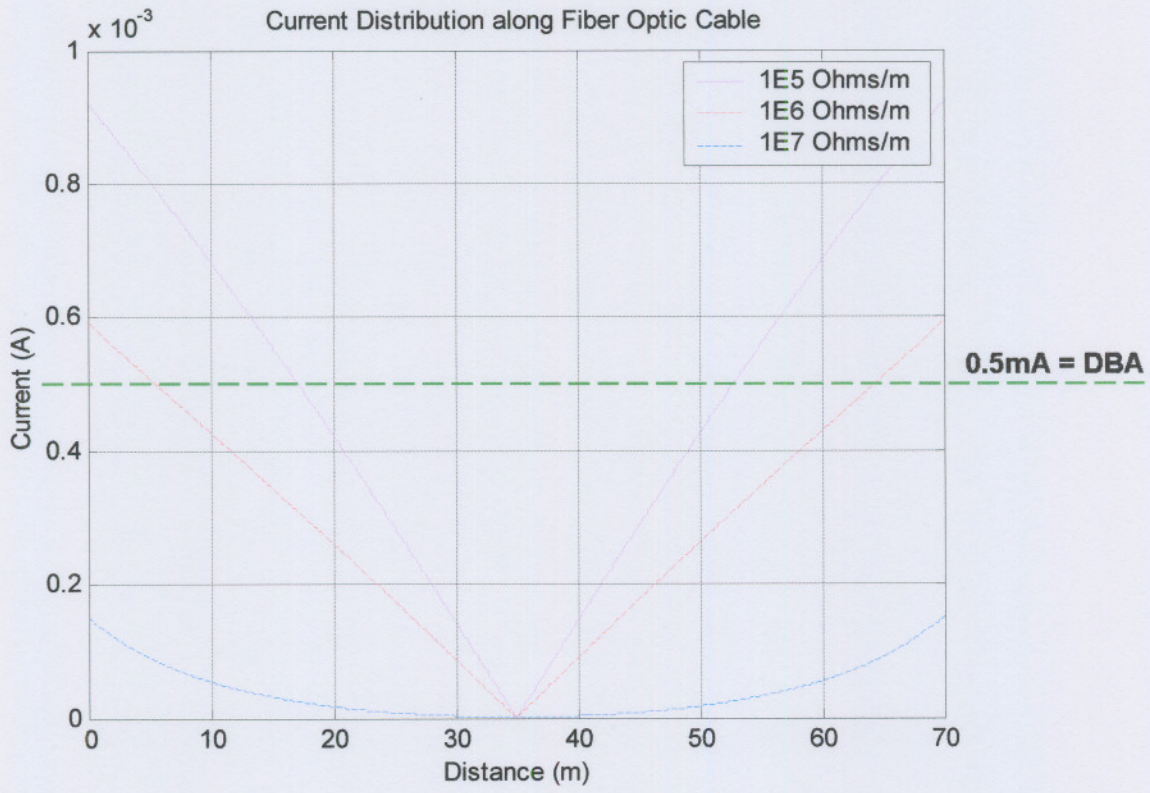

Figure 60: Leakage Current distribution for span length of 70m and sag = 8%

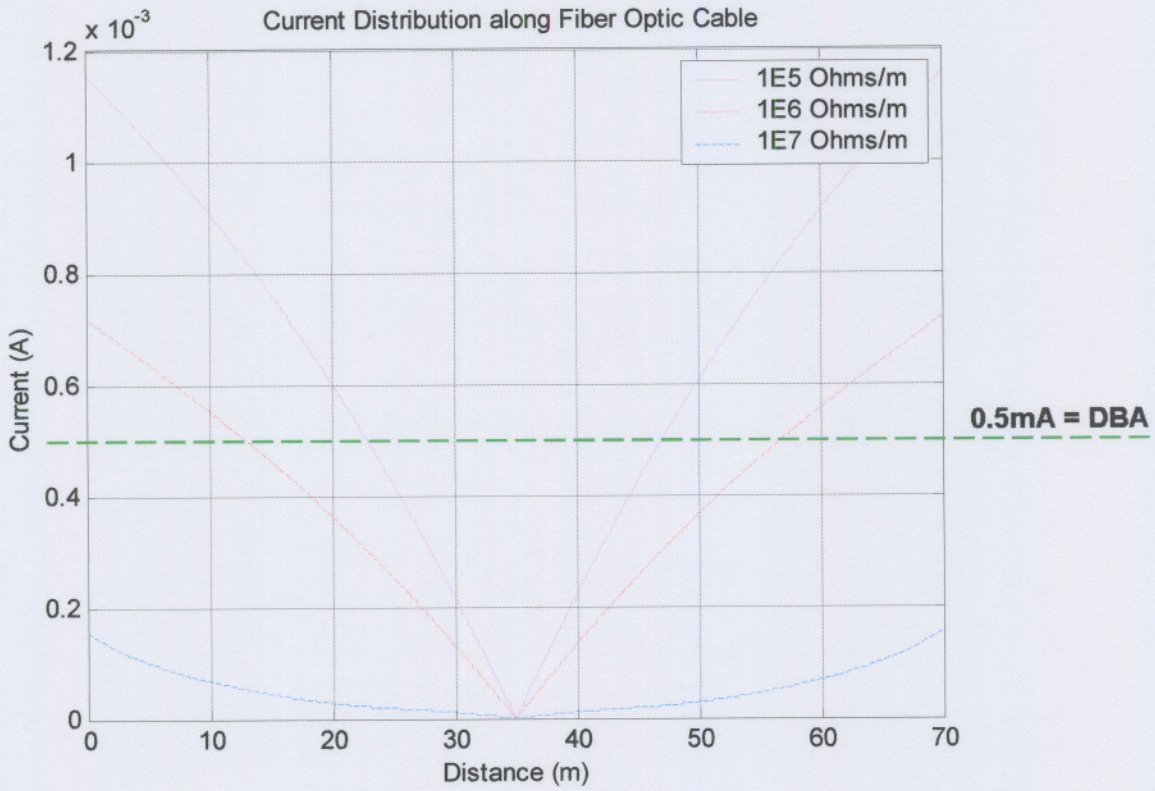

Figure 61: Leakage Current distribution for span length of 70m and sag = 10%

Discussion:

For figure 49, at a span length of 70m and with a 2% sag the cable with a light pollution level has a leakage current of 0.15mA. The cable with a medium pollution level has a leakage current of about 0.53mA and the cable with a heavy pollution level has a leakage current of about 0.7mA.

Now for figure 58 with 4% sag, the leakage currents are 0.14mA for a cable with a light pollution level, 0.54mA for a cable with a medium pollution level and 0.84mA for a cable with a heavy pollution level.

For figure 59 with 6% sag, the leakage currents are 0.14mA for a cable with a light pollution level, 0.56mA for a cable with a medium pollution level and 0.86mA for a cable with a heavy pollution level.

For figure 60 with 8% sag, the leakage currents are 0.15mA for a cable with a light pollution level, 0.58mA for a cable with a medium pollution level and 0.93mA for a cable with a heavy pollution level.

Finally for figure 61 with 10% sag, the leakage currents are 0.16mA for a cable with a light pollution level, 0.72mA for a cable with a medium pollution level and 1.66mA for a cable with a heavy pollution level.

The amount of sag increases the amount of current flowing on the cable. For the 10% sag the enormous change in the voltage is also reflected in the leakage current. The leakage current increased steadily from 2% sag to 8% sag where after it suddenly increased from about 0.93mA for a cable with a heavy pollution level at 8% sag to 1.66mA for a cable with a heavy pollution level at 10% sag. This is a 178% increase whereas for the 4% sag it was 120% increase, for the 6% sag it was a 102% increase and for the 8% sag it was a 178% increase.

This shows that although it is desirable to lower the fibre cable, caution should be taken as to keep the sag at 2% and not lower the cable to close to the ground.

We now want to see what the effect would be on the induced voltage and leakage currents if the cable has a span of 70m, a sag of 2% but it is moved one meter closer to the feeder, and then again one meter further from the feeder. The coordinates will thus be (0.64, 4.43) for closer and (0.64, 6.43) for further.

5.4. Effects of pollution on induced voltage and leakage current at different distances from the feeder cable

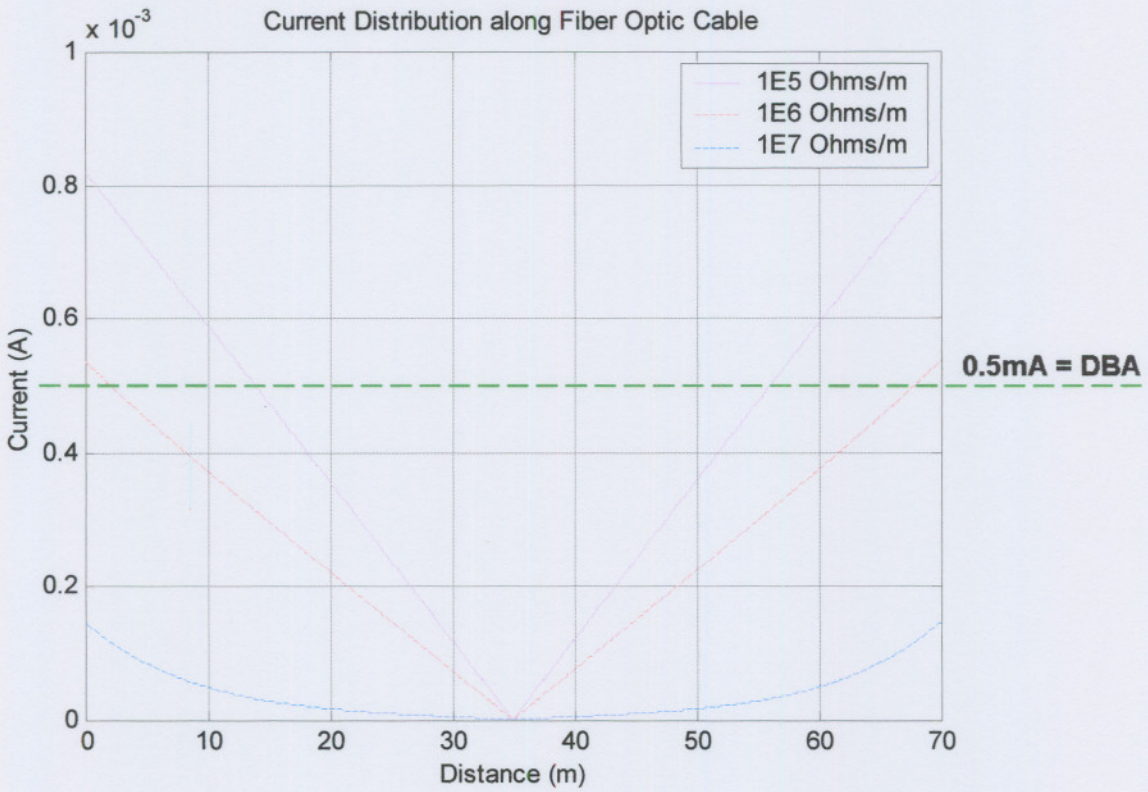

Figure 62: Leakage current distribution for fibre cable at its normal position of (0.64, 5.43) with a span length of 70m and three differ pollution levels

Figure 62 shows the cable at it's current position with a span length of 70m and sag of 2%, we also see that the leakage current is about 0.14mA for a cable with a light pollution level, 0.54mA for a cable with a medium pollution level and 0.82mA for a cable with a heavy pollution level. This is as described previously.

One would expect the leakage currents to increase when the fibre cable is brought closer to the feeder cable and to decrease when the fibre cable is taken further away from the feeder cable. What would the effect on the leakage current be if we lowered it by one meter to (0.64,4.43)?

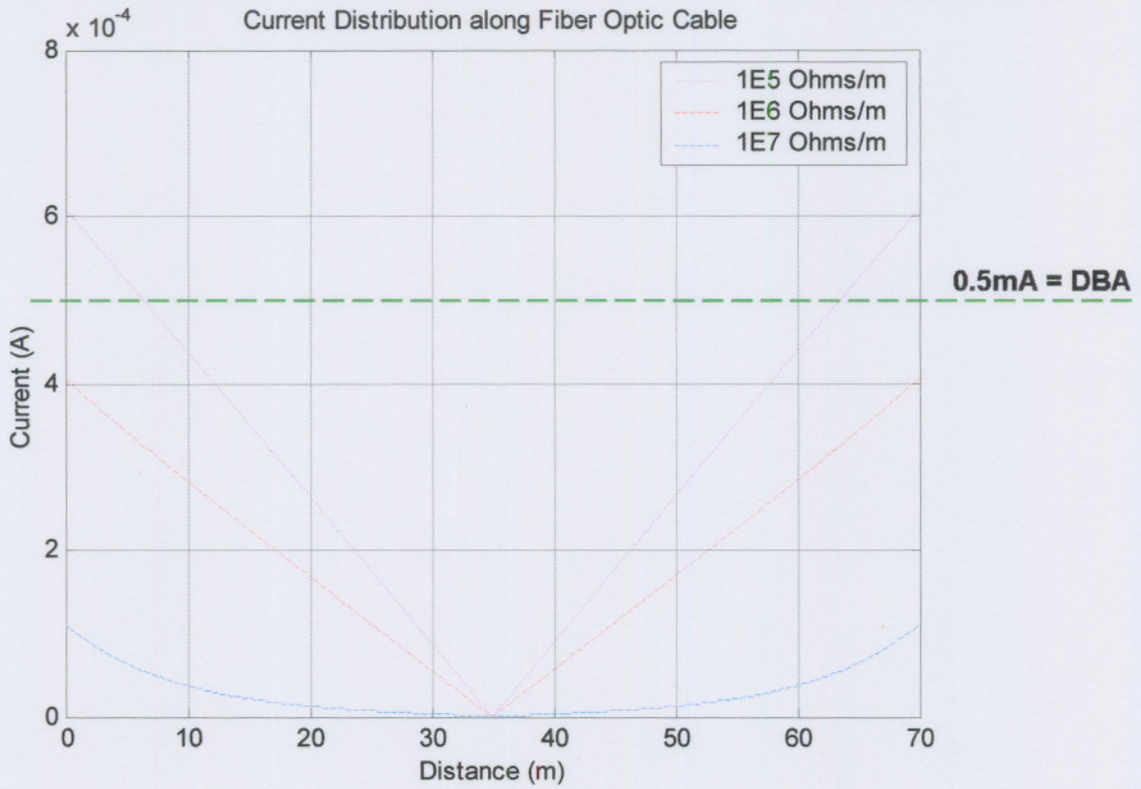

Figure 63: Leakage current on fibre cable when lowered to (0.64, 4.43) with a span length of 70m and sag of 2%

Figure 63 proves what we expected. When the fibre cable is lowered by one meter to (0.64, 4.43), the leakage currents was reduced by 78% from 0.14mA to 0.11mA for a cable with a light pollution level, it decreased by 76% from 0.54mA to 0.41mA for a cable with a medium pollution level and it decreased by 74% from 0.82mA to 0.61mA for a cable with a heavy pollution level. Although 0.61mA is still 0.11mA above the threshold value of 0.5mA, the chances of all the factors working together to allow DBA to occur is minimal and even if it does occur, the extent of the damage will be much less than what it would currently be.

This indicates that by lowering the fibre, thus taking it further away from the source, but keeping the sag at 2%, the leakage currents on the fibre cable can be significantly reduced by up to 74%, thereby reducing the probability of DBA occurring on the fibre cable. It is therefore strongly advised that for this case the fibre be lowered by at least one metre, specifically in areas affected by DBA.

The induced voltage distribution for the cable lowered by one meter can be seen in Figure 64.

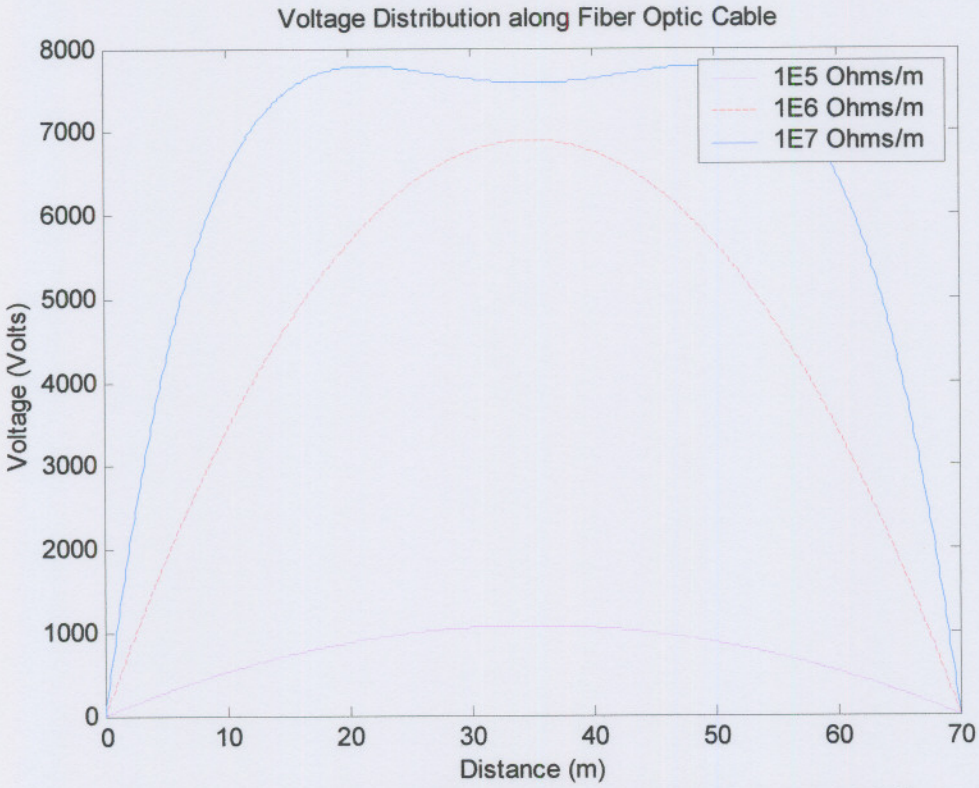

Figure 64: Induced Voltage distribution for cable lowered to (0.64,4.43)

In figure 64 we can see that when one compares this figure to figure 44, the induced voltage was lower from 1500V to about 1200V for a cable with a light pollution level, from 9200V to 6800V for a cable with a medium pollution level and from about 9800V to 7600V for a cable with a heavy pollution level. This also proves to show that by lowering the fibre cable, the risk and probability of DBA is decreased.

Now we want to look at the effect of bringing the cable closer to the feeder has on the leakage current and induced voltages. The cable was placed at (0.64, 6.43) and the result can be seen in figure 65.

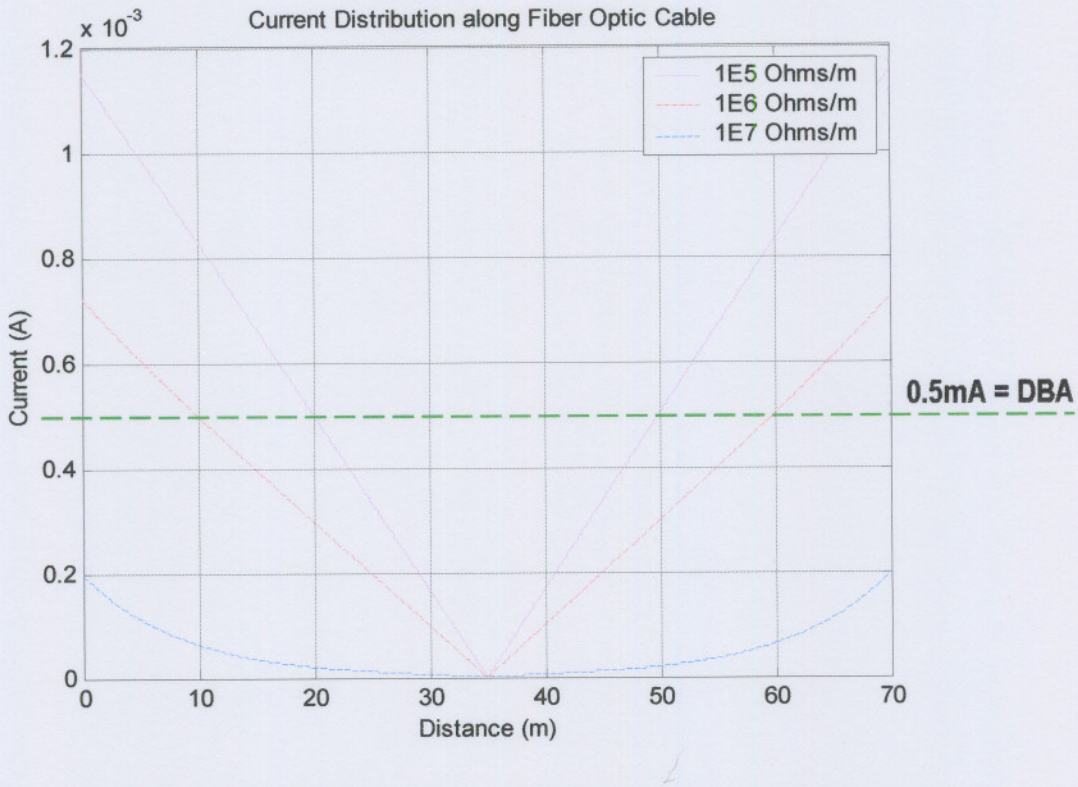

Figure 65: Leakage current distribution for OFC cable lifted to (0.64, 6.43)

In figure 65 we can see that the leakage current increased from 0.14mA to 0.19mA for a cable with a light pollution level. The leakage current increased from 0.54mA to 0.72mA for a cable with a medium pollution level and the leakage current increased from 0.82mA to 1.14mA for a cable with a heavy pollution level. That means that even at medium pollution levels the chances of DBA occurring is greater when the cable is close to the feeder than for a cable with a heavy pollution level, one meter lower than normal. Looking at the induced voltage distributing in figure 66 emphasises this fact.

Lifting the cable by one meter has almost the same effect as putting up the fibre with sag of about 9%. The induced voltage was increased from 1500V to about 2000V for a cable with a light pollution level, increased from 9200V to about 12200V for a cable with a medium pollution level and increased from 9800V to about 12600V for a cable with a heavy pollution level.

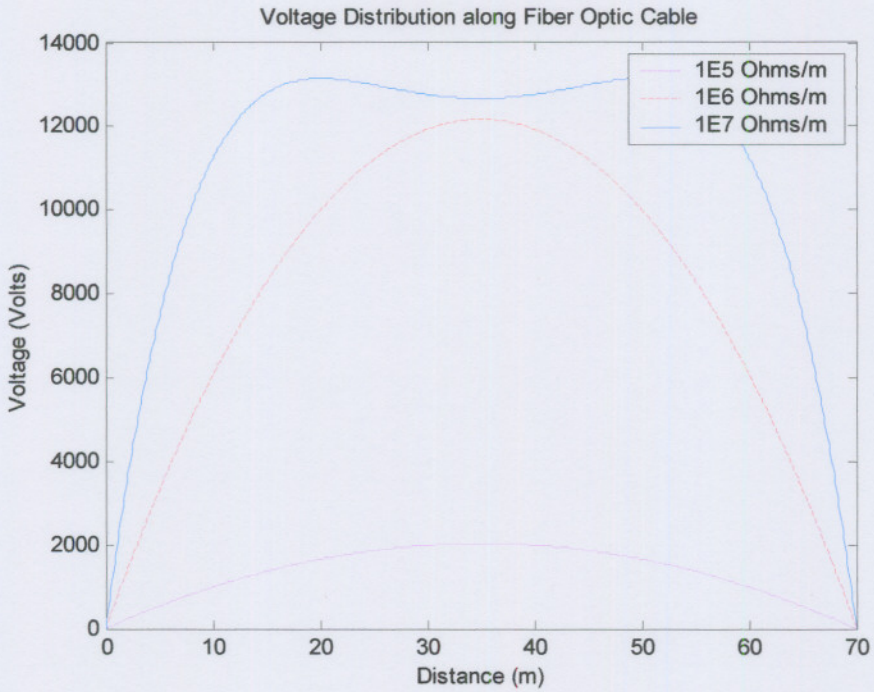

Figure 66: Induced voltage distribution for cable lifted by one meter

Distance from the feeder definitely plays a significant role in the probability of DBA occurring, more so than any other factor.

6. CONCLUSION

This chapter has shown that for a new optical fibre cable installed at the current position, there should be no occurrence of DBA. This correlated well with what is being experienced in the field. It is however when these cables become polluted and they are installed in areas of high humidity and salt rich air areas that the risk of DBA increases. Our simulations using both MATLAB and MAXWELL have shown that the pollution on the cable as well as excessive span lengths increases the probability of DBA occurring.

There are many factors to consider in finding a permanent solution to this problem. Both the MAXWELL simulation and the MATLAB simulation showed that by lowering the OFC by between one and one and a half meter should reduce the risk of DBA irrespective of the level of pollution present on the cable.

The MATLAB model also showed the percentage of sag, span length and distance from the feeder plays an definite role in the occurrence of DBA since all these factors contribute to either an increase or decrease in the induced voltage and leakage current on the cable.

Currently the optic fibre cable is being isolated from the masts and the span length is varying. It is recommended that the fibre cable be earthed at regular intervals, every mast if possible and that the span lengths be kept as short as possible.

Figure 34 showed an interesting occurrence, there seems to be a small surface potential ("hot spot") present on the inside surface of the OFC. The potential of these "hot spots" are of very low magnitude, but it could indicate where DBA might occur if the pollutant is spread evenly around the cable. No explanation for the occurrence of the small "hot spot" could be postulated.

CHAPTER 6 - CONCLUSION AND FUTURE WORK

1. CONCLUSION

In this study we used existing packages that implement completely different modelling methods to try and determine what effect the level of pollution on the cable and the position of the cable has on the occurrence of DBA. The real world structure was taken and simplified somewhat to use as a reference model in various simulations and to try and give meaningful recommendations concerning the occurrence and prevention of DBA.

Both software package simulations have shown that for a newly installed optical fibre cable at the current position, there should be no occurrence of DBA. Both software packages have also shown that as the level of pollution on the optic fibre cable increases, the risk of DBA occurring increases. This is especially true for cables installed closer to the coastal regions, up 100km inland, due to the prolonged exposure to pollution and salt rich air. This proves that the occurrence of DBA is not only dependent on the pollution on or around the cable, neither is it only dependant on the voltage source close to the OFC but also to the span length and the sag of the cable.

Also, due to insufficient collectable data concerning weather conditions before, during and after the occurrence of DBA, it is difficult to predict what the exact effects of wet-dry cycles are on the occurrence of DBA for this specific stretch of OFC. It has been shown by [15], [16] that the presence of both pollution and water, gives better chance for DBA to occur. There are many factors to consider in finding a permanent solution to this problem. One solution could be to lower the OFC by about one and a half meter.

The MAXWELL software package as well as the mathematical model showed that lowering the fibre cable should reduce the probability of DBA occurring. This can be seen in section 3.1 and 5.4. It is also apparent from both of these software packages

that DBA should not occur at the centre of the span. This is true although very few cases have been reported where DBA actually occurred near mid-span. This is however very unlikely.

In section 3.1 the effect of the optic fibre cable on the electric field was observed and it was found that the presence of the fibre cable, had no effect on the form or intensity of the electric field. In section 5 however, we could see that the electric field had a profound effect on the fibre cable in terms of the potential build-up and leakage currents that was induced on the fibre cable. As expected, from section 5, the leakage currents and induced voltages on a newly installed fibre cable is much less than that for a polluted fibre cable. From this we know that cables can't be continuously replaced in order to keep the pollution level as low as possible, but it might be feasible to clean the cables on occasion.

The accuracy of the MAXWELL program is sufficient to the scope of this study, but where higher degrees of accuracy is required, some research could be done to the feasibility and availability of software and support. The mathematical software program running in MATLAB had a much higher degree of accuracy and reliability and was developed and refined using work done by several well-known researchers in this field of study. Again, due to the complex nature of this specific situation, only known and controllable parameters where used. This does limit the accuracy of the results, yet it relates very well to the physical reality.

It might also not be feasible to lower the fibre cables throughout the whole configuration since DBA does not occur countrywide. It is however advisable to lower the cable whenever maintenance is done or in the event of cable failure. This would help in reducing the occurrence of DBA at the specific problem area. Once again this is derived from what could be seen in both sections 3.1 and 5 of Chapter 5.

2. FUTURE WORK

The model consisted of a single mast with a 25kV Feeder connected to the catenary, an earth wire was connected on top of the masts to the supporting beam for the catenary and an OFC installed about 1.8m below the feeder. This model can be made

more complex by adding another Mast opposite this one, but instead of a feeder, one could place a three-phase system on top of the second mast to see what the influence of the two masts would be on one another. This could be done to see what the effect would be on the OFC in areas where a double rail system is used. The case viewed in this study only considered a single-track system.

The influence that a passing train has on the potential fields could also be of interest, but this would require extensive as well as dynamic 3D modelling software package and an extensive knowledge of the electric fields at work in this area. Remember that these fields are not stationary but dynamic.

The 0.5mA threshold value was taken from research done in a balanced three-phase system; the accuracy and relevance under these circumstances could also be investigated.

Physical measurements can also be done although this has proven to be extremely difficult since any interference in the system changes the whole configuration. Trains running in the system and passing the point of interest also plays a significant role in the currents generated at the specific voltage level of the feeder cable.

Pollution levels were obtained from the University of Natal in South Africa, where several samples were taken and measured. Some other test and simulations in this regard could also be conducted.

I believe that the occurrence of DBA is more or less predictable, and that some very easy preventative measures can be taken to reduce to probability of DBA occurring. It is however where these easy solutions fails, that more in-depth studies need to be conducted.

REFERENCES

[1] KARADY, G.G., TORGENSON, M., TORGENSON, D., WILD, J., & TUOMINEN, M.: "New Test Method for evaluation of Corona-caused Aging of Fibre-optic Cables". IEEE Transmission and Distribution Conference, Vol. 2, pp. 734-738, April 11-16 1999.

[2] KARADY, G.G. 2002. Utility application of fibre optic cables. [In Arizona State University] http://www.pserc.wisc.edu/cgipserc/getbig/generalinf/presentati/psercsemin1/psercsemin1/WWWhttpwwwpsercwiscedupserc bintestgetpublicatio2000publicKaradypdf.url] [Date of access: 16 April 2002].

[3] CARTER, C.N. & WALDRON, M.A. 1992. "Mathematical model of dry band arcing on self-supporting all dielectric optical cables strung on overhead power lines", IEEE Proceedings – C., Vol. 139, No. 3, pp.185-196, May 1992.

[4] FREUDENRICH, C.C. 2002. How fibre optics work. [In Howstuffworks: http://www.howstuffworks.com/fibre-optic.htm] [Date of access: 12 March 2002].

[5] PEDROW, P.D., OLSEN, R.G. & EDWARDS, K.S. Portable ADSS Surface Contamination Meter. Proceedings of the 1999 IEEE Conference on Electrical Insulation and Dielectric Phenomena. Volume I. 1999. pp. 158-161.

[6] HALLIDAY, D., RESNICK, R. & WALKER, J. 1997. Fundamentals of Physics Extended, Fifth Ed. USA: John Wiley & Sons, Inc. 1142 p.

[7] STEVENSON, W.D. Jr. 1982. Elements of Power System Analysis, Fourth Ed. McGraw-Hill Book Co – Singapore. Pp.68-87.

[8] NEL, G. 2003. TRANSTEL, South Africa. Personal correspondence.

[9] MAXWELL 2D Field Simulator, Student Version, Version 9 [In http://www.ansoft.com/about/academics/sv.cfm?sv=Max&CFID=68185&CFTOKEN=91779188] [Accessed on 5/6/2003].

[10] CARTER, C.N. & WALDRON, M.A. 1992. Mathematical model of dry-band arcing on self-supporting, all-dielectric, optical cables strung on overhead power lines. IEEE Proceedings-C, Vol. 139, No.3, May 1992.

[11] VAN ZYL, P. 2003. ATC, South Africa. Personal correspondence.

[12] CARTER, C.N, "Arc control devices for use on All Dielectric Self Supporting optical cables," *IEE Proceedings-A*, September 1993, Vol. 140, No 5, pp. 357-361.

[13] KARADY, G.G. & DEVARAJAN, S. Algorithm to predict Dry-Band Arcing in Fiber-Optic Cables, IEEE Transactions. On Power Delivery Vol.16, No.2, April 2001.

[14] KHAN, M.F. & HOCH, D.A. Performance of All Dielectric Self-Supporting fibre optic cable in High Voltage environments. University of Natal, South Africa, September 2003.

[15] VOSLOO, W.L. & HOLTZHAUSEN, J.P. Observation of discharge development and surface changes to evaluate the performance of different outdoor insulator materials at a severe coastal site. 13th International Symposium on High Voltage Engineering, Netherlands 2003, Smit (ed.) Millpress, Rotterdam, ISBN 90-77017-79-8.

[16] VOSLOO, W.L. & HOLTZHAUSEN, J.P. The electric field of polluted insulators. Africon 20002, George, South Africa, October 2002.

[17] HOCH, D.A. University of Natal. 2004.

[18] ALLAN, W.B. 1980. Fibre Optics. Engineering Design Guides. Vol. 36. p. 3-4, 21-23. 25 p.

[19] CORNING GROUP. 2002. Fibre Optic Technology. [In Corning: http://www.iec.org/online/tutorials/fibre_optic/index.html] [Date of access: 4 April 2002].

[20] NELSON, G. 2002. Fibre Optics. [In Arcelect: http://www.arcelect.com/fibrecable.htm] [Date of access: 15 March 2002].

[21] SENIOR, J.M. 1985. Optical Fibre Communications. London: Prentice Hall International. 558. p.

[22] ERICKSON, D.C. & HOGUTA, K. 1983. Fibre Optic Application in Electrical substations. IEEE. p. 15-29. 38 p.

[23] GOWAR, J. 1984. Optical Communication Systems. London: Prentice Hall International. 577p

APPENDIX A

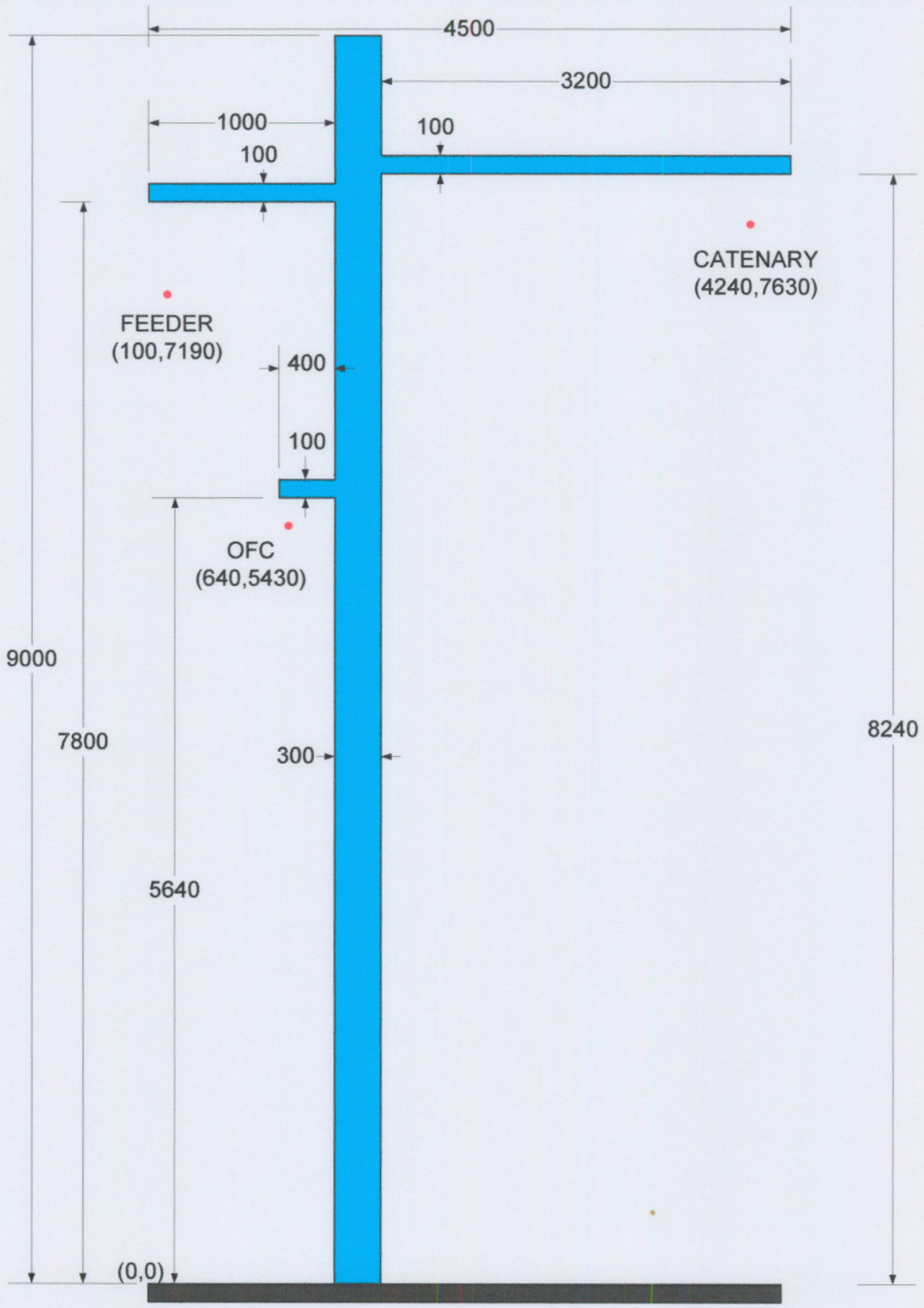

Figure 67: Detailed drawing of mast and cables

APPENDIX B

Determination of Leakage current as determined in Carter and Waldron [10].

A system was devised that accurately calculates the current and voltage at specific points on the cable. One needs a way of calculating how earth leakage currents flowing on the surface of the conductor modify the induced voltages. Thevinin'e theorem may be used to replace the system of phase conductors by an equivalent conductor, at potential V_s relative to ground.

Consider an infinitesimal element of the cable, of length *dx*, whose capacitances per unit length to line and ground are C_1 and C_2, respectively. If we assume that C_1, C_2 and R, the resistance per unit length of the wet polluted cable are independent of position in line with the assumptions made above to calculate V_0 and J_0, the problem can be treated quite simple. If the element has a potential relative to ground of V and carries a current I, then current continuity gives

$$d\mathbf{I} = j\omega C_1 \mathbf{V}_s dx - j\omega \mathbf{V}(C_1 + C_2)dx \tag{B.1}$$

and the resistive voltage drop along the cable gives

$$d\mathbf{V} = -\mathbf{I}Rdx \tag{B.2}$$

It is convenient at this point to define normalised parameters for voltage, current, position and specific resistance, which simplify the algebra greatly. Thus

$$\begin{aligned} &\mathbf{v} = \mathbf{V}/\mathbf{V}_0, \qquad \mathbf{i} = \mathbf{I}/\mathbf{J}_0 L, \\ &\lambda = x/L, \quad \textit{and}\ \mathbf{k}^2 = \mathbf{J}_0 RL^2/\mathbf{V}_0 \end{aligned} \tag{B.3}$$

where L is the half-span

$$\mathbf{V}_0 = \frac{C_1 \mathbf{V}_s}{(C_1 + C_{2)}} \tag{B.4}$$

is the cable potential when R tends to infinity, and

$$\mathbf{J}_0 = j\omega C_1 \mathbf{V}_s, \tag{B.5}$$

is the charging current when R tends to zero, which relate C_1 and C_2 to the calculated values of V_0 and J_0. Equations (B.4) and (B.5) now read

$$\mathbf{v} = 1 - \frac{d\mathbf{i}}{d\lambda} \tag{B.6}$$

$$\frac{d\mathbf{v}}{d\lambda} = -\mathbf{i}\mathbf{k}^2 \tag{B.7}$$

hence

$$\frac{d^2\mathbf{i}}{d\lambda^2} = \mathbf{k}^2\mathbf{i} \tag{B.8}$$

which has a solution

$$\mathbf{i} = Ae^{\mathbf{k}\lambda} + Be^{-\mathbf{k}\lambda} \tag{B.9}$$

If we choose $\lambda = 0$ at mid-span, then the boundary condition $i = 0$ at $\lambda = 0$ yields $A = -B$ and B $\boldsymbol{i} = 2A \sinh \boldsymbol{k}\lambda$.

The cable is taken as earthed at the support so that $\mathbf{v} = 0$ at $\lambda = 1$, so from eqns. (B.6) and (B.7) we can obtain expressions for the normalised voltage and current as functions of position

$$\mathbf{v}(\lambda) = 1 - \frac{\cosh \mathbf{k}\lambda}{\cosh \mathbf{k}} \quad \text{and} \quad \mathbf{i}(\lambda) = \frac{\sinh \mathbf{k}\lambda}{\mathbf{k} \cosh \mathbf{k}} \tag{B.10}$$

giving the normalised earth-leakage current as

$$\mathbf{i}(1) = \frac{\tanh \mathbf{k}}{\mathbf{k}} \tag{B.11}$$

The parameter **k** is complex, if we write:

$$\mathbf{k} = (1+j)\frac{L}{\delta}, \text{ where } \delta^2 = \frac{2}{\omega R(C_1 + C_2)} \tag{B.12}$$

then eqn. 11 can be rewritten as

$$\mathbf{i}(1) = \frac{\delta}{2L}\left[\frac{\sinh\frac{2L}{\delta} + \sin\frac{2L}{\delta}}{\cosh\frac{2L}{\delta} + \cos\frac{2L}{\delta}} - j\frac{\sinh\frac{2L}{\delta} - \sin\frac{2L}{\delta}}{\cosh\frac{2L}{\delta} - \cos\frac{2L}{\delta}}\right] \tag{B.13}$$

Where $L >> \delta$, as it always will be in the problem at hand, then eqn. (B.13) reduces to

$$\mathbf{i}(1) = \frac{\delta}{2L}(1-j) \tag{B.14}$$

and so the earth-leakage current will have the magnitude

$$I_1 = V_s \omega C_1 \delta \tag{B.15}$$

The two ends of the span are thus independent of each other and of the span length. The magnitude of the earth-leakage current is as though drawn from the line through a

capacitor of value $C_1\delta$. Here δ, which we will call the active length, represents the length of cable adjacent to the support from which the majority of the earth-leakage current is drawn.